BRANZ

# STUDY REPORT

## No. 189 (2008)

# Seismic performance of brick veneer houses

# Phase 1. Cyclic and elemental testing of clay brick veneer construction


## S.J. Thurston and G. J. Beattie



FUNDED BY
THE BUILDING
RESEARCH LEVY
BUILDING RESEARCH

The work reported here was funded by Building Research Levy.





ISSN: 1178-4938

# Preface

This is the first full-scale investigation of the performance of clay brick veneer houses when subjected to simulated seismic loading. In the 1990s, an investigation was conducted of the out-of-plane performance of New Zealand brick veneer construction and out of that study came the standardised requirements for brick veneer ties to be screw-fixed to timber framing. A second requirement was that the ties were required to be fully encapsulated in the mortar joint. Further investigations were conducted in the early 2000s which concluded that full encapsulation of the ties was not necessary and the ties remained well bound when seated directly on the top of the brick.

The current study is intended to improve the understanding of the performance of brick veneer construction in earthquakes, in particular:

- To determine if brick veneer can be relied upon to carry a part of the building seismic load or whether the light timber-framed (LTF) construction of the building should be designed to carry the entire load.
- To identify the damage that might be expected to occur in modern brick veneer construction, particularly at building corners where the face-loaded and in-plane loaded veneers meet.

# Acknowledgments

This work was funded by the Building Research Levy. Elephant Plasterboard New Zealand donated the wall linings used in the testing. MonierBricks donated the bricks and Eagle Wire Products Ltd the brick-ties used in the testing.

# Note

This report is intended for DBH (Department of Building Housing) standards committees, structural engineers, architects, designers, plasterboard and brick manufacturers and others researching this topic.

# Seismic performance of brick veneer houses
# Phase 1. Cyclic and elemental testing of clay brick veneer construction

## BRANZ Study Report SR 189


## S.J. Thurston and G. J. Beattie


## Reference


Thurston SJ and Beattie GJ. 2008. 'Seismic performance of brick veneer houses. Phase 1. Cyclic and elemental testing of clay brick veneer construction'. BRANZ *Study Report 189*. BRANZ Ltd, Judgeford, New Zealand.


## Abstract


Historically brick veneer houses have not performed well in earthquakes. However, modern construction using better brick-ties which are screwed to studs and the use of bricks with internal holes is expected to result in a better performance.

BRANZ cyclically racked two large brick veneer rooms (including ceilings) using a system which allowed the total load carried by the brick veneer to be measured directly. One room incorporated windows and had a door opening, while the other had fully separated brick veneer elements. Brickwork cracking patterns were identified and rationalised. It was determined that in-plane brickwork slip was significantly resisted by adjacent perpendicular walls and the mortar in brickwork holes acted as dowels which resisted slip along horizontal mortar cracks.

Elemental tests were used to measure brickwork tension bond and slip strengths and the in-plane brick tie load versus deflection relationship. These were used to determine the theoretical lateral load strength of the veneer and a theoretical model was calibrated by comparing with the measured room strengths. A new design philosophy has been proposed.

**Contents** **Page**

## Figures Page

## Tables Page



Notation used

| Variable | Reference | Description |
|---|---|---|
| $B_{net}$ | Eqn. (6) | Net bending moment of forces about pivot of Figure 20 |
| $C_{EQ}$ | Section 5.2.3 | Seismic lateral load coefficient acting on the brickwork in the in-plane direction |
| CrackHeight | Figure 20 | Height of horizontal crack from the bottom of the veneer |
| D | Section 5.3.1 | T/2 at Corner 1 and (L2-T/2) at Corner 2 of Figure 21 |
| Deflection stud | Table 4 | Name used in plots corresponding to $\Delta_{\text{Stud at gauge}}$ |
| DeltaX | Figure 19 | Horizontal deflection of the LTF stud at Tie j based on the “trapezoidal assumption” |
| EQ | Figure 20 | Horizontal earthquake force on brick veneer pier |
| $f_{mv}$ | Section 5.2.3 | Shear bond strength of brick-to-brick or substrate below |
| $f_{mt}$ | Section 5.2.3 | Tension bond strength of brick-to-brick or substrate below |
| ForceXj | Figure 20 | Horizontal force on brick pier from Tie j |
| ForceYj | Figure 20 | Vertical force on brick pier from Tie j |
| GaugeHeight | Section A.5.2 | Height of gauge above base of veneer |
| H | Figure 20 | Height of pier of brick |

| | | |
|---|---|---|
| H1 | Figure 21 | Height R acts above base crack |
| L | Figure 20 | Length of pier of brick |
| LTF | – | Light Timber Frame |
| LTFdef | Figure 19 | Deflection of LTF wall top plate |
| LTFheight | Figure 19 | Height of LTF wall |
| LTFtoBrick | Table 4 | Name used in plots corresponding to $\Delta_{LTFtoBrick}$ |
| Pier rotation | Table 4 | Name used in plots corresponding to $\Delta_R$ |
| R | Figure 21 | Horizontal shear force on L-shaped corner veneer elements from the sum of the horizontal forces in the end wall brick-ties |
| T | Section 5.3.1 | Brickwork thickness = 0.07 m |
| Shear slip | Table 4 | Name used in plots corresponding to $\Delta_{shear}$ |
| SW | Figure 20 | Brick veneer pier self-weight = $\rho$LH |
| Tie j | - | A typical tie called Tie j |
| TieDefXj | Eqn. 4 | Horizontal deformation of Tie j |
| TieDefYj | Eqn. 5 | Vertical deformation of Tie j |
| trapezoidal assumption | Figure 19(a) | LTF wall deflects in a trapezoidal shape with no stud bending. |
| TXj | Figure 20 | Horizontal distance between pivoting end of brick pier and brick-tie J |
| TYj | Figure 19 | Height of Tie j above bottom of the veneer |
| W1 | Figure 21 | Weight of wall length L2 = $\rho$ x L2 x H2 |
| W2 | Figure 21 | Weight of the return wall = $\rho$ x (L1 – T) x H2 |
| $\Delta_{Brick\ at\ j}$ | Section 5.2.2 | Horizontal movement of the brickwork at Tie j |
| $\Delta_{LTF\ at\ j}$ | Section 5.2.1 | Deflection of the LTF wall at Tie j = DeltaX – $\Delta_{Stud\ at\ j}$ |
| $\Delta_{LTFtoBrick}$ | Section A.5.2 | Relative deflection between a LTF wall and the brick veneer at a brick-tie, deflection gauge or top of the brick wall |
| $\Delta_R$ | Section A.5.2 | Deflection of a point in a brick pier (brick-tie, deflection gauge or top of wall) due to pier rotation |
| $\Delta_{shear}$ | Eqn. 3 | Horizontal slip of brickwork on a crack |
| $\Delta_{Stud\ at\ gauge}$ | Section A.5.2 | In-plane deflection of a stud due to stud bending |
| $\Delta_{Stud\ at\ j}$ | Figure 19 | In-plane defection of the stud at Tie j due to deviation from trapezoidal assumption |
| $\mu$ | Section 5.2.3 | Friction coefficient along a crack line |
| $\phi$ | Section 6.2 | Strength reduction factor |
| $\theta$ | Figure 20 | Rotation of pier of brick by pivoting at one end |
| $\rho$ | Section 5.2.3, 5.3.1 | Brick veneer weight per unit area = 130 kg/m$^2$ |

# 1. INTRODUCTION

## 1.1 Historic performance and reasons for the study

The BRANZ building database shows that clay brick veneer is used in 37% of new buildings in New Zealand. Concrete brick veneer (as against masonry block) is used in a further 7% of buildings. Occasionally the brickwork is plastered to give a monolithic appearance. In 75% of new veneer construction, brick is used as the sole cladding material.

Historically brick veneer has performed poorly in earthquakes. Cracking, particularly at building corners, and partial collapse of the veneer have been common (Figure 1). There have been resulting concerns over the safety of veneer construction which are no longer likely to be relevant because significant changes have been made to the way brick veneer cladding is constructed.

**Figure 1. Examples of veneer damaged in the 1987 Edgecumbe earthquake**

Traditionally, the brick veneer has been assumed to be a driving element (mass) under earthquake loading and that the timber framing has been the load-resisting element. Currently NZS 3604 (SNZ 1999) assumes the brick veneer does not carry any in-plane load and it is a cladding element only, applying inertial load to the timber-framed bracing walls.

There is a basic deflection incompatibility between the stiff veneer and the relatively flexible timber-framed wall under in-plane loading which may lead to the development of damage in either in an earthquake. At the corners of a building there is likely to be a deflection incompatibility between the veneers in the two orthogonal directions which could lead to significant cracking if the in-plane strength was lost.

A complex inertial load transfer interaction is expected between the veneer and the timber frame because of the significant stiffness of the ties. The extent and effect of this load transfer was unknown before the commencement of the testing at BRANZ. The veneer ties were assumed to accommodate expected deflections between the framing and the veneer and the ties were expected to transfer the inertial forces from the face-loaded veneer panels to the timber framing. However, in modern veneer construction, the pick-up of load by the veneer may indeed assist the overall performance of the building in an earthquake by reducing the displacement of the frame. On the other hand, it may also result in damage to the brick veneer.

The study is intended to improve the understanding of brick veneer construction in earthquakes, in particular:

- To determine if brick veneer can be relied upon to carry most of the building seismic load or whether the building light timber-framed (LTF) construction should be designed to carry the entire load.
- To identify the damage that can be expected in modern brick veneer construction.

## 1.2 Changes in veneer construction materials

Brick veneer has historically consisted of solid clay or concrete bricks, possibly with frogs (indentions) in their top surfaces. These bricks were generally between 90 and 100 mm thick. The method of securing the veneer to the supporting timber framing was with a length of 8g wire ("No. 8" wire) bent into a figure eight form. One end of the tie was buried in the fresh mortar and the other was fixed with fence staples to the framing. No account was taken of the presence of water in the cavity between the veneer and the framing. Mortar droppings often accumulated on the tops of the ties during construction of the veneer and the water draining down the back of the veneer kept the mortar wet. This was a recipe for corrosion of the wire tie to occur. When an earthquake struck houses constructed with this method of attachment, many of these veneers fell away from the framing because of a failure of the connection (either because of rotted ties or because the staples pulled from the mortar) (Figure 1).

In the last 20 years, lighter weight clay bricks have been available. These are typically 70 mm thick and have vertical penetrations along their length, which allows the fresh mortar to form a mechanical interlock with the bricks. Flat "L-shaped" ties were developed that were laid on the brick and covered with mortar. The timber framing end of the tie was nail-fixed to the adjacent face of the timber.

## 1.3 New Zealand building standards

Since the early 1990s changes have been instigated to improve the seismic performance of brick veneer, particularly under face-loading. Shelton (1996) investigated the face-load resistance of brick veneer ties and determined that for satisfactory out-of-plane performance of the veneer it was necessary to screw-fix the ties to the timber framing. This new requirement was incorporated in the construction requirements for brick veneers in NZS 4210:2001 (SNZ 2001). This Standard includes a requirement that the ties are to be screw-fixed to the studs and that the tie-to-brick joints have sufficient strength and stiffness. It also requires the ties to be fully encapsulated in the mortar. There is therefore a mix of prescriptive and performance requirements included in the Standard. It has since been found that ties may be dry-bedded and still satisfy the performance requirements of the Standard for ties under face-loading (Beattie 2006). No requirements are contained in the New Zealand Standards for the in-plane performance of the ties. AS/NZS 2699.1 (SA/SNZ 2000) provides a test procedure to establish the rating of the veneer ties in terms of their axial stiffness and strength. The test method notes that when cycling the ties horizontally in the wall plane direction, "designers may find the loads resisted and stiffness encountered during this regime useful", and it suggests that manufacturers collect this information. However, this has not generally been done by any testing agencies.

## 1.4 Previous investigations

Literature searches have shown that little work has been done either in New Zealand or overseas to understand the in-plane performance of the combination of veneer and framing, particularly at wall corners (Beattie 2006). Beattie found that research had been undertaken on the in-plane performance of veneers by Lapish and Allen in the late 1980s (Lapish 1991, Allen and Lapish undated). Lapish noted that "because of the rigid, brittle nature of unreinforced masonry veneers and the limited ductile nature of reinforced veneers, the in-plane seismic design loads generated within the mass of the veneer must be at a high level to assume full or near-elastic response to the earthquake forces". The report went on to state that the veneer must have a separation from the flexible seismic load-resisting structure to prevent altering the intended seismic response.

Allen and Lapish described full-scale in-plane racking tests. The panels were approximately 2.4 m high by 2.4 m long. Load was applied to the top plate of the timber-framed wall and, during the tests, the veneer panel was observed to lift off the foundation as it was pulled by the ties connecting it to the timber frame (similar behaviour was observed in research undertaken by Beattie (2003)). No distress was observed in the brickwork. Allen and Lapish concluded that:

1. The brick panels of these dimensions were able to sustain lateral deflections up to ±25 mm without any real damage to the face-fixing capacity of the stiff strip metal ties and the brick panel rocked in concert with the racked framing.
2. The design of timber-framed buildings with stiff wall tie anchorage into brick veneers should take account of higher earthquake loads than for those situations where the veneer connectors do not materially influence the racking capability of the timber-framed walls.
3. Conventional stiff masonry ties should be used only where veneers are designed and detailed into individual panels which are free to rock as units under lateral loads.
4. Stiff brick veneer ties should be ductile.

Johnson and McGinley (2003) conducted in-plane shear tests on small (900 x 600 mm) veneer panels connected to timber stud wall sections with corrugated metal ties. The tests were monotonic. In their introduction they note that the 2000 International Residential Code (ICBO 2000) restricts the height of masonry veneer that can be used in higher seismic zones to one-storey structures. They note that "there may be a substantial in-plane shear transfer between the wood frame and the brick veneer…" resulting in the participation of the veneer in the lateral load-resisting system. They go on to show that there is sufficient strength to resist significant wind loads but there is no mention of cyclic response in earthquakes. While the authors refer to whole house testing in Australia and Japan, their reference list does not include relevant papers from either of these countries.

Choi and LaFave (2004) carried out cyclic in-plane tests on brick couplets fixed to timber stud members with 22g, 28g and 16g corrugated metal ties. The ties were nailed into the stud elements. Strengths were reported for the three gauges of metal but little information was provided on the large displacement performance.

Heath et al (2006) conducted in-plane shear tests on brick veneer panels 3 m long by 2.4 m high with an included window opening. Because they were interested in the development of cracks in the veneer due to underground blasting, they carried out a monotonic racking test in accordance with ASTM standard E72 (2005) after cutting a significant proportion of the ties joining the veneer to the framing. In-plane load was applied directly to the top of the veneer and the end of the veneer was restrained vertically. Cracks were observed to develop at the corners of the window opening. These began to form at a top displacement of 12 mm and continued to form up to 30 mm. However, because there was no interest in interaction between the veneer and the framing, no comment was made on this in the paper.

Heath et al (2008) undertook shake table testing on a 2.6 x 2.8 m room with brick veneer cladding to simulate ground vibrations from blasting. The specimen included window and door openings but the veneer panels on the four sides were not connected together at the corners. While the development of cracking in the individual panels was closely monitored as the excitation was increased, there was no cracking at the corners related to interaction of the face-loaded and in-plane loaded veneer elements.

While the aim has been to maintain the link between the veneer and the frame under face-loading, the effectiveness of these measures had not been proven in any reasonable scale investigations.

## 1.5 BRANZ investigations

BRANZ undertook an investigation to determine the in-plane shear strength of two brick ties typically used in New Zealand (Beattie 2007). The results of these tests showed that there was both a significant transfer of in-plane forces between the timber frame and the veneer and that the veneer ties were able to accommodate large differential in-plane displacements between the veneer and the framing while transferring this load.

## 1.6 Investigations in USA

Through email contacts (Shing, personal communication), BRANZ is aware of a research programme being undertaken in the USA by a consortium of four universities and industry organisations. The programme is concerned with the performance of reinforced masonry walls, but a part is concerned with the seismic performance of brick veneer attached to timber framing with American-style ties. These ties are considerably weaker and less flexible than those used in New Zealand. A one-directional shake table test is planned on a 6 x 6 m single-storey structure in January 2009.

## 1.7 New Zealand brick veneer construction

A typical modern clay brick veneer house is shown in Figure 2. It comprises bricks of usual size 220-260 mm long x 80-90 mm high x 70-90 mm wide with brick-ties mortared into the brickwork at every third or fourth brick course. The other ends of the brick-ties are screwed to timber studs. The veneer is penetrated by windows and doors. Usually no brickwork is used above these openings and instead it is framed out and sheathed with lightweight cladding as shown in Figure 3. This is the construction simulated in the tests described in this report. Brickwork lintels above the windows, similar to that shown in Figure 4, are less common.

The column of brickwork between the veneer window openings is referred to as "piers" in this report. Isolated brick veneer walls which are completely separated from other brickwork are referred to as "isolated veneer panels". The brickwork on both sides of a corner tends to act as a single unit and is referred to as an "L-shaped corner veneer element".

Occasionally the brickwork is penetrated by full wall height windows, as shown in Figure 5. Such isolated veneer panels are expected to result in a significantly different seismic behaviour as these panels are free to slide at the base, as discussed in Section 4. Sometimes large windows commence one block above the concrete foundation, shown in Figure 6, and these may also demonstrate some base slip.

Veneers formed using concrete blocks of usual size 240-400 mm long x 100-200 mm high x 70-100 mm wide, as shown in Figure 6 and Figure 7, are also common in New Zealand. These do not have the good shear bond characteristics of the typical modern clay-bricks shown in Figure 10, and are not expected to perform as well in an earthquake.  Expansion joints, such as shown in Figure 8, will also influence seismic performance, creating a weakness in the veneer.

Most brick veneer houses in New Zealand are single-storey. However, two-storey veneer (Figure 9) and concrete brick veneer is becoming more common. Some houses are almost entirely clad with masonry veneer while others often have it only in small areas.

**Figure 2. Typical brick veneer house**

**Figure 3. Lightweight cladding infill is usually used above windows in New Zealand**

**Figure 4. Brickwork lintels**

**Figure 5. Full height windows resulting in isolated veneer panels**

**Figure 6. Large window heights and veneer**

**Figure 7. Concrete block veneer showing a tie**

**Figure 8. Expansion joints used in concrete veneer**

**Figure 9. Two-storey brick veneer**

## 1.8 Bricks, brick-ties and mortar used in the testing

Details of the brick construction used in the tests described in the appendices are given below. The choice of these products is expected to have a significant influence on the test results. Further tests are required before general applicability can be determined.

The average strength of the standard cured 28 day mortar was 20.2 MPa (see Appendix C) which is 62% more than the 12.5 MPa minimum strength specified by NZS 4210.

The MonierBricks brand clay bricks used had dimensions 230 mm long x 76 high x 70 mm wide. When assembled using the standard 10 mm of mortar between bricks, the veneer weighs approximately 130 kg/m$^2$.

The bricks used had five vertical holes, of cross-section 32 x 23 mm, for the full brick depth which partially filled with mortar, as shown in Figure 10.

The bricks were laid by tradesmen using Dricon Trade Mortar with approximately 10 mm thick mortar being used between the bricks on both horizontal and vertical surfaces. This mortar was stated to comply with NZS 4210 (SNZ, 2001) for masonry construction.

Hot-dipped galvanised steel, 85 mm long, 70 series, Eagle brand brick-ties were dry-bedded onto the bricks rather than being fully encapsulated within the mortar. The ties were stated to be rated “heavy earthquake to NZS 3604:1999 and the draft AS/NZS 2699 Standards”.

Ties were secured to the face of the timber studs using galvanised, self-drilling, 35 mm long, Tek screws which are supplied with the ties.

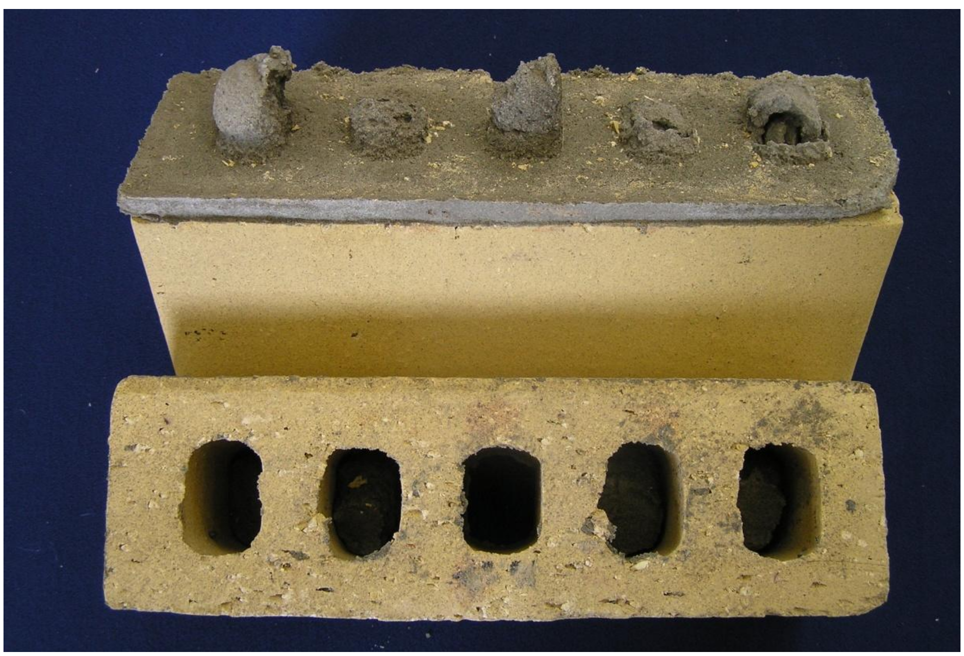

**Figure 10. Holes in bricks - mortar formed dowels linking bricks**

## 1.9 Limitations of this study

Many (particularly older) houses only used brick veneer on the front façade for economy. Modern houses sometimes use a mixture of brick veneer and other claddings for architectural reasons. This report only considers houses with brick veneer around the complete house perimeter.

In the tests described herein, slow cyclic displacements were imposed on room ceilings and the load transferred to the brick veneer was measured. There was no real time shaking performed. Thus, the testing performed did not simulate the out-of-plane inertia forces on the brick veneer and the ability of the brick-ties to transfer this load to the LTF construction was therefore not tested. The AS/NZS 2699.1:2000 brick-tie tests are intended to ensure the brick-ties are adequately strong in their axial direction. It is possible that out-of-plane inertia forces may induce vertical cracking at the veneer corners which would separate the veneer sides from the ends.

## 1.10 Outline of test report

Section 2 summarises the results of slow cyclic testing of a 6.7 x 3.9 m timber-framed room, with ceiling and brick veneer cladding. This testing is described in greater detail in Appendix A. The construction incorporated windows and door openings. The brickwork cracking pattern, the load carried by the veneer and various deflections were monitored.

Section 3 summarises the results of the slow cyclic testing of a second similar timber-framed room but in this instance the brick veneer cladding only consisted of isolated 4.8 m and 3.2 m veneer panels loaded in-plane and an L-shaped corner veneer element.

Section 4 uses the observations of the testing described above to describe the racking behaviour and cracking mechanisms qualitatively.

Section 5 calls on the behaviour described in Section 4 to develop a computer model of brick veneer behaviour under lateral load from which the relationship between LTF wall deflection and load carried by the veneer can be determined. To achieve this, it uses the measured brick-tie stiffness characteristics given in Appendix D. Plots that can be used in house design, developed using the model, are presented in Figure 26.

Section 7 compares the measured test results with the predictions from Section 5 to help validate the theory.

Conclusions and recommendations are given in Section 8.

Appendix A describes in detail the slow cyclic testing of the first room.

Appendix B describes in detail the slow cyclic testing of the second room.

Appendix C describes the measurement of the brickwork mortar bond strength in both shear and tension and in both brick-to-brick and brick-to-foundation concrete. Some test specimens incorporated the Mulseal™ surface on the foundation slab as stipulated in NZS 3604.

Appendix D describes the determination of brick-tie load versus relative movement between LTF and veneer.

# 2. CYCLIC TESTING OF ROOM 1

Appendix A provides the details of the racking tests on Room 1. This was a single-storey nominally 2.4 m high room shown in Figure 11 which incorporated windows and a door. It had plasterboard-lined LTF walls, a timber-framed plasterboard-lined ceiling and brick veneer on all four sides. The outside plan dimensions of the room were 6.73 x 3.93 m.

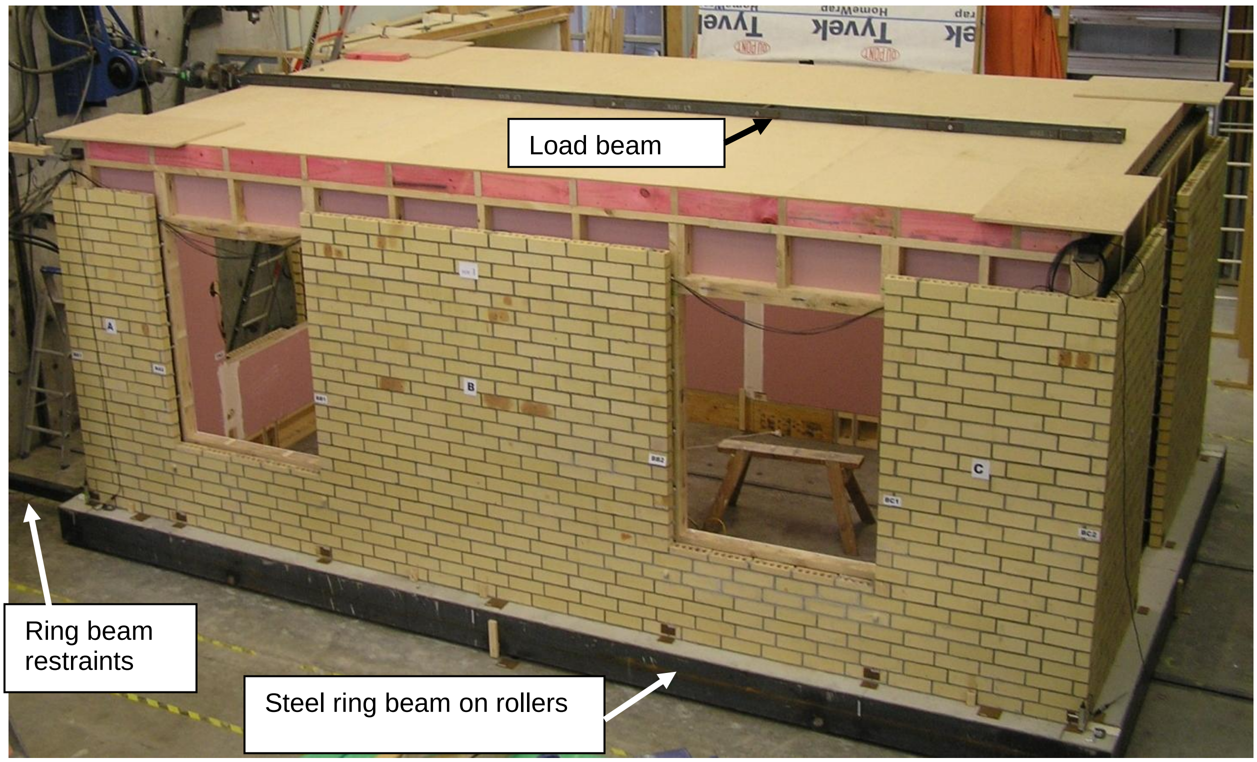


**Figure 11. Photograph of Room 1 before testing**

The brick veneer was constructed on a steel ring beam with concrete infill which was supported on rollers. An arrow in Figure 11 points to this ring beam. Appendix A explains how this enabled the force in the brick veneer to be measured using the ring beam restraints. In Stage I of the testing no windows were installed in the openings.

The LTF ceiling was horizontally displaced using an actuator which moved a load beam connected to the ceiling as shown in Figure 11. In Stage II of the testing, three aluminium windows were installed in side wall openings. The windows were fitted into the timber-framed walls so that they extended out into the plane of the veneer. Any relative movement between the brickwork and the LTF walls required the window framing to deform. This was observed to occur by distortion of the window frames into a trapezoidal shape and rotation of the glazing within the window frames. No window damage or glass breakage was observed.

Stage III involved adding timber framing acting as a packer above window and doorway openings. This simulated the construction shown in Figure 3.

Hysteresis loops of the measured horizontal load carried by the brick veneer versus ceiling displacement are given in Figure 27. The resisted load had levelled off at ±16 mm LTF wall deflection for construction without windows. This was because all veneer elements above cracks were “rocking” about crack corners. Thus, the lateral strength was largely limited by the panel widths and weights. In Stage II peak loads increased by 23% at ±24 mm LTF wall deflection. Stage III peak loads were 45% greater than Stage I.

The cracks tended to form at the bottom of the window level as shown in Figure 12 and the veneer piers above rotated on these cracks as shown in Figure 17. Near doorways these cracks formed at the bottom course of mortar of the brickwork. No shear slip occurred along the cracks.

No cracks occurred at the base of the Room 1 veneer except for a small length of Panel G (Figure 51 to Figure 53). As the total length of brickwork (including the end walls) was 13.5 m, and the brick-to-concrete foundation interface strength was measured at 409 kPa (see Table 6), the predicted total bond strength between brickwork and concrete foundation = 13.5 x 0.07 x 409 = 387 kN which is far greater than the applied loads shown in Figure 27. So it is not surprising that no brick veneer base slip was observed in Room 1. The slip observed in Panels A and B of Room 2 is expected to be because the bond was ruptured by rocking before the slip occurred. No brick-to-brick slip occurred along crack lines in either room. It is expected that once the bond had been ruptured by rocking the mechanical action of the dowels resisted any slip.

Timber stud weak axis (in the wall plane direction) bending deflections are of significance in that they result in a lesser differential displacement (hence lesser load transfer) between the LTF and veneer. Stud flexural bending deflections in the LTF walls adjacent to two 2.4 m long brick piers between windows, were not significant for LTF deflections less than 24 mm. Subsequently, the lining became ineffective and large stud bending deflections occurred at stud mid-height.

Generally, the magnitude of the timber stud flexural deformation and differential movement between brick veneer and LTF was very low for the L-shaped corner veneer elements at all LTF deflections, showing that almost the entire movement of this veneer was due to rocking of each L-shaped corner as a single unit, as shown in Figure 16.

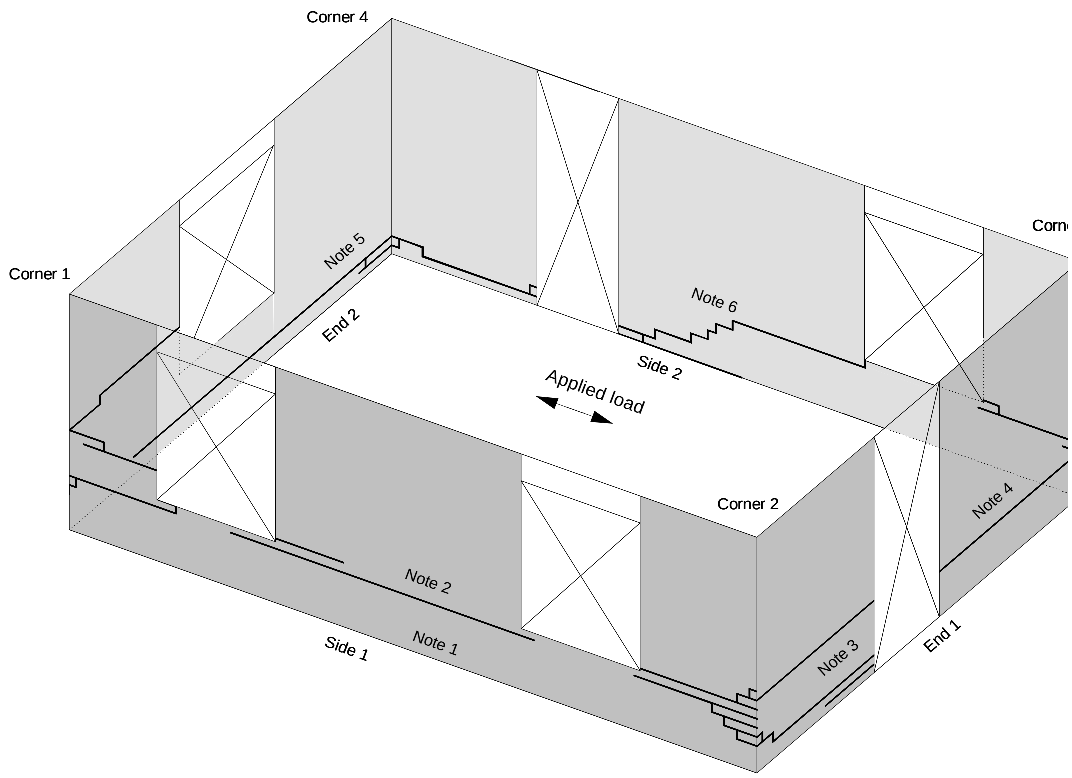


| Note number | Explanation |
|---|---|
| Note 1 | No cracks or in-plane shear slip occurred at junction between the base of brickwork and concrete foundation beneath the side walls. It is expected that the end brick walls prevented this movement. The reason is that the end walls were forced to move in the out-of-plane direction by the same amount as the end LTF walls as they were interconnected by brick ties which were stiff in this direction. The base of the end LTF walls did not move in the out-of-plane direction. Thus, the base of the end brick veneer walls also did not move. No vertical cracks occurred in the brick veneer corners. Thus, the side brick veneer did not slip in the direction of the load at the base. |
| Note 2 | Cracks occurred early along horizontal brickwork mortar courses at approximately the level of the base of the windows due to the flexural in-plane moment on the pier above. The pier subsequently rocked about the crack line from the imposed cyclic loading. No shear slip occurred along the crack probably because the bricks had holes on top and bottom faces into which the mortar had penetrated during placement. These effectively formed a series of small dowels which resisted sliding along the crack line. |
| Note 3 | The brickwork on the end walls was forced to deform the same as the LTF walls in the out-of-plane direction due to the presence of the brick ties which were stiff in this direction. Thus, there was a tendency for the end walls to form a crack near the base of the walls and rock about this crack. However, the brickwork between openings in the side and end walls tended to act as a unit at a corner and this resulted in cracks in the end walls forming at the level of the bottom of the side wall window opening as the corner unit rocked as a single body under the applied loading. |
| Note 4 | Corner element rocked about at crack at the level of the bottom of the window. |
| Note 5 | Corner element rocked about at crack at the level of the bottom of the door. |
| Note 6 | Crack stepped down from bottom of window to bottom of door. |

**Figure 12. Measured cracking in Room 1 and explanation**

# 3. CYCLIC TESTING OF ROOM 2

Appendix B summarises the racking tests on a single-storey nominally 2.4 m high room called Room 2. It had plasterboard-lined LTF walls and a timber-framed plasterboard-lined ceiling. There were three isolated brick veneer elements, as shown in Figure 13 to Figure 15. These were:

- An isolated 4.8 m long veneer panel, called Panel A, on Side 1.
- An isolated 3.2 m long veneer panel, called Panel B, on Side 2.
- An L-shaped corner veneer element with a 1.43 m length on Side 2, called Panel C, and a 0.86 m length on End 1 called Panel D.

Panel A (see Figure 13 and Figure 14) deformed by sliding on a crack in the mortar at the junction of the brick veneer and the foundation concrete. The panel exhibited almost zero rotation. The ratio of lateral load during panel slip to panel weight gave an effective slip coefficient of friction of 0.63. Up to 16 mm LTF displacement the brickwork ties accommodated most of the movement. Subsequent slip of the brickwork on the concrete foundation almost equalled the additional LTF deflections.

Panel B deformed by sliding on a crack between the brick veneer and foundation concrete but also had significant rotation. Otherwise the monitored movements were similar to Panel A.

Stud flexural deflection was not significant near the top of the LTF walls next to Panel A and B. At mid-height of the panels stud flexural deflection only became significant for LTF deflections exceeding 24 mm, when the lining became ineffective.

With the L-shaped corner veneer element, cracks occurred in the mortar course one brick above the intersection of the brickwork and concrete foundation. There was only a small amount of shear slip on this crack. The horizontal differential displacement between the LTF wall and adjacent veneer was also small. This was expected as the connection between the end brick veneer and LTF walls would have resisted such movement. Stud bending in the LTF wall next to Panel C was also small.

Calculations showed that the cracking resistance due to brickwork to mortar tension bond, $f_{mt}$, was negligible. Also the cracking resistance due to mortar shear bond between brick veneer and concrete foundation, $f_{mv}$, was small.

In summary, as there were no windows in Room 2, a single crack formed at the base of the veneers and the isolated veneer panels above the crack either slipped or rotated on these cracks.

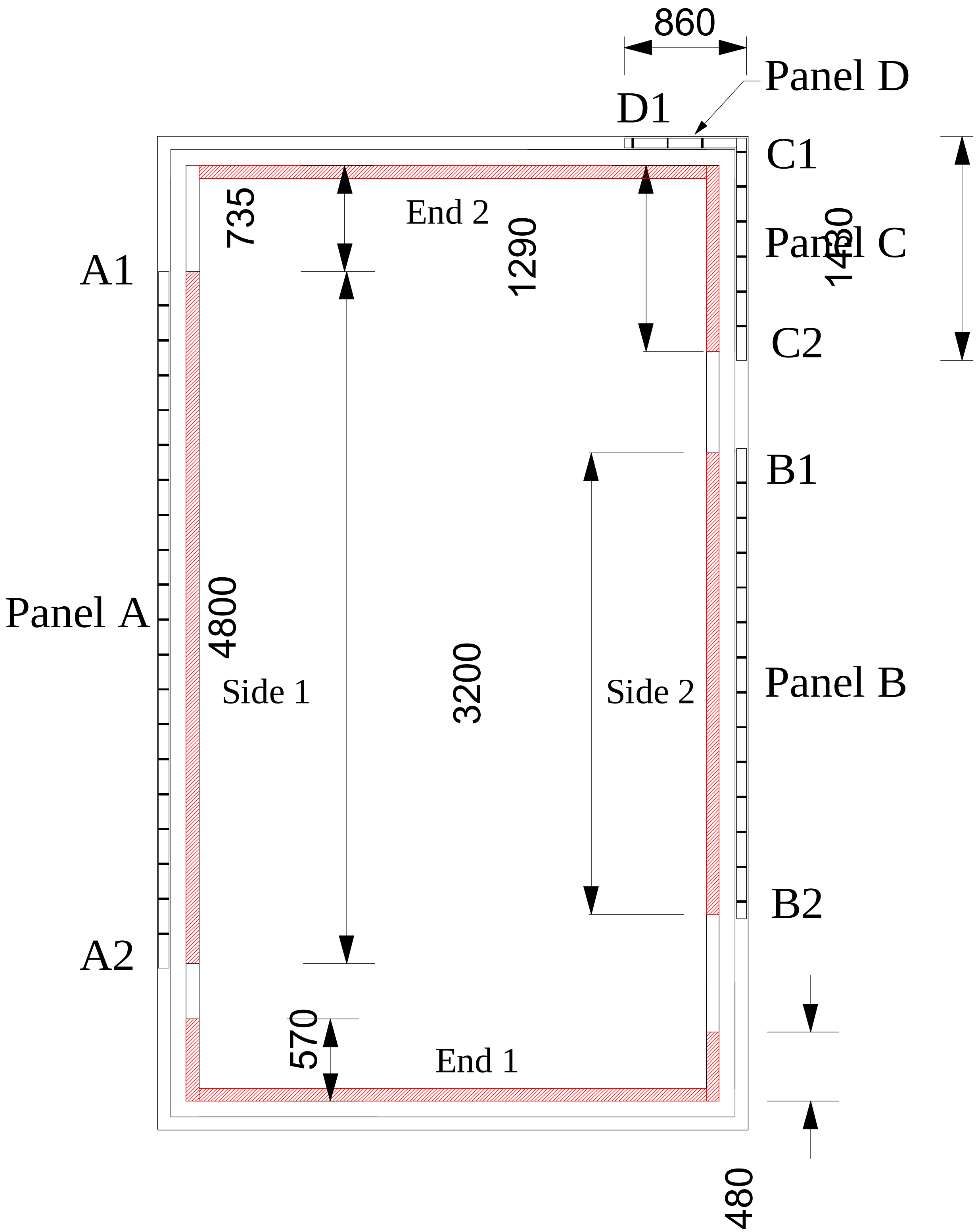


**Figure 13. Plan view of Room 2**


**Figure 14. Room 2 - Panel A on Side 1 before testing**


**Figure 15. Room 2 - Panel B and C on Side 2 before testing**

# 4. BRICK VENEER MOVEMENT AND CRACK PATTERNS IN EARTHQUAKES

## 4.1 Introduction

This section gives a general discussion of brickwork cracking and load sharing between LTF and veneer walls based on the observations in the tests summarised in Sections 2 and 3. This generalised behaviour forms the basis for the development of the computer model of brick veneer performance in earthquakes given in Section 5.

## 4.2 Veneer cracking and deformation

A sheathed LTF wall deforms in a trapezoidal shape under lateral racking load, as shown in Figure 16. In the Room 1 tests, described in Appendix A, it was found that the brick veneer deformed as shown in Figure 17. Figure 17 labels the veneer panels or piers from 1 to 10. The L-shaped corner veneer elements responded as a single unit (i.e. no vertical cracks occurred in the corners). This behaviour is generalised below using the “Note numbers” depicted in Figure 17 for reference:

*Note 1*. The brick-ties between the end wall of the room and the brick veneer are not expected to buckle or fail in tension. Hence, the brick veneer in the end wall will be forced to follow the out-of-plane room deformation of the adjacent LTF wall. Thus, Panels 1 and 10 will act as a unit to rock as shown. Panels 8 and 9 will do likewise.

As Panels 1 and 8 will have the same horizontal deflection as the LTF walls, there will be no horizontal deformation of, and hence no in-plane load in, the brick-ties in these panels. Further, if the corners stay intact, and the end brickwork does not move relative to the LTF wall, Panels 1 and 8 will not slip horizontally along the base crack lines in the direction of the load.

The brickwork at End 1 will crack at the level of the bottom of the windows and could additionally crack at the bottom of the wall from the out-of-plane movement (although this additional cracking was not observed in the Room 1 test).

*Note 2*. Similar behaviour is expected except the cracking will be near the bottom of the brick veneer as the nearest opening in the side walls is a door rather than a window. Panels 3 and 4 (and also Panels 5 and 6) will rock about the bottom of the brickwork.

*Note 3*. The piers will rock about a line joining the bottom of the adjacent openings – in this case a window and door. As the brick-ties must transfer the force to make the piers rock the brick-ties must have horizontal deformation and thus there will be significant differential movement between veneer and LTF wall. Hence, the rocking deflection of the pier will be less than the LTF deflection.

No slip is expected along the crack line for construction using bricks with holes as the mortar will penetrate into the holes to act as dowels. (In contrast to this, in Room 2, where the panels were fully isolated, both rotation and slip occurred in a single crack at the bottom of the brickwork, as mortar dowel action was not present at this junction.)

## 4.3 Recommended assumptions regarding mortar bond strength to use in design

The L-shaped corner veneer elements shown in Figure 17 cracked at low LTF wall deflections as the brick-tie connection between the end veneer and adjacent LTF wall forced the veneer to rock as shown. Hence, earthquake loading at 45º to a building main axis will cause all brick veneer to crack at low LTF wall deflections as all veneer walls will experience out-of-plane rocking. Thus, shear and tension bond strength along the crack lines shown in Figure 17 should be assumed to be zero (i.e. $f_{mt}$ and $f_{mv}$ = 0). However, mortar dowel interlock shown in Figure 10 is expected to prevent shear slip along brick-to-brick mortar cracks. The test evidence was that in the BRANZ lateral load tests described in this report, brickwork did not slide along horizontal mortar cracks between bricks but an isolated veneer panel did slide on cracks in the mortar course at the junction of the brickwork and the foundation concrete where mortar dowels did not occur.

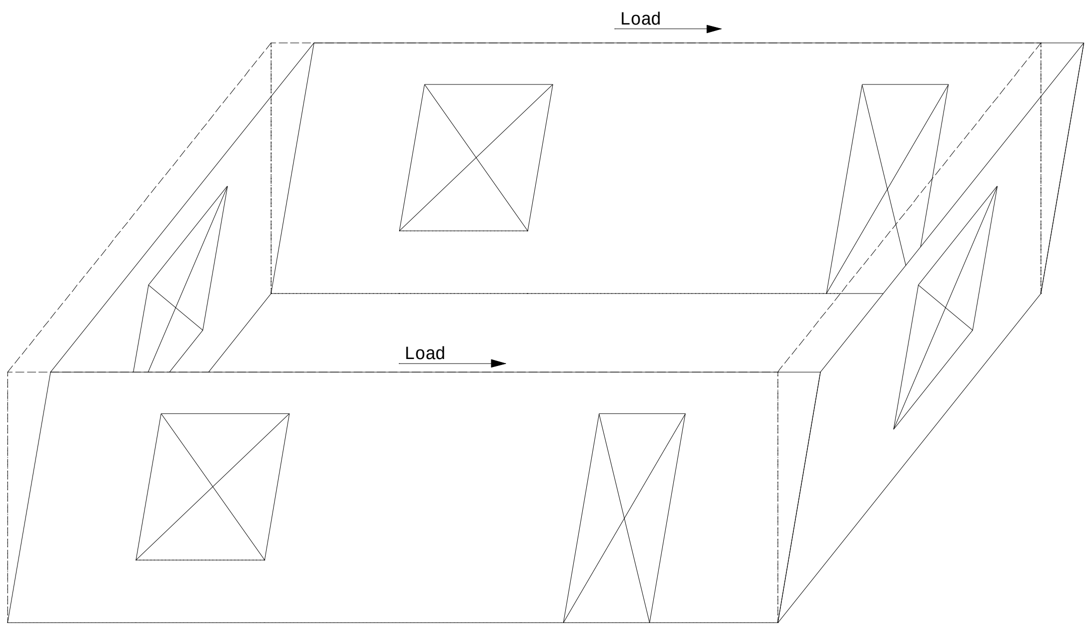


**Figure 16. Deformation of LTF room under lateral load**

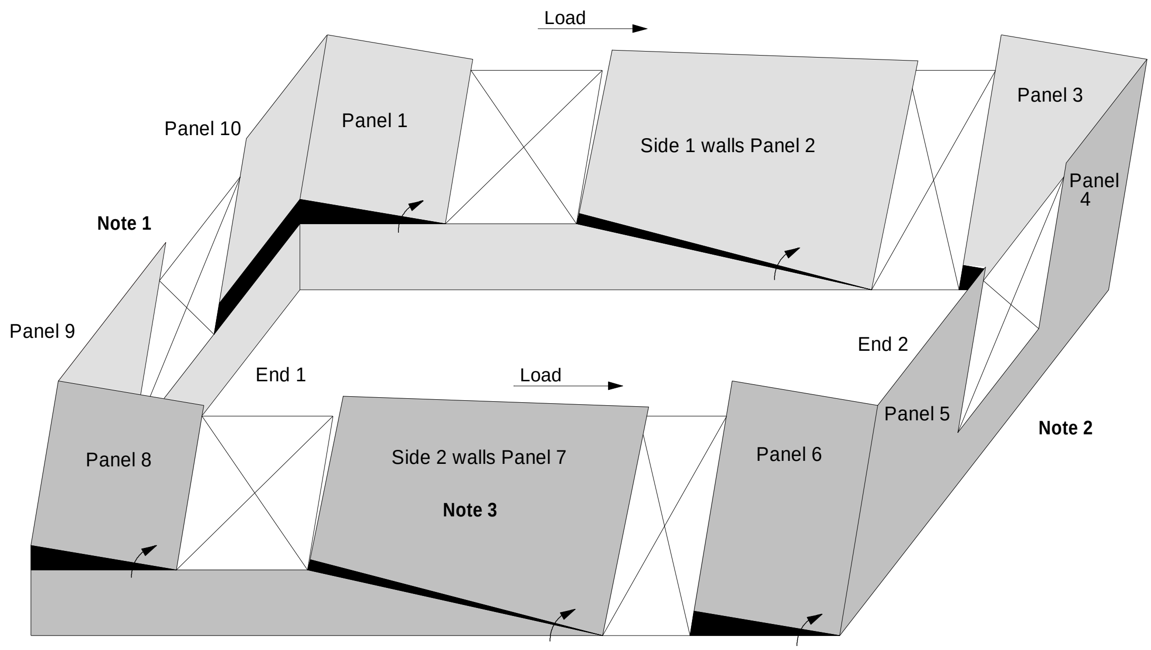


**Figure 17. Expected cracking and deformation mechanisms of brick veneer**

# 5. COMPUTER MODEL OF BRICK VENEER PIERS

## 5.1 Qualitative description of brick-tie deformations and forces

Figure 18(a) shows the in-plane deformation of brick-ties relative to the timber frame assuming the brick pier does not slide at the base but rotates on a crack at the base of the wall as shown in Figure 20. It also assumes that the LTF wall deforms in a trapezoidal shape, with no stud bending, no member separation and no rocking or uplift of the LTF wall itself.

With these assumptions:

- The LTF wall deflection varies linearly from maximum at the top to zero at the bottom.
- The horizontal tie deformation equals the LTF wall deflection at the tie height less the deflection attributable to rotation of the pier.
- Using the notation of Figure 20, the vertical deformation of Tie j = $\theta$ x TXj ( i.e. will vary linearly with horizontal distance from the pivot and will thus be the same magnitude up each stud as shown in Figure 18(a)).
- The force in the brick-ties depends on the vector sum of the horizontal and vertical deformations factored by the stiffness of the ties at that angle.
- The brick-tie force on the brick veneer is equal and opposite to the brick-tie force on the timber frame.

Figure 18(b) shows the in-plane deformation of brick-ties relative to the timber frame assuming the brick pier slides along a base crack rather than rotating. Near the bottom of the LTF wall (where the LTF wall horizontal deflection is close to zero), the tie horizontal deformation is shown to equal veneer slip which is in the reverse direction of the tie deformations further up the stud.

Stud bending, member separation and rocking or uplift of the LTF wall itself will affect the brick-tie forces and make the analysis more complex.

The tests and analysis in this report attempt to identify the importance of these parameters to allow a brick veneer seismic analysis to be performed.

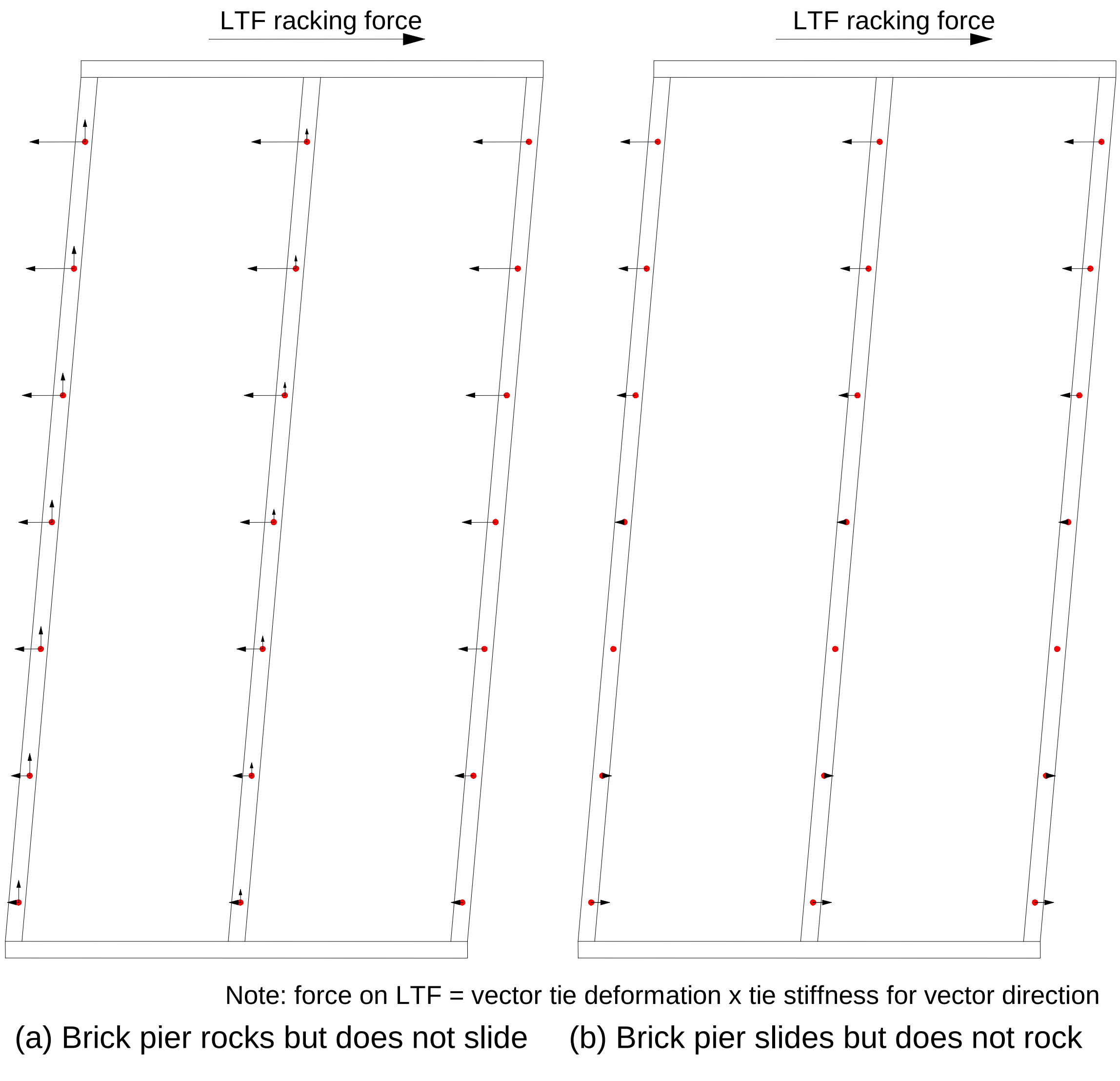


**Figure 18. Deformation of brick-ties relative to timber frame**

## 5.2 Theory for in-plane load carried by a brick pier

### 5.2.1 Deflection of LTF wall at brick Tie j

Consider a LTF wall, of height LTFheight, which deforms in a trapezoidal shape with studs remaining straight as shown in Figure 19(a). In this figure it is assumed that the studs do not bend in the wall in-plane direction and there is no slip between stud ends and adjacent timber plates. If the LTF wall has a top deflection of LTFdef then the horizontal deflection, DeltaX, of the LTF stud at Tie j (assumed to be at height TYj), based on this trapezoidal assumption, is given by:

$$\text{DeltaX} = \text{LTFdef x (TYj/ LTFheight)} \quad \ldots \qquad (1)$$

If the linings do not hold the stud rigidly in the in-plane direction and the stud flexes, and/or if there is slip between stud ends and adjacent timber plates, such that the stud has moved a horizontal distance of $\Delta_{\text{Stud at j}}$ at Tie j from the trapezoidal assumption, then the corrected deflection of the LTF wall at Tie j is given by:

$$\Delta_{\text{LTF at j}} = \text{DeltaX} - \Delta_{\text{Stud at j}}$$

i.e., $$\Delta_{\text{LTF at j}} = \text{LTFdef x TYj/ LTFheight} - \Delta_{\text{Stud at j}} \quad \ldots\ldots\ldots. \qquad (2)$$

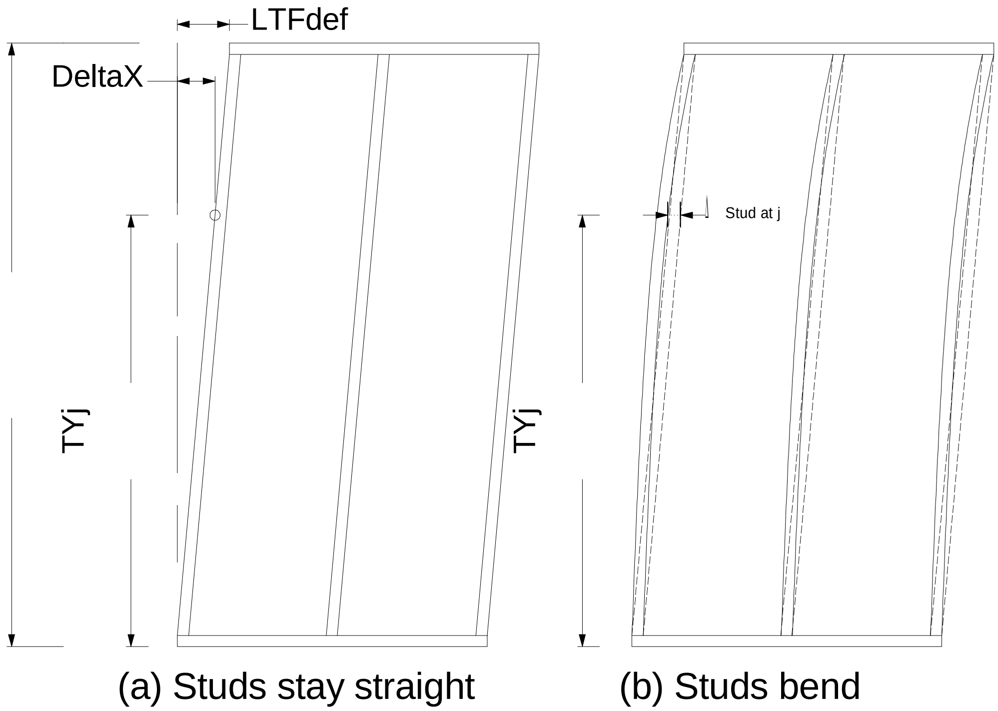


**Figure 19. Geometry for discussion of movement of LTF wall relative to brick veneer**

### 5.2.2 Relative deflection between LTF wall and brick veneer at brick-tie j

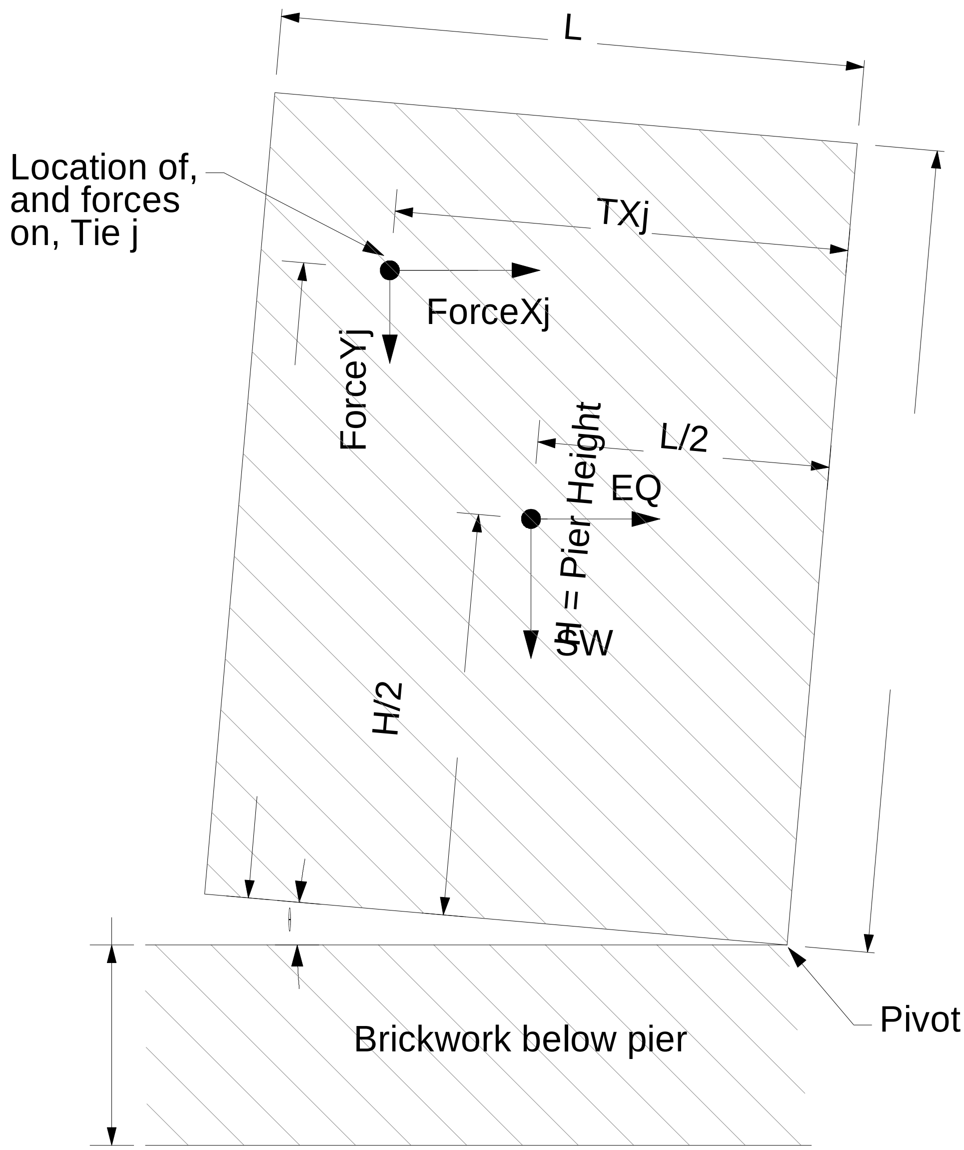


**Figure 20. Forces on a rocking brick pier**

Figure 20 shows the forces on a rocking pier of brick, of height H and length L, which has rotated by $\theta$ radians by pivoting at one end. The figure shows the location of Tie j, with coordinates TXj, TYj. The rotation occurs at a crack at height, CrackHeight, from the bottom of the veneer. The pier is assumed to have slipped by $\Delta_{shear}$ along the crack. Thus the horizontal movement of the brickwork at Tie j is given by:

$$\Delta_{Brick\ at\ j} = (TYj - CrackHeight) \times \theta + \Delta_{shear} \ldots \qquad (3)$$

It is assumed that there is negligible slip of the brick-ties in the mortar and slip of the ties at the screw interface with the timber stud. Hence, the differential deflection between the timber stud and brickwork at a brick-tie is the deformation of the tie. Thus, from Eqn.s 2 and 3, the horizontal deformation of the Tie j is given by:

$$\text{TieDefXj} = \text{LTFdef} \times \text{TYj} / \text{LTFheight} - \Delta_{\text{Stud at j}} - (\text{TYj} - \text{CrackHeight}) \times \theta - \Delta_{\text{shear}} \ldots (4)$$

Similarly, the upwards vertical deformation of the Tie j relative to the stud is given by:

$$\text{TieDefYj} = \text{TXj} \times \theta - \text{“Uplift of stud”} \ldots (5)$$

### 5.2.3 Forces on a brick veneer pier assuming studs remain straight

The value of $\Delta_{\text{Stud at j}}$ used in the above Eqns. is a function of the lining, stud connections and stud stiffness. While the lining is still firmly fixed to the studs this value is expected to be small and as the basic assumption for this section is that studs remain straight, it follows that $\Delta_{\text{Stud at j}} = 0$. For this case, Eqns. are derived below which enable the forces on, and rotation of, a brick pier to be found. However, at high LTF wall deflections, when the lining is semi-detached, this assumption is expected to lead to errors.

The value of the tie deformations TieDefXj and TieDefYXj can be determined from Eqns. (4) and (5) at each LTDfdef, if $\theta$, $\Delta_{\text{shear}}$ and “Uplift of stud” are known. Thus, with knowledge of the tie load versus deflection behaviour, detailed in Appendix D, then the corresponding horizontal and vertical forces on Tie j can be calculated. These are called ForceXj and ForceYj respectively.

As the LTF wall deflects horizontally further than the brick pier the force, ForceXj, in Figure 20 is shown as a driving force tending to open the crack. ForceYj resists this upward movement.

The “net bending moment”, $B_{net}$, of the forces about the pivot in Figure 20 is given by:

$$B_{net} = \text{EQ} \times H/2 - \text{SW} \times L/2 + \Sigma\text{ForceXj} \times \text{TYj} - \Sigma\text{ForceYj} \times \text{TXj} \ldots (6)$$

where:
$EQ = C_{EQ} \times \rho \times H \times L$
$C_{EQ}$ = the seismic lateral load coefficient
$\rho$ = the brick veneer weight per unit area in kN/m$^2$
$SW = \rho \times H \times L$

To induce a flexural crack at the base of a pier, $B_{net} = f_{mt} \times Z$

where:
Z = section modulus = $T \times L^2/6$

$f_{mt}$ = the brick-to-brick mortar flexural tensile bond strength
T = the brick width = 70 mm for 70 Series brick.

Provided $B_{net}$ from Eqn. (6) is less than the cracking moment and the applied shear force is insufficient to induce shear failure, then the section will remain uncracked and $\theta = 0$. The seismic load carried by the brick pier can be found directly for each LTF wall deflection (= $\Sigma$ForceXj + EQ).

If a crack has formed then the pier will slide on the crack surface until the shear friction balances the horizontal force and then it will rotate about the pivot in Figure 20 until the net moment on the pier is zero.

The net shear to induce cracking at the base of the pier = $f_{mv} \times T \times L + \mu \times \rho \times H \times L$

where:
$\mu$ = the friction coefficient along a crack line
$f_{mv}$ = the shear bond strength

A bending moment on the pier will concentrate the shear force near one end of the crack but, in theory, will not reduce the total shear resistance as the same axial load will be carried.

Based on test measurements this analysis assumes that no shear slip will occur along a horizontal mortar course for bricks with holes because of mortar dowel action.

A two stage incremental solution is used in the computer model:

(1) When the shear force in the brick veneer exceeds the shear friction + shear bond resistance for brickwork without holes, or when considering the brick-to-concrete foundation interface of isolated veneer panels, then this step must be actioned. For each LTF wall deflection, the slip deflection, $\Delta_{shear}$, is incremented along the crack until the shear friction balances the horizontal brick pier demand force given by EQ + $\Sigma$ForceXj.
(2) $\theta$ is incremented until $B_{net}$ from Eqn. (6) is zero.

## 5.3 Theory for horizontal load resistance of an L-shaped corner veneer element

### 5.3.1 Deflection of LTF wall at brick-tie j

The deformation of, and forces on, an L-shaped corner veneer element under lateral loading is shown in Figure 21. As discussed in Section 4, the presence of brick-ties on the end return walls prevents differential horizontal movement between the brick veneer and adjacent LTF side walls. Thus, Tie j shown in Figure 21 does not transfer a horizontal force between the brick veneer and LTF wall but it will transfer a vertical force, Force Yj, as the brick veneer lifts relative to the LTF wall.

By taking moments about the pivot at Corner 1 of Figure 21:

$$R \times H1 = W1 \times D + W2 \times L2/2 + \Sigma(\text{Force } Yj \times TXj) + f_{mt}Z \ldots \quad (7)$$

where:

R = the horizontal shear force on Panel E from the sum of the horizontal forces in the brick-ties joining Panel E to the LTF return wall

H1 = the height this resultant acts

H = the height of the brick veneer above the base crack

Force Yj = the vertical force on Tie j (including the return wall).

W1 = the weight of Panel S = $\rho$ x L2 x H2

W2 = the weight of Panel E = $\rho$ x L1 x H

$\rho$ = brick veneer weight per unit area ($\approx$ 130 kg/m$^2$ for 70 series brick veneer)

T = brickwork thickness = 0.07 m

D = T/2 for Corner 1 and (L2-T/2) for Corner 2

Z = section modulus of the "L-shaped" section

$f_{mt}$ = the brick-to-brick mortar flexural tensile bond strength

It is assumed that the end ties are strong enough to crack the veneer-to-concrete foundation bond at low LTF wall deflections and thus $f_{mt}$ is assumed to be zero. This is discussed further in Section 5.4. As it was observed in the tests that cracking at the base of the L-shaped corner veneer elements only occurred at approximately 5 mm LTF wall deflection, the value of R used for LTF deflections between zero and 5 mm was linearly interpolated between zero at zero LTF deflection and the value of R calculated from Eqn. (7) at 5 mm LTF wall deflection.

All values on the right-hand side of Eqn. (7) are known. The height H1 is not known and is difficult to determine theoretically. It was assumed to be 0.67 H, which enabled R to be determined.

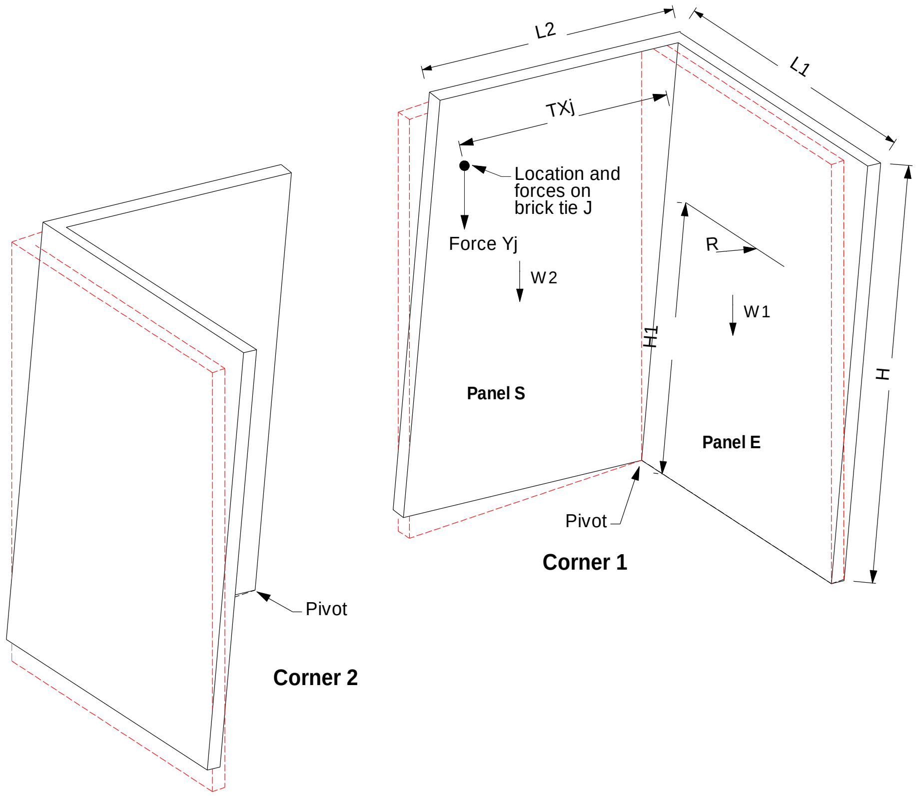


**Figure 21. Forces on, and deformation of, L-shaped corner veneer elements**

## 5.4 Geometry of L-shaped corner veneer elements for rocking to be initiated by end ties

The theory in Section 5.3 assumes the bending moment imposed on the veneer by the end ties is strong enough to crack the veneer-to-concrete foundation bond and to induce rocking of the L-shaped corner veneer elements at low LTF wall deflections. If L2 shown in Figure 21 is large and L1 is small, the number of end wall ties may be inadequate to achieve this and the LTF walls will need to deflect further for the ties to “drag” the veneer into rocking as described for the piers in Section 5.2. Even for this situation, sliding of the L-shaped corner veneer along the foundation is unlikely as it will be resisted by both friction between the brickwork and the foundation and the resistance of the end ties.

Consider a northerly direction LTF movement, as shown in Figure 22, to generate tension in the end wall ties. The veneer will tend to rock about the “heel”, denoted in Figure 22, and as illustrated in Corner 1 of Figure 21. For earthquake loads in the southerly direction the end wall ties will be in compression and the veneer will tend to rock about the “toe”, denoted in Figure 22, and as illustrated in Corner 2 of Figure 21.

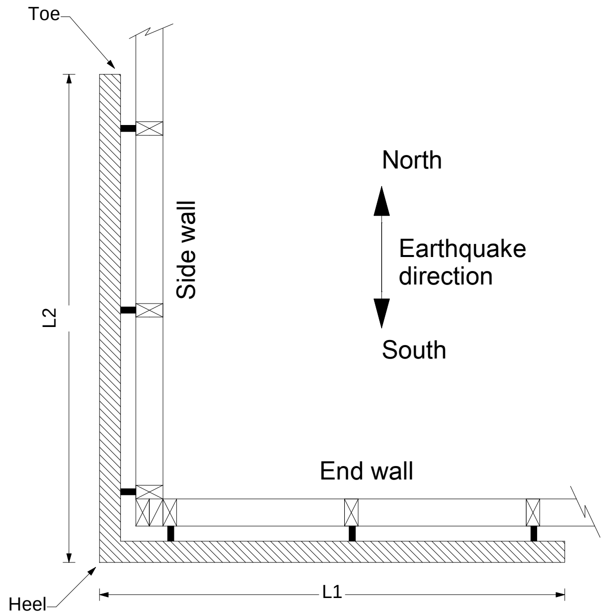


**Figure 22. Geometry of an L-shaped corner veneer element**

If the force in every end wall tie on the corner element shown in Figure 22 is $T_{axial}$ then the bending moment imposed on the veneer = $\Sigma$ $H_j$ x $T_{axial}$ where $H_j$ is the height of tie j above the base of the veneer. This can be used to replace R x H1 in Eqn. (7). The term Force Yj in this Eqn. can be set to zero as there is no upward veneer movement at low LTF deflection. Thus, Eqn. (7) can be re-expressed as:

$$\Sigma H_j \times T_{axial} = W1 \times D + W2 \times L2/2 + f_{mt}Z \qquad (8)$$

Table 1 was derived using Eqn. (8) and gives the length, L2, of side wall veneer that can theoretically be rocked by end wall ties for the case of $f_{mt}$ = 0 and $f_{mt}$ = 50 kPa. It uses the tie characteristic axial strengths defined in Table 2 of AS/NZS 2699.1 (SA/SNZ 2000). (Note that the measured direct tension (plucking) strength of brick from concrete given in Table 9 is 34 kPa.) It can be seen that generally the end wall ties will be adequate to induce rocking without any help from the side wall ties, particularly for the tension case, for stronger ties, where L1 is large, and where the brick-to-brick mortar flexural tensile bond strength, $f_{mt}$, is low.

**Table 1. Maximum length of side wall brick veneer that can be rocked by end wall ties**

$f_{mt}$ = 0 kPa

| No of columns of ties | L1 (mm) | Ties in tension | | | Ties in compression | | |
|---|---|---|---|---|---|---|---|
| | | Maximum L2 length in metres to rock veneer for tie strength in kN | | | | | |
| | | **0.5** | **0.75** | **1.5** | **0.5** | **0.75** | **1.5** |
| 1 | 255 | 1.72 | 2.10 | 2.97 | 1.54 | 1.93 | 2.80 |
| 2 | 855 | 2.43 | 2.97 | 4.20 | 1.78 | 2.30 | 3.50 |
| 3 | 1455 | 2.97 | 3.64 | 5.15 | 1.91 | 2.52 | 3.95 |
| 4 | 2055 | 3.43 | 4.20 | 5.94 | 2.00 | 2.68 | 4.29 |
| 5 | 2655 | 3.84 | 4.70 | 6.65 | 2.06 | 2.80 | 4.56 |
| 6 | 3255 | 4.20 | 5.15 | 7.28 | 2.11 | 2.89 | 4.78 |

$f_{mt}$ = 50 kPa

| No of columns of ties | L1 (mm) | Ties in tension | | | Ties in compression | | |
|---|---|---|---|---|---|---|---|
| | | Maximum L2 length in metres to rock veneer for tie strength in kN | | | | | |
| | | **0.5** | **0.75** | **1.5** | **0.5** | **0.75** | **1.5** |
| 1 | 255 | 1.21 | 1.71 | 2.44 | 1.19 | 1.52 | 2.24 |
| 2 | 855 | 1.62 | 2.36 | 3.37 | 1.25 | 1.67 | 2.64 |
| 3 | 1455 | 1.94 | 2.86 | 4.09 | 1.28 | 1.75 | 2.88 |
| 4 | 2055 | 2.20 | 3.28 | 4.69 | 1.29 | 1.79 | 3.04 |
| 5 | 2655 | 2.44 | 3.65 | 5.21 | 1.30 | 1.83 | 3.16 |
| 6 | 3255 | 2.65 | 3.98 | 5.69 | 1.31 | 1.85 | 3.25 |

# 6. COMPARISON OF LATERAL STRENGTH OF PIERS BETWEEN WINDOWS AND L-SHAPED CORNER VENEER ELEMENTS

A comparison of the predicted shear force resisted by brick piers and L-shaped corner veneer elements is given in Figure 23 for a 2.445 m long veneer panels, based on the software described in section 5. The L-shaped corner veneer elements was assumed to have equal length walls in the two directions. Plots are given for the corner return wall in tension as well as compression. Being in tension means that the return wall weight helps resist the overturning moment.

It can be seen that it is conservative to assume that the resistance of the L-shaped corner veneer elements equals that of a pier with a length the same as the corner element in the loaded direction.

There are two processes in action. The pier deflection will lag the deflection of the L-shaped corner veneer elements as the former has differential movement between veneer and LTF wall. However, as the ties yield, the height of the line of action drops in the pier theory whereas it remains at 0.67 times the panel height in the L-shaped corner veneer element theory of Section 5.3.

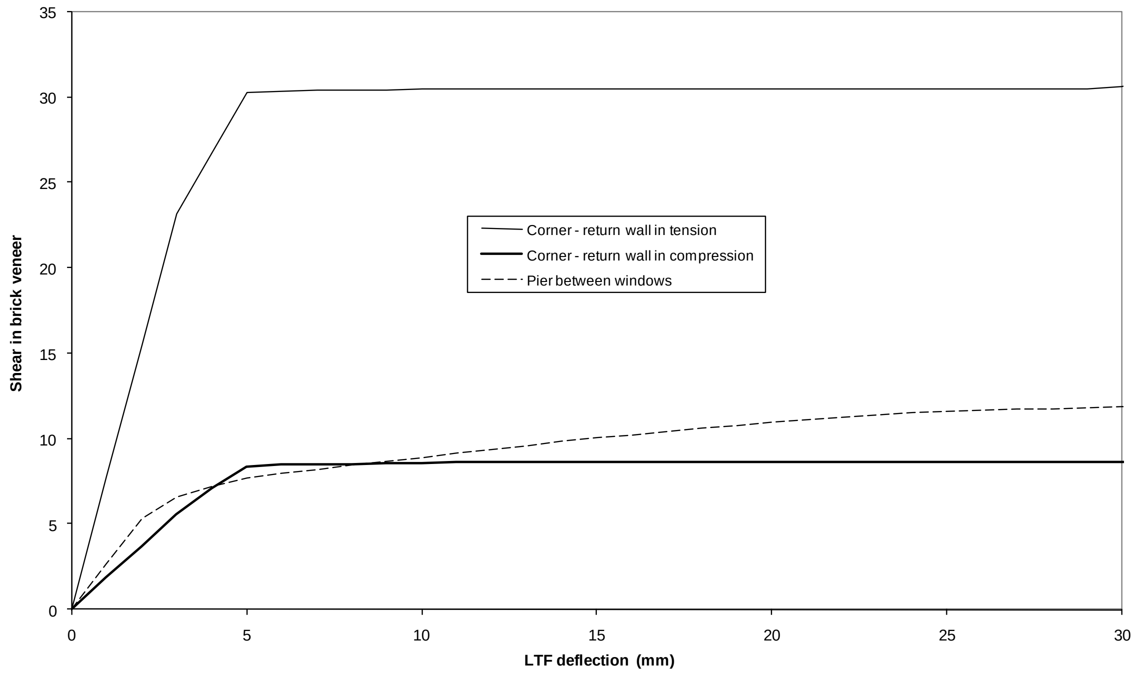


**Figure 23. Shear force taken by 2.445 m long brick veneer**

## 6.1 Application of theory

### 6.1.1 Zero seismic shear coefficient acting on brick inertia (i.e. the test situation)

The software based on the above theory has been used to predict the shear force carried by brick piers for the case of zero seismic shear coefficient (i.e. $C_{EQ} = 0$). Figure 24 plots the shear force expected to be resisted by the veneer for various lengths of brick piers versus LTF wall deflection. However, the shear load that is transferred from the LTF to the brick veneer must first get transferred into the LTF walls. This could be the weak link if the LTF sheathing is not strongly fixed to the top of the LTF wall.

The following assumptions were made for Figure 24:

- The mortar bond tension strength, $f_{mt} = 0$ kPa.
- Crack height = 600 mm.
- Pier height = 2220 mm.
- Tie type and tie spacing corresponding to those described in Section 1.8.
- Studs spaced at 600 mm centres.
- Piers analysed were of length n x 600 + 45 mm where n = 1, 2, 3, 4 etc.
- Mortar interlock fully resists the shear forces at mortar crack lines.

Figure 25 plots the crack rotation at the bottom of brick piers for various lengths of brick piers versus LTF wall deflection. The plot shows pier lengths greater than 3 m will have small crack rotations due to load transfer from LTF walls for LTF deflections less than 20 mm. It also predicts that short lengths of brick veneer piers will crack at the base and rock about this crack under seismic loading.

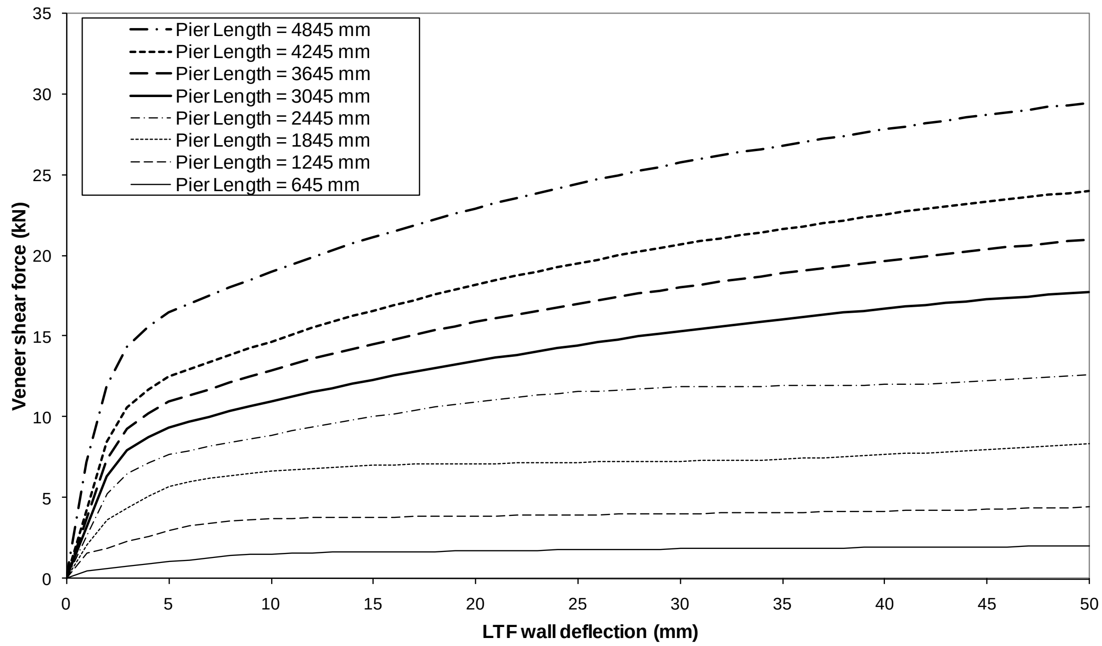


**Figure 24. Shear force taken by brick piers**

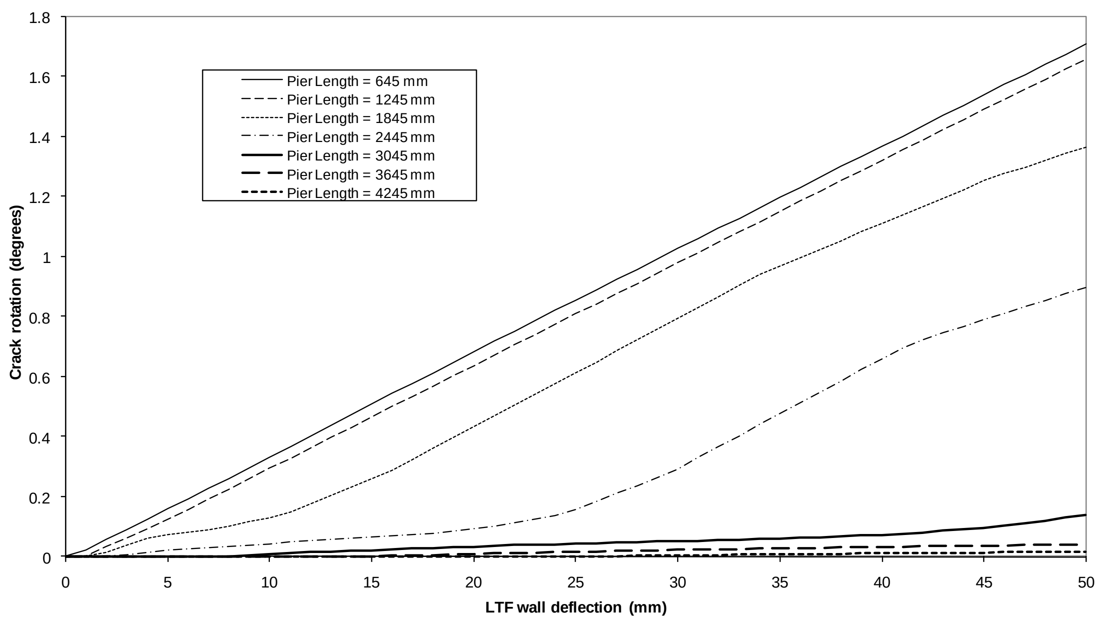


**Figure 25. Crack rotation versus LTF wall deflection for various brick pier lengths**

### 6.1.2 Including seismic inertial shear in brick itself

A plot of the lateral load taken by the brick veneer versus the pier length is given in Figure 26. It includes the self-weight induced seismic shear plus the load transferred from the LTF wall to the brick veneer. The former was calculated using the lateral load coefficient assumed by NZS 3604 for seismic Zone A (i.e. $C_{EQ}$ =

0.24). It was assumed that $f_{mt} = f_{mv} = 0$ and CrackHeight = 0.6 m. A lower crack height reduces the shear carried by short piers but increases it for long piers. Figure 26 can be used as a design chart for the brickwork type tested for brick piers bounded by windows or corners. It is recommended that the brick design load be based on 16 mm LTF wall deflection.

Brick panels which are isolated by full height openings (i.e. as tested in Room 2) can slip at the interface of the brickwork and the concrete foundation and the lateral load taken by the veneer is then lower, as also plotted in Figure 26.

To examine the proportion of seismic load that can be carried directly by the brick veneer, two examples are given below for houses in Zone A (the highest earthquake demand zone in New Zealand). The results showed that the brick veneer of the example single-storey house had the capacity to carry 166% of the demand seismic load and the two-storey house had the capacity to carry 75% of the demand load.

Example 1

Consider a brick veneer, single-storey, 16 m long x 12 m wide rectangular house founded on a concrete slab, with light roof of pitch 25º. From NZS 3604, the demand seismic load = 5.2 BUs/m$^2$ giving a total demand load of 5.2/20 x 16 x 12 = 49.2 kN. However, NZS 3604 assumes that the cladding weight for a heavy cladding = 220 kg/m$^2$ rather than the actual value of 130 kg/m$^2$ for the veneer used in this investigation. Based on the actual weights a revised demand load was calculated to be 39.2 kN.

Assume each side of the house has brick veneer piers between windows, or corners, of nominal lengths 1.2, 1.8, 2.4 and 3.0 m (total length = 8.4 m). From Figure 26, at 16 mm LTF deflection the capacity of the brick veneer in each direction = 2x(3.5+6.1+9.7+13.5) = 65.6 kN. This capacity is greater than the 39.2 kN demand load.

Example 2

This example is as per Example 1 except that the building is two-storeys with the upper storey having lightweight cladding. From NZS 3604, the seismic demand load for the lower storey is 13.5 BUs/m$^2$ which results in a total demand load of 13.5/20 x 16 x 12 = 129.6 kN. However, NZS 3604 assumes that the cladding weight for a heavy cladding = 220 kg/m$^2$ rather than the actual value of 130 kg/m$^2$ for the veneer used in this investigation. Based on the actual weights a revised design load was calculated to be 88.2 kN. If the brick veneer capacity is 65.6 kN as derived in Example 1 it will only be able to carry 75% of the demand load.

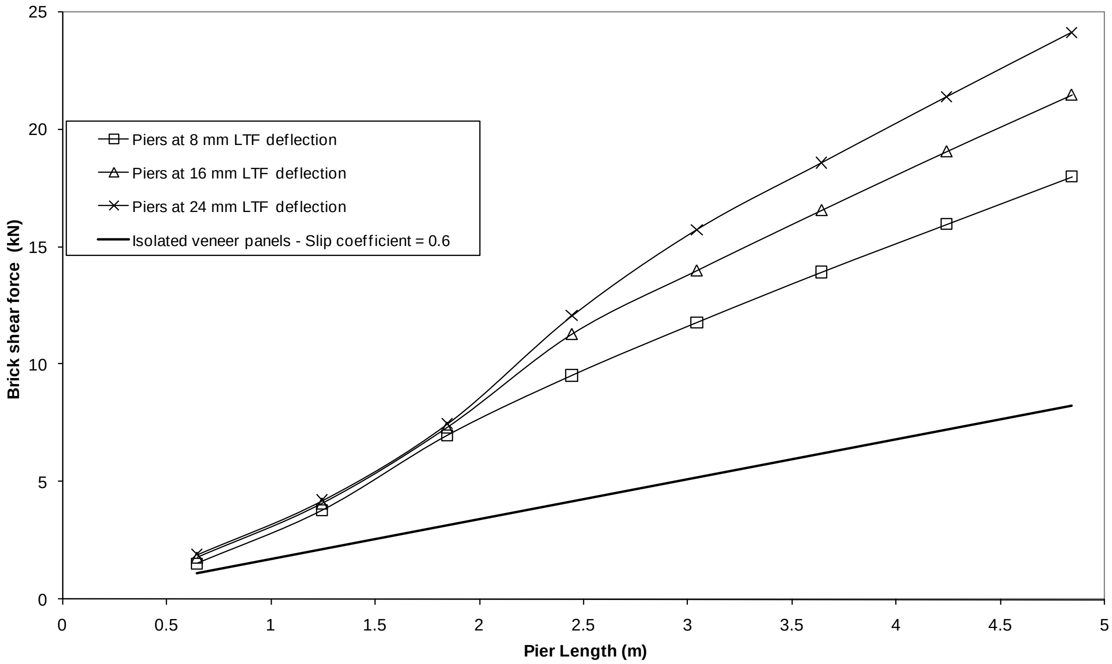


**Figure 26. Design chart - load taken by veneer versus pier length**

## 6.2 Proposed design philosophy

Brick veneer will stiffen the house and add mass, both of which will affect the natural period. When brick has cracked the period will increase.

The seismic hazard acceleration coefficient, $C_h(T_1, \mu)$ (= 0.3) used to derive the NZS 3604 seismic demand tables was based on an elasto-plastic ductility, $\mu$ = 3, and a building period, $T_1$, of 0.4 seconds (Shelton 2007). Because the Room 1 test showed the brick veneer had the capacity to deflect to 50 mm with little decay in load-resistance, it is considered reasonable and conservative to retain this value of $C_h(T_1, \mu)$.

A design philosophy is proposed for construction using the brick and brick-tie types used in this investigation. The method conservatively assumes that the inertia forces of the brick veneer and LTF core of the house respond to the seismic excitation in phase. It is envisaged that each brick manufacturer may choose to produce design curves similar to Figure 26 for their own brick systems based on the model given in Section 5. This may require them to perform some elemental tests.

The proposed method is intended to be conservative relative to the design of houses without brick veneer. Bond strength, both in tension and shear, is assumed to be zero except for the mechanical shear strength of the mortar dowels in brickwork with holes. Horizontal cracks are expected in the brick mortar in major earthquakes but these will be fine and can be repaired by re-pointing. The method assumes no vertical cracking at corners and good performance from out-of-plane loading. However, as this performance needs to be confirmed by future testing <u>the proposed method should not be used until verified</u>.

It is proposed that earthquake or wind lateral load, used for house LTF bracing wall design, be taken as the <u>greater</u> of the following two calculations:

(1) Calculate the lateral demand load using normal methods (NZS 3604 tables or software currently available from manufacturers which takes actual weights into account). Subtract $\phi$ times the resistance plotted in Figure 26 where $\phi$ is recommended to be 0.7. (Note: isolated veneer panels or use of bricks without holes will need to be based on the lower shear slip line plotted in Figure 26.)

(2) Calculate the lateral load using normal methods but assuming lightweight cladding. This is because it is considered important to retain a reasonable level of LTF construction bracing resistance.

NZS 3604 stipulates the minimum bracing resistance which must be provided for each bracing line. It is proposed that brick veneer can be used to provide up to 50% of this resistance on exterior bracing lines.

# 7. COMPARISON OF TEST AND MODEL PREDICTION OF BRICK VENEER HORIZONTAL LOADS

## 7.1 Horizontal load in Room 1

Figure 27 gives a comparison of the measured horizontal load carried by the brick veneer and the predictions from the theory presented in Section 5.2. A moderate agreement was obtained up to the stage when windows were installed. The subsequent additional restraints when windows and framing above windows were added increased the load transferred to the veneer and the prediction becomes even more conservative. It is expected that these additional restraints effectively lowered the value of H1 in Eqn. (7) which would therefore increase the shear force required to rock the veneer. These additional restraints were not modelled in the theory presented in Section 5.

Note, Figure 27 has been adjusted from the original presentation of this report due to use of new test data on the relationship between tie displacement and tie upward load as summarised in Appendix D.

## 7.2 Horizontal load in Room 2

### 7.2.1 Side 1 of Room 2

The 4.82 m long isolated veneer panel in Room 2, called Panel A, simply slipped along the mortar crack between the veneer and the concrete foundation and had no rotation or additional cracking. Its resistance was assumed to be the coefficient of friction, $\mu$, factored by the panel self-weight, W. Figure 28 provides a comparison of the measured load in Panel A and the prediction assuming $\mu = 0.63$. The agreement is good.

### 7.2.2 Side 2 of Room 2

Side 2 of Room 2 consisted of a 3.2 m long isolated veneer panel called Panel B and an L-shaped corner brick veneer element. Initially the main deflection of Panel B was due to rocking, but by 22 mm LTF wall deflection the shear slip deflection equalled the rocking deflection and most of the subsequent movement was by shear slip along the mortar crack between the veneer and the concrete foundation.

Figure 29 gives a comparison of the measured load in the Side 2 veneer and the predictions from the theory in Section 5.2. The theory predicted that Panel B would rock until a deflection of 1.6 mm and then slip on the base whereas the L-shaped corner brick veneer element would simply rock with no slip. A slip coefficient of 0.63 was assumed for Panel B. A moderate and conservative agreement was obtained for the total load-resisted by Side 2.

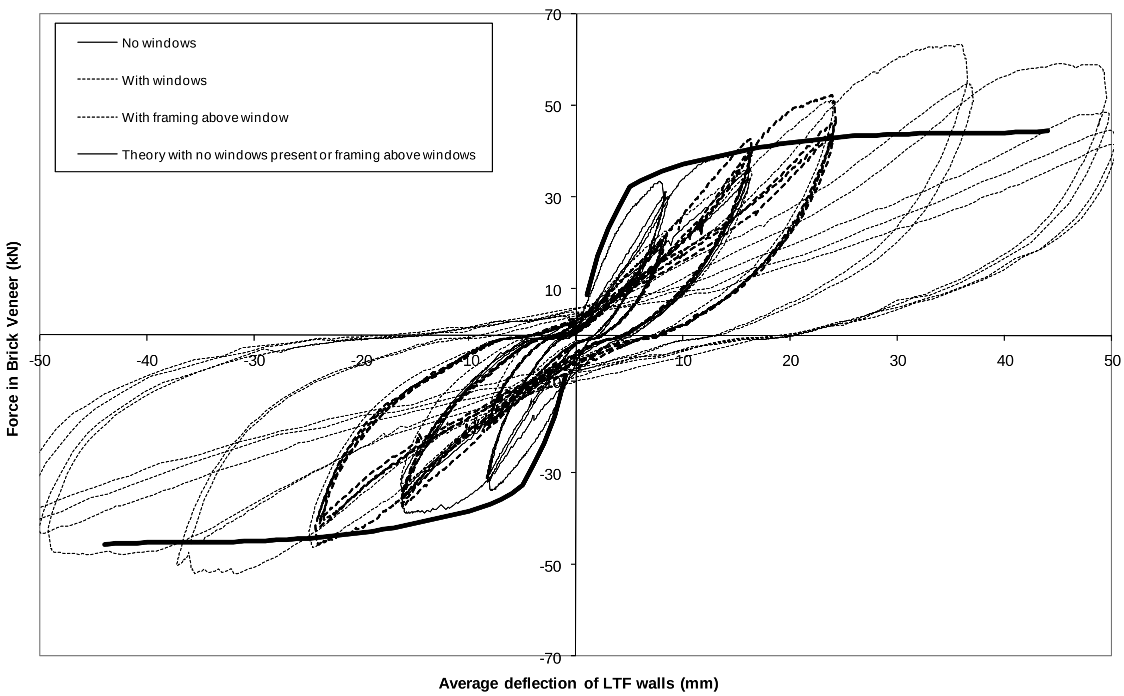


**Figure 27. Comparison of measured and predicted load in Room 1 brick veneer walls**

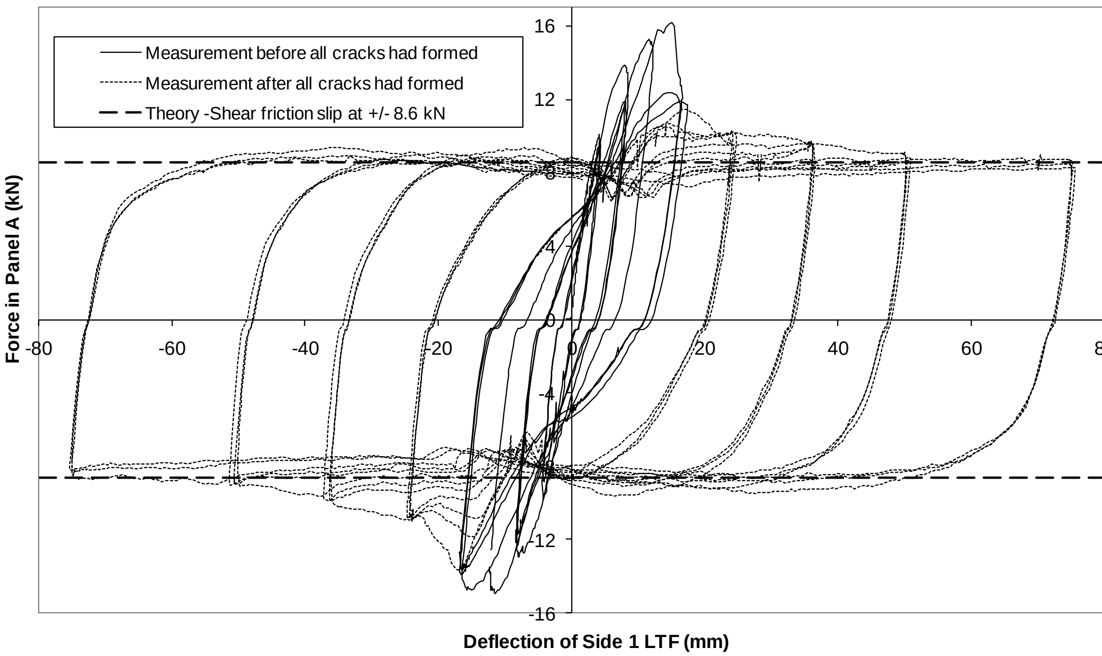


**Figure 28. Comparison of measured and predicted load in Room 2 Side 1 brick veneer walls**

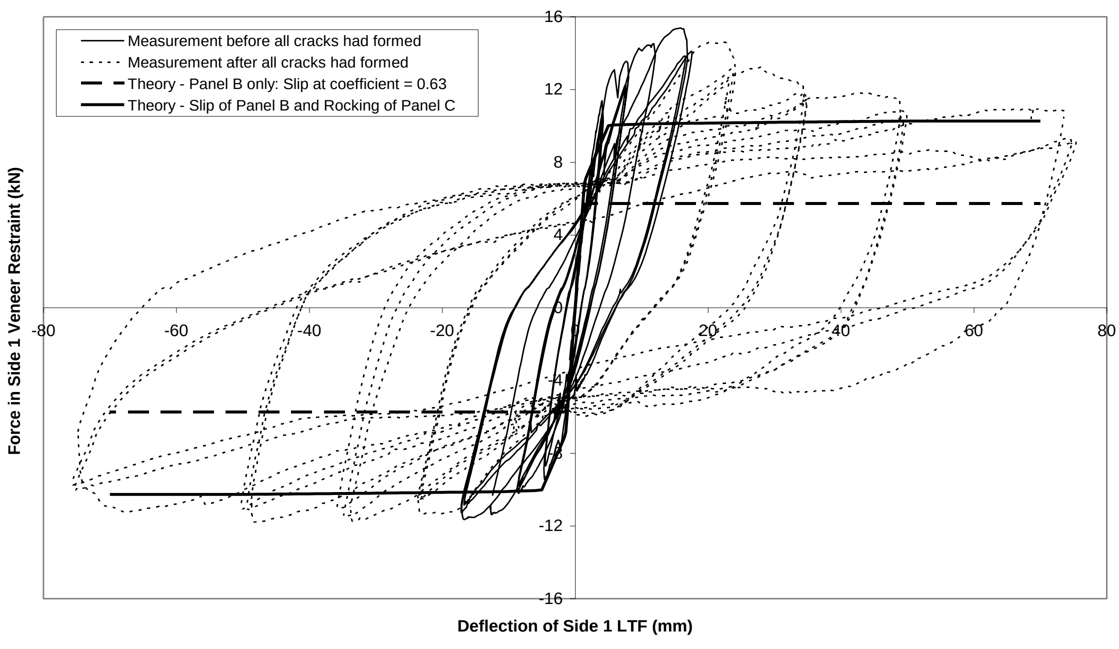


**Figure 29. Comparison of measured and predicted load in Room 2 Side 2 brick veneer walls**

## 7.3 Slip coefficient measured in elemental tests (Appendix C)

The slip coefficient (0.63) calculated for the room tests was far lower than the average (0.90) measured in elemental testing described in Appendix C. Three reasons for this incompatibility are possible:

- The brick ties may have been applying a net uplift force on the veneer panels in the room tests.
- The concrete surface in Room 2 was trowelled smoother than used for the small sample tests.
- The measurement of shear force carried by the veneer in Room 2 may have been underestimated due to possible friction in the UC support beam rollers.

# 8. SUMMARY/CONCLUSIONS/RECOMMENDATIONS

## 8.1 Objective

Historically brick veneer construction has not performed well in earthquakes. Recent changes in construction are expected to result in a much improved performance. This is discussed in Section 1. This study was intended to improve the understanding of modern brick veneer construction in earthquakes. In particular the study was undertaken:

- To determine if brick veneer can be relied upon to carry some of the building seismic load or whether the building light timber-framed (LTF) construction should be designed to carry the entire load.
- To identify the damage that can be expected in modern brick veneer construction during earthquakes.

## 8.2 Test observations

The LTF portion of two large rooms clad with clay brick veneer was racked under cyclic loading and the horizontal load that was transferred to the veneer was measured. Figure 17 and Figure 88 show the cracking mechanisms that formed. The bricks used had five vertical holes, of cross-section 32 x 23 mm, for the full brick depth which partially filled with mortar during construction, as shown in Figure 10. This effectively formed mortar dowels which greatly enhanced the horizontal shear strength between bricks. Thus, any conclusions made below apply only to veneer constructed using such bricks.

Conclusions regarding the movement of the veneer and LTF and veneer cracking were:

- Cracks in the veneer tended to form at the mortar courses just below the bottom of the window openings. The piers of brickwork between window openings rotated on these cracks. Near doorways, the cracks formed at the bottom mortar course of the brickwork rather than between the veneer and the concrete foundation. No shear slip occurred along the cracks. No individual bricks cracked.

- Isolated veneer panels cracked at the mortar course between the brickwork and concrete foundation. Piers rocked on these cracks, slid with a coefficient of friction of 0.63, or did both.
- It is possible that out-of-plane inertia forces may induce vertical cracking at the veneer corners which would separate the veneer sides from the ends. This report shows that the integrity of this connection improves the sliding resistance of the side veneer panels. The rocking behaviour of the L-shaped corner veneer elements would also be affected if cracking occurs in the corners.
- Timber stud in-plane bending deflections are significant in that they reduce the horizontal deformations (hence load transfer) between the LTF and veneer. Stud flexural bending deflections in the LTF walls adjacent to two 2.4 m long brick piers between windows was not significant for LTF deflections less than 24 mm. Subsequently, the lining became ineffective and large stud bending deflections occurred at stud mid-height.
- The magnitude of the stud flexural deformation and slip between the brick veneer and LTF was very low for the L-shaped corner veneer elements at all LTF deflections. Almost the entire movement of this veneer was due to rocking of each L-shaped corner as a single unit. As the brickwork did not crack vertically at the corner, and the ties between the end walls and LTF did not buckle or fail in tension, it was concluded that the end wall brick-ties forced the L-shaped corner veneer elements to have the same horizontal deflection as the LTF walls. This meant the veneer rocked at cracks near the base and there was no base shear slip. Many investigations by others have not used fully interlocked veneer corners and therefore missed this feature.
- In both test rooms the brick veneer reached large deflections in the loading direction in a very stable manner, giving “fat” energy absorbing hysteresis loops showing little load decay under repeated cycles or increased deflection.
- Calculations using data from Room 2 tests showed that the cracking resistance due to brickwork to mortar tension bond, $f_{mt}$, was negligible. Also the cracking resistance due to mortar shear bond between the brick veneer and concrete foundation, $f_{mv}$, was small.

## 8.3 Elemental tests

Elemental test results are given in Appendix C and D. These provided:

- mean shear strength and shear friction coefficients for the brick-to-mortar and mortar-to-coated (or bare concrete) surfaces:
    1. The waterproof coating increased the shear bond strength of the joint but reduced the shear friction coefficient.
    2. The values were sufficiently high that shear slip of an uncracked joint would not be expected unless the joint was pre-cracked by panel rocking.

- Bond wrench tests were performed to measure the tensile strength of brick-to-brick mortared joints using a method described in NZS 4210. Values were high and calculations showed that rocking would generally not occur if this was the true strength. It is expected that mortar dowels effectively strengthened the joints in this test. This mechanism would not occur in a real structure as the load is applied as a direct tension. Thus, the NZS 4210 bond wrench test is suspected to be inapplicable for bricks with internal holes where mortar dowel action can occur.
- Pure tension tests were also performed on the above joints and this gave values more in keeping with the observed cracking in the tests on Room 1.
- Mortar cylinder compressive tests indicated that the mortar used in the room tests had a crushing strength 62% greater than the 12.5 MPa minimum strength specified by NZS 4210.

The strength and stiffness of brick ties, both parallel and perpendicular to the tie main axes, was measured and used in the development of the theoretical behaviour prediction.

## 8.4 Comparison with theory

The relationship between brick-tie deformation and load was measured and reported in Appendix D. The shear and tension mortar bond strengths between stacked bricks, between bricks and foundation concrete with and without surface coating and the coefficient of friction between these surfaces was measured and reported.

Based on the observed crack formations a theoretical model of veneer shear capacity was developed. A reasonable agreement was obtained with the full-scale test measurements up to the stage when windows were added. Subsequently, the theory was a little conservative.

## 8.5 Proposed brick veneer seismic design methodology

Based on the developed theoretical model, design charts of the shear load carried by the veneer in brick veneer houses versus brick pier length were prepared and a design methodology has been presented which takes advantage of the inherent strength of the veneer. It was concluded that brick veneer could be used to partially brace New Zealand houses. However, this requires verification by further testing before adoption. The methodology is currently limited to single-storey design.

## 8.6 Damage to modern brick veneer construction expected in a design earthquake

Damage to modern, single-storey, brick veneer houses using either the current or proposed methodology is expected to be low. The veneer will crack but the residual post-earthquake cracks can readily be re-pointed with little loss of function or appearance. The house interior is expected to rack less and therefore will sustain less damage than similar houses with no veneer cladding.

# 9. REFERENCES


Allen D. and Lapish E. Undated. 'The interaction of timber framed walls with a tied masonry veneer under cyclic racking loads'. Publication details unknown.

ASTM. 2005. *E72-2005: Standard Test Methods of Conducting Strength Tests of Panels for Building Construction*. American Society for Testing Materials, USA.

Beattie GJ. 2003. 'Repair and Reinstatement of Earthquake Damaged Houses Phase II – Derivation of Repair Techniques'. BRANZ *Study Report 123*. BRANZ Ltd, Judgeford, New Zealand.

Beattie GJ. 2006. 'Literature Survey on Two-storey Brick Veneers and Proposed Tie Strength Investigation' BRANZ *Consultancy Report SC1161-1*. BRANZ Ltd, Judgeford, New Zealand.

Beattie GJ. 2007. 'Shear Strength of Brick Ties in the Horizontal Direction in the Plane of the Wall'. BRANZ *Consultancy Report SC1186*. BRANZ Ltd, Judgeford, New Zealand.

Choi Y-H. and LaFave J. 2004. 'Performance of Corrugated Metal Ties for Brick Veneer Wall Systems'. *Journal of Materials in Civil Engineering*, (*May/June)*: 202-211.

Heath D, Gad E, Wilson J. and Simeoni L. 2006. 'Behaviour of Brick Veneer Walls Under In-Plane Racking Load'. *Proceedings of the 19th Australasian Conference on the Mechanics of Structures and Materials.* Christchurch, New Zealand, 29 November – 1 December 2006.

Heath D, Gad E and Wilson J. 2008. 'Shaking Table Test of Full-scale Brick Veneer House'. *Proceedings of the 14th International Brick and Block Conference.* Sydney, Australia. 17 – 20 February 2008.

ICBO. 2000. 'International Residential Code'. International Code Council, USA.

Johnson E. and McGinley M. 2003. 'The In-Plane Performance of Brick Veneer and Wood Stud Walls'. *Proceedings of the 9th North American Masonry Conference.* South Carolina, USA. *June 1 - 4 2003*, 226-237.

Lapish E. 1991. 'Aseismic Designs of Brick Veneer and the NZ Building Codes'. *Proceedings of the Pacific Conference on Earthquake Engineering*. New Zealand, 20 – 23 November 1991, 291-302.

Shelton RH. 1996. 'Seismic Performance of Brick Veneers and Ties'. BRANZ *Study Report 53*. BRANZ Ltd, Judgeford, New Zealand.

Shelton RH. 2007. 'The Engineering Basis of NZS 3604'. BRANZ *Study Report 168*. BRANZ Ltd, Judgeford, New Zealand.

Shing. 2008. Personal communication.

SA/SNZ. 2000. AS/NZS 2699.1. *Built-in Components for Masonry Construction – Part 1: Wall Ties.* Standards Australia, Sydney, Australia and Standards New Zealand, Wellington, New Zealand.

SNZ. 1999. NZS 3604 *Timber-framed Buildings*. Standards New Zealand, Wellington, New Zealand.

SNZ. 2001. NZS 4210 *Masonry Construction: Materials and Workmanship.* Standards New Zealand, Wellington, New Zealand.

# APPENDIX A CYCLIC TESTING OF ROOM 1

## A.1 Construction

Room 1 was a single-storey nominally 2.4 m high room as shown in Figure 42. It had plasterboard-lined light timber-framed (LTF) walls, brick veneer on all four sides and a timber-framed plasterboard-lined ceiling. Figure 31 defines the labelling of the corners, sides and ends. Details are tabulated below:

General:

- The outside plan dimensions of the room were 6.73 x 3.93 m.
- The walls incorporated windows and a door as shown in Figure 34 to Figure 36.
- The LTF wall framing was constructed from 90 x 45 mm kiln dried radiata pine timber with maximum stud spacing being 600 mm.

Brickwork:

- The veneer consisted of 26 courses of clay bricks placed in running bond. Hot-dipped galvanised steel ties were placed on top of the 2$^{nd}$, 6$^{th}$, 10$^{th}$, 14$^{th}$, 18$^{th}$, 22$^{nd}$ and 24$^{th}$ level of bricks and were screwed to timber studs spaced at a maximum of 600 mm centres. The bricks were interlocked at the corners as shown in Figure 39.
- Details of the bricks, brick-ties and mortar are summarised in Section 1.8.

Foundations:

- The LTF was constructed on a timber foundation beam bolted to the laboratory strong floor, as shown in Figure 31 to Figure 33.
- The brick veneer was constructed on a 250 universal column (UC) steel ring beam laid on its side. The top portion of the UC was filled with concrete to provide a bed for the brick veneer. The ring beam was supported on rollers as shown in Figure 32 and Figure 33 which enabled it, when filled with concrete, to be rolled on the laboratory strong-floor with a horizontal force of 0.3 kN. However, horizontal movement of the ring beam was precluded during the test by using horizontal ring-beam restraint elements that incorporated load cells as shown in Figure 31 and Figure 33.

## A.2 Test method

The LTF construction was horizontally displaced using an actuator which moved a load beam connected to the ceiling, as shown in Figure 32 and Figure 33. The load was transferred to the brick veneer by the various connections between the LTF and veneer (brick-ties, window frames and framing above openings). This load was measured using the load cells in the ring beam restraint elements, as shown in Figure 31.

The deflection regime imposed on the side LTF walls is summarised in Table 2. At ±8 mm deflection, in Stage I, the vertical plasterboard joints cracked at the corners of the openings in the LTF walls. Under subsequent loading these cracks widened and extended to the ceiling. However the wall to ceiling joints and the joints at the junctions of the walls remained uncracked for the duration of testing described in Table 2.

In Stage II, three aluminium windows with 4 mm thick float glass supported on rubber mounting blocks were installed in the side wall openings. The window framing butted up against the brickwork and therefore any relative movement between the brickwork and the LTF walls required the window framing to deform. This was observed to occur by distortion of the window frames into a trapezoidal shape and rotation of the glazing within the window frames. No window damage or glass breakage was observed.

In an estimated 80% of recent New Zealand brick veneer houses, brick is not used as a lintel above window and door openings. Instead this is framed out and clad with a light sheeting material, often being fibre-cement cladding. This is usually painted a similar colour to the brickwork and slightly overlaps the window head to form a weather seal.

Stage III involved adding 90 x 45 mm timber-framing, acting as a packer between veneer panels above window and doorway openings, to simulate construction as described above, but this framing was not clad as the cladding was expected to add little strength. NZS 3604 is silent on the connection required between the packer and LTF and any clearance requirements between the packing and brick veneer. For the purposes of this test the clearance was zero and the packer was connected to the LTF by a total of six 90 x 3.15 mm power-driven skew nails.

## A.3 Instrumentation

Potentiometers were used to measure:

- The deflection of the brickwork relative to the timber framing at four places on the side walls in the direction parallel to the brick veneer, as shown in Figure 40.
- The deflection of the brickwork relative to the timber framing at four places on the end walls in the direction perpendicular to the brick veneer.
- The in-plane horizontal displacement of the top of both Side 1 and Side 2 LTF walls relative to the ground.
- The horizontal displacement of the room ceiling relative to the ground at the actuator loading point.

A steel rule was used to measure:

- Uplift and horizontal slip of the LTF walls in many positions.
- Horizontal slip of the brick veneer relative to the ring-beam.

- Vertical and horizontal movement of the ring beam.
- Vertical changes in length (effectively brickwork crack widths) between lines drawn on the brickwork. Some lines were added subsequently to cover cracks that had formed in the locations shown in Figure 51 to Figure 53.

The following forces were measured by load cells:

- Horizontal load in the brick veneer via the horizontal ring beam restraint elements shown in Figure 31 and Figure 33.
- The total load applied to Room 1 at the ceiling level, at room mid-width, using the load cell in the actuator shown in Figure 33.

## A.4 Test results

### A.4.1 Hysteresis loops for load in brick veneer

A plot of the total horizontal load recorded by the ring beam restraints (i.e. transferred through the brick veneer) versus average side wall deflection is shown in Figure 48 for construction before the timber packing was placed above openings and in Figure 49 for the complete test series.

The hysteresis loops had levelled out at ±16 mm for construction without windows which is not surprising as the veneer panels were "rocking" about cracks and the lateral strength is largely limited by the weight of the brick piers in this case. This levelling out can be more readily seen by viewing only the backbone portion of the hysteresis curves which are shown in Figure 50.

Following the addition of the three windows the average resisted load increased by 9.2 kN (23%) at ±24 mm LTF wall deflection. The addition of windows plus framing above the windows increased the average resisted load by 18.1 kN (45%) at ±34 mm LTF wall deflection from the construction without windows or framing above.

Before the windows were installed the load at corresponding deflections carried in Side 1 and Side 2 brick veneers was almost identical. However, at ±24 mm deflection for construction with the windows, the load carried by Side 2 was 15% less than that carried by Side 1. This may be because Side 2 had only one window plus an unfilled door opening whereas Side 1 had two windows. The total length of brickwork on Side 2 was greater than for Side 1.

**Table 2. Deflections imposed on LTF Side 1 and Side 2 walls**

| Stage | Windows installed? | Framing installed above openings? | Deflections (mm) imposed | Number of cycles |
|---|---|---|---|---|
| I | No | No | ± 8 | 3 |
| I | No | No | ± 16 | 3 |
| | | | | |
| II | Yes | No | ± 8 | 3 |
| II | Yes | No | ± 16 | 3 |
| II | Yes | No | ± 24 | 4 |
| | | | | |
| III | Yes | Yes | ± 8 | 1 |
| III | Yes | Yes | ± 16 | 1 |
| III | Yes | Yes | ± 24 | 1 |
| III | Yes | Yes | ± 36 | 2 |
| III | Yes | Yes | ± 48 | 4 |

## A.4.2 Theoretical forces resisted by the brick veneer

The theoretical lateral shear load carried by the sum of the two nominal 2.4 m long brick piers and also by the four L-shaped corner veneer elements is plotted in Figure 30 based on the computer model explained in Section 5. The plots are the average from the push and pull directions. Although the total length of the side walls in the corner elements is 91% of the piers, the load taken by the piers is proportionally greater (e.g. the piers take more than 60% of the load at 24 mm LTF deflection).

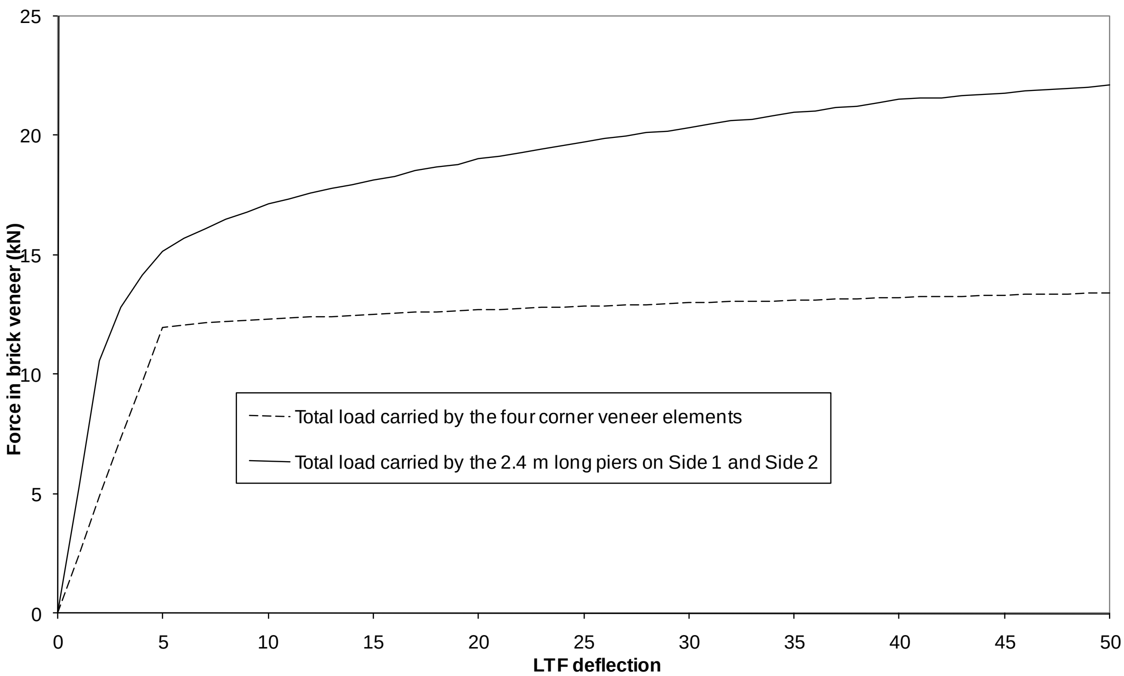


**Figure 30. Theoretical load carried by L-shaped corner veneer elements and side wall piers**

## A.4.3 Brickwork cracking

Cracking observed in the brickwork mortar was marked with a felt pen at the peak loads. These are sketched in Figure 51 to Figure 53. No cracks occurred within the bricks themselves and no cracks occurred between the concrete base and the bottom layer of bricks. Brickwork movement in all cases was by a rocking action at one end of the crack. Observations made at scratch marks across cracks showed that there was negligible shear slip along the cracks. All cracks first occurred in the ±8 mm cycling of the LTF wall except as noted in Figure 51 to Figure 53.

Crack widths were determined by using a steel rule to measure the vertical distance between horizontal pencil marks placed on the brickwork on either side of the crack(s). The crack labels given in Figure 51 to Figure 53 depict where crack width measurements were made and the results are summarised in Table

3. Only the crack widths across the arrows depicted in these figures were measured.

**Table 3. Crack width measurements**

| LTF wall deflection (mm) | Crack width (in mm) at the locations shown | | | | | | | | | | | | | | | | | |
|---|---|---|---|---|---|---|---|---|---|---|---|---|---|---|---|---|---|---|
| | **A1*** | **A2** | **B1** | **B2** | **C1** | **C2** | **D1** | **D2** | **E1** | **E2** | **F1** | **G1** | **G2** | **H1** | **H2** | **J1** | **J2** | **K2** |
| **8** | 2 | 0 | 0 | 0 | 3 | 0 | | | | | 4 | | | | | | 4 | |
| **-8** | 0 | 4 | 0 | 0 | 0 | 2 | | | | | 0 | 0 | 1 | | | 0 | | 0 |
| **+16** | 5 | 0 | 3 | 0 | 8 | 1 | | | | | 7 | 2 | 0 | 4 | 1 | 4 | 7 | 3 |
| **-16** | 0 | 8 | 0 | 4 | 0 | 4 | | | 4 | 5 | 0 | 0 | 5 | | 10 | 0 | 2 | 1 |
| **+24** | 6 | 0 | 8 | 0 | 12 | 1 | | | | | 11 | 7 | 1 | 7 | 1 | 7 | 10 | 3 |
| **-24** | 0 | 11 | 0 | 9 | 0 | 7 | | | 5 | 8 | 0 | 0 | 15 | | 17 | 0 | 2 | 0 |
| **48** | 7 | 0 | 29 | 0 | 25 | | | | | | 22 | 29 | 0 | 13 | | 10 | 15 | 4 |
| **-48** | 0 | 24 | 0 | 21 | 1 | | 17 | 11 | 10 | 17 | 2 | 0 | 23 | | 28 | | | 1 |

*Note: Width of the crack which formed at 16 mm LTF deflection not included in A1.

Cracks in the side walls tended to propagate from the bottom of openings in the brickwork (i.e. at window and door edges) or from building corners at approximately the same height as the bottom of adjacent brickwork openings. Generally only a single horizontal crack occurred between openings, although it sometimes deviated along a vertical mortar course (perpend) between bricks. An exception was the line of cracking on Panel G of Side 2 which followed the line of least resistance along the mortar courses between the bottom of the window at G2 and the bottom of the door at G1 (Figure 52, Figure 58 and Figure 59).

Generally, once a crack had formed no additional cracks occurred in the same pier. Exceptions were in Panel C (Figure 51) and Panel D (Figure 53) where a new crack formed at a ceiling displacement of 24 mm. Under further imposed LTF wall cycling most of the crack opening in Panel D occurred at the new crack and the amount of opening of the previously formed crack reduced.

The deformation mechanism of the brickwork of Room 1 under the imposed lateral load was that each pier simply "rocked" about the influential crack at its base and the pier otherwise remained uncracked. Usually it rocked backward and forward under the cyclic load over the same crack (Figure 58 and Figure 59), except that at location C1-C2 (Figure 51) the rocking occurred on the bottom cracks under "push" load but on the top cracks under "pull" load as shown in Figure 55 and Figure 56.

Cracks in the veneer of the end walls tended to be near horizontal and formed at the identical levels to the cracks which reached the corners of the side walls. The L-shaped corner veneer elements tended to rotate as a unit along these cracks due to the rocking action as shown in Figure 54. This can also be seen in Figure 53 and Figure 60.

The four corners of the room are labelled 1 to 4 in Figure 51 to Figure 53. The crack mechanisms at these corners is described below:

- Corner 4 was adjacent to a door in Side 2. Corner 4 L-shaped elements rotated about a crack one brick up from the base of the brick veneer as shown in Figure 54(a).

- Corner 3 was adjacent to a window in Side 2. Corner 3 L-shaped elements rotated about a crack at the base of the window as shown in Figure 54(b).
- The mechanism at Corner 3 also occurred at Corner 1 at $\pm16$ mm and greater deflections, although previously a crack had occurred four bricks higher in Side 1 and another crack occurred two bricks up from the base of End 2.
- This mechanism was also predominant at Corner 2 at $\pm24$ mm and greater deflections in the pull direction, but in the push direction the crack started from the window opening in the side wall and then stepped down to two bricks from the base at the corner and along End 1.

The following summary can be made. The brick-ties in the end walls did not change in length and so the L-shaped corner veneer deflection was forced to be the same as the adjacent LTF wall. Hence, the brick veneer ends were forced to rotate about a crack near the base. If there is a doorway in the side walls the crack will originate from near the base of the opening (i.e. near the base of the veneer) and propagate at this level along the end walls. If there is a window in the side walls nearest the corner, there are two competing locations for the crack to form in the end walls, these being at the base of the windows and the base of the wall. This was reflected in the cracking observed in the tests.

## A.4.4 Movement of brick veneer relative to LTF wall

Uplift of both the LTF wall and base beam was measured at the edges of wall openings and room corners and horizontal slip was measured at mid-length of wall elements. The maximum movement monitored did not exceed 1 mm.

The out-of-plane movement between brick veneer and the LTF wall was measured at four locations on the end walls. The maximum movement monitored did not exceed 1 mm.

Eqn. (4) is reproduced below for ease of discussion of displacements on the side (in-plane loaded) walls. The horizontal deformation of the Tie j is given by:

$$\text{TieDefXj} = \text{LTFdef x TYj/ LTFheight} - \Delta_{\text{Stud at j}} - (\text{TYj} - \text{CrackHeight}) \times \theta - \Delta_{\text{shear}} \quad \text{... (9)}$$

At each deflection gauge measuring the relative deflection between brick veneer and LTF wall, measured values are substituted into Eqn. (9) to estimate the values of the unknown parameters. As the point of interest is at the deflection gauge, TYj (i.e. the height of Tie j) is replaced with the gauge height (GaugeHeight) and $\Delta_{\text{Stud at j}}$ is replaced with $\Delta_{\text{Stud at gauge}}$.

The relative deflection between veneer and LTF wall is referred to as "$\Delta_{\text{LTFtoBrick}}$". $\Delta_{\text{LTFtoBrick}}$ can be used to replace TieDefXj in Eqn. (9) as TieDefXj is just the differential deflection at a specific location.

The term (TYj – CrackHeight) x $\theta$ in Eqn. (9) is the deflection at Tie j due to pier rotation and this is replaced with the calculated brickwork deflection at the gauge location, $\Delta_R$, due to measured brick pier rotation. $\Delta_R$ is taken as:

$$\Delta_R = \text{(Measured crack width from Table 3)/(Pier length) x GaugeHeight} \quad \text{… (10)}$$

Thus, Eqn. (9) reduces to:

$$\Delta_{LTFtoBrick} = \text{LTFdef x GaugeHeight / LTFheight} - \Delta_{Stud\ at\ gauge} - \Delta_R - \Delta_{shear}$$

Reorganising, this becomes:

$$\Delta_{Stud\ at\ gauge} + \Delta_{shear} = \text{LTFdef x GaugeHeight / LTFheight} - \Delta_{LTFtoBrick} - \Delta_R \quad \text{… (11)}$$

Note that observations at scratch marks made perpendicular to the cracks showed that $\Delta_{shear} = 0$ and so this term is deleted from Eqn. (11) for Room 1.

In the plots in this section a different notation is used due to the limitations of the plotting software. Table 4 provides the relationship between the names of the variables as used in this report and those used in the plots.

**Table 4. Nomenclature used in plots**

| Name used in report | Name used in Excel plots | Description |
|---|---|---|
| $\Delta_{LTFtoBrick}$ | LTFtoBrick | Relative deflection between a LTF wall and the brick veneer at a brick-tie, deflection gauge or top of the brick wall |
| $\Delta_{Stud\ at\ gauge}$ | Deflection stud | In-plane deflection of a stud at a gauge due to stud bending |
| $\Delta_{shear}$ | Shear slip | Horizontal slip of brickwork on a crack |
| $\Delta_R$ | Pier rotation | Deflection of a point in a brick pier (brick-tie, deflection gauge or top of wall) due to pier rotation |

Figure 62 plots $\Delta_{LTFtoBrick}$, $\Delta_R$ and $\Delta_{Stud\ at\ gauge}$ for a gauge near the top of the veneer versus LTF deflection where $\Delta_{Stud\ at\ gauge}$ was calculated from Eqn. (11). The figure averages the results from the “push” and “pull” directions for the two nominally 2.4 m long piers referred to as Panel B and Panel G in Figure 51 and Figure 52 respectively. The magnitude of $\Delta_{Stud\ at\ gauge}$ is low for LTF deflections less than 24 mm. Above this deflection, the lining became ineffective and significant stud bending was observed. This is reflected in the plot. Deflection due to pier rotation, $\Delta_R$, was zero at 8 mm LTF deflection as a crack had not formed at that stage. This subsequently increased until it surpassed $\Delta_{LTFtoBrick}$. Up to 16 mm LTF deflection most of the contribution to the LTF deflection was due to $\Delta_{LTFtoBrick}$.

Similar conclusions can be reached from Figure 63 for a gauge near the mid-height of the veneer, except that the brickwork rotation component was smaller (simply because the gauge was lower).

The relative deflection between veneer and LTF wall $\Delta_{LTFtoBrick}$ was not measured in the L-shaped corner veneer due to lack of available gauges. Thus, $\Delta_{LTFtoBrick}$ was moved to the left-hand side of Eqn. (11) and Figure 64 plots $\Delta_R$ and $\Delta_{Stud\ at\ gauge} + \Delta_{LTFtoBrick}$ for the top of the veneer versus LTF deflection for the three L-shaped corner veneer elements which had short panels on the side walls adjacent to windows (i.e. a crack height of approximately 516 mm). Figure 64 plots the results for both the "push" and "pull" directions as a different performance is expected for both directions due to the "L–shape" of the brickwork element. The magnitude of ($\Delta_{Stud\ at\ gauge} + \Delta_{LTFtoBrick}$) was very low for all LTF deflections showing that almost the entire movement of the panels was due to rocking of the veneer.

As the brickwork did not crack vertically at the corner, it is not surprising that $\Delta_{LTFtoBrick}$ was so low as the ties between the end wall and LTF would have prevented this movement unless they buckled in compression or extended in tension.

At Corner 4 there was a door opening in the adjacent side panel and the side panel was longer. A similar conclusion to the other corners can be reached with reference to Figure 65 for the pull direction. However, in the push direction $\Delta_{Stud\ at\ gauge} + \Delta_{LTFtoBrick}$ was of similar magnitude to the deflection due to panel rotation. One explanation of this could be that the ties slipped in the mortar under tension at the end wall at this corner and allowed the large veneer panel to move horizontally relative to the LTF. A post-test examination revealed that the bricklayer had omitted a full row of ties at 600 mm from the top of the end wall at this corner, which adds credence to this explanation.

### A.4.5 Summary on deflection components

The cracks in the veneer tended to form at the window sill level and the piers of brickwork above rotated on these cracks. Near doorways these cracks formed at the bottom brickwork mortar joint. No shear slip occurred along the cracks and this may have been due to the bricks having a series of large holes (as shown in Figure 10), with the mortar partially penetrating these holes and thus forming a series of small dowels which prevented slip from occurring.

Within the 2.4 m long brick panels, the stud flexural deformation was not significant for LTF deflections up to 24 mm. At deflections greater than 24 mm, the lining became ineffective and significant stud bending occurred. Deflection due to pier rotation was zero at 8 mm LTF deflection as no crack had formed. Pier rotation subsequently increased until it surpassed the slip between brick veneer and LTF (i.e. tie deformations). Up to 16 mm LTF deflection most of the LTF deflection was taken by the differential movement between the brick veneer and LTF.

For three of the four L-shaped corner veneer elements, the magnitude of the stud flexural deformation and slip between brick veneer and LTF was very low for all LTF deflections showing that almost the entire movement of the panels was due to pier rocking. The rotation was significant for the fourth corner, which had an adjacent door in the side wall for the direction which placed the end wall veneer panel into tension. With this exception it was concluded that the L-shaped corner veneer elements rocked with little horizontal load being transferred from LTF to brickwork via side wall brick-ties (i.e. there were only minor tie deformations). As the brickwork did not crack vertically at the corner, it is not surprising that the differential movement between LTF and brickwork was very low as the ties between the end wall and LTF would have prevented this movement unless they buckled or extended in tension. The difference in result in the fourth corner may have been due to the crack height being lower (as there was an adjacent door in the side walls), a longer length of brickwork or omission of some ties on the end wall.

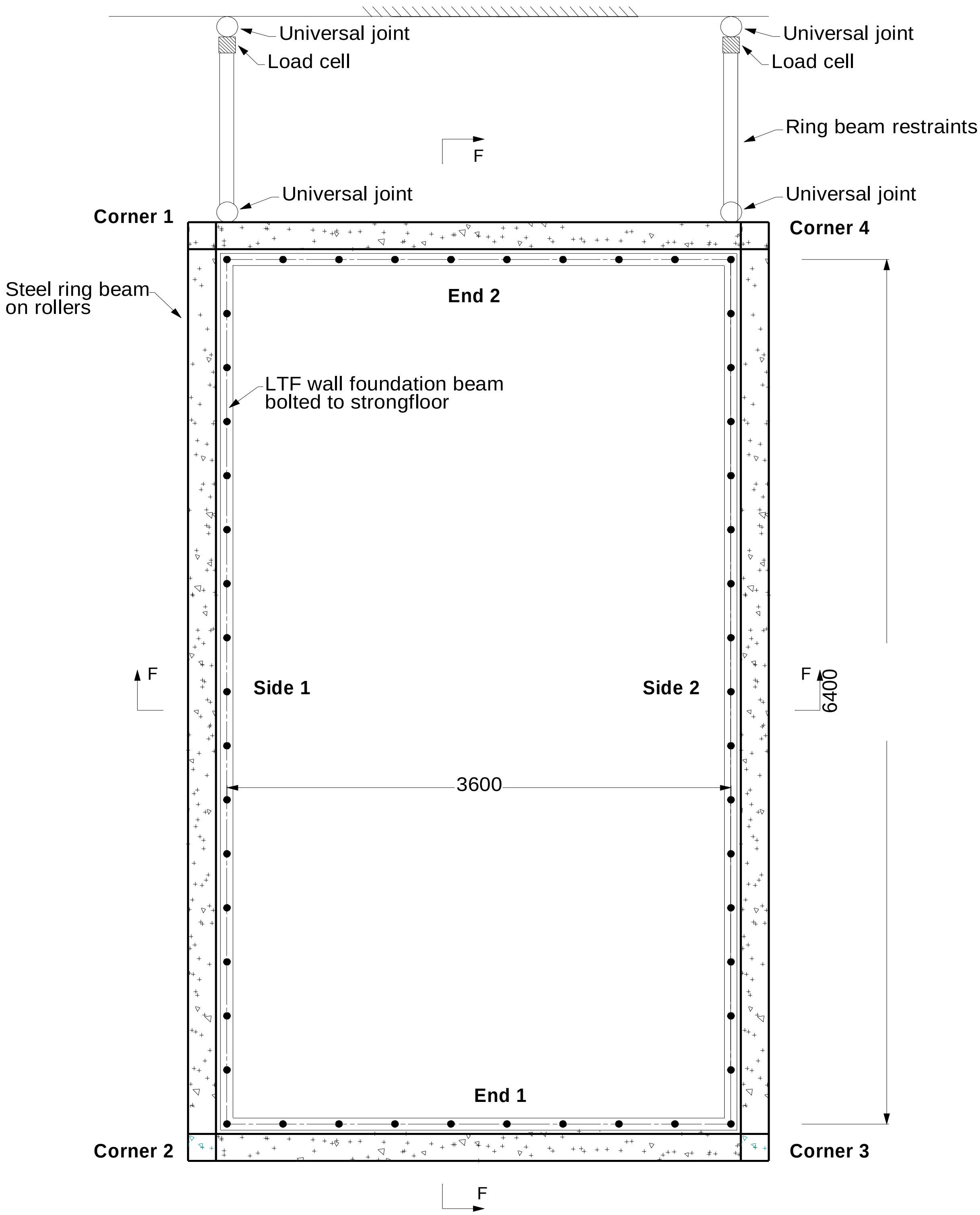


**Figure 31. Plan view of Room 1 foundation ring beams supporting the veneer and the LTF foundation beams**

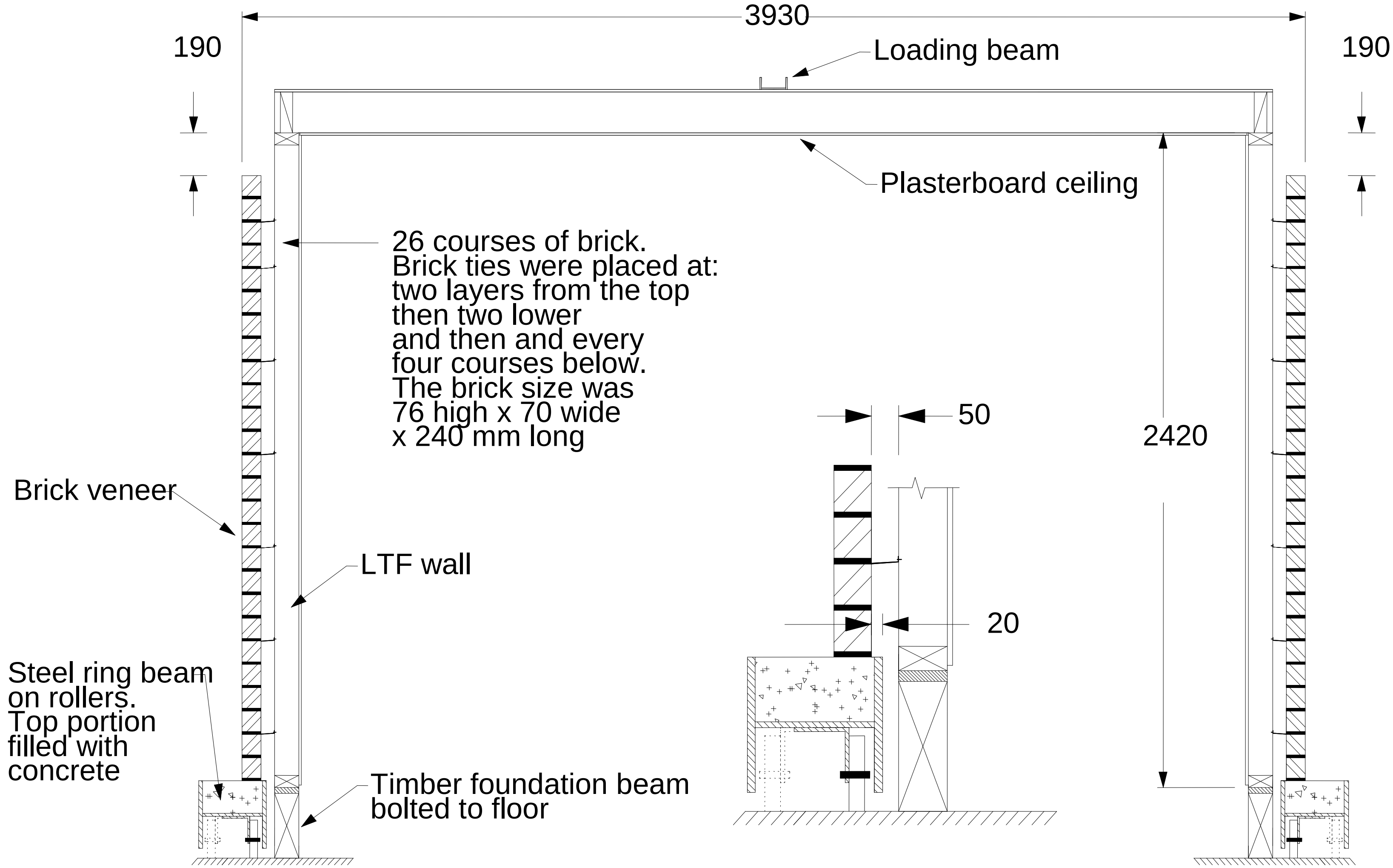


**Figure 32. Section E-E through Room 1 (see Figure 31 for location)**

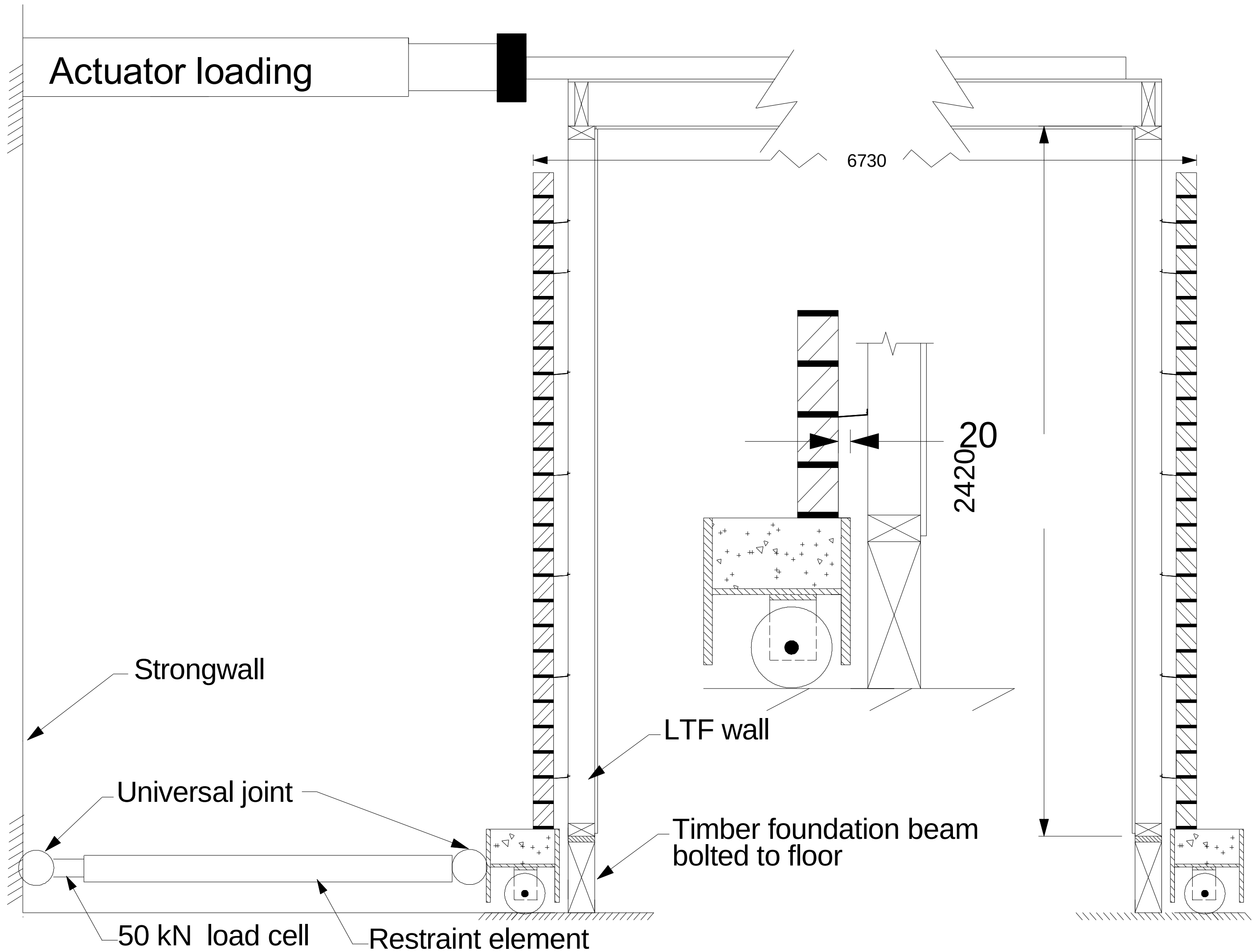


**Figure 33. Section F-F through Room 1 (see Figure 31 for location)**

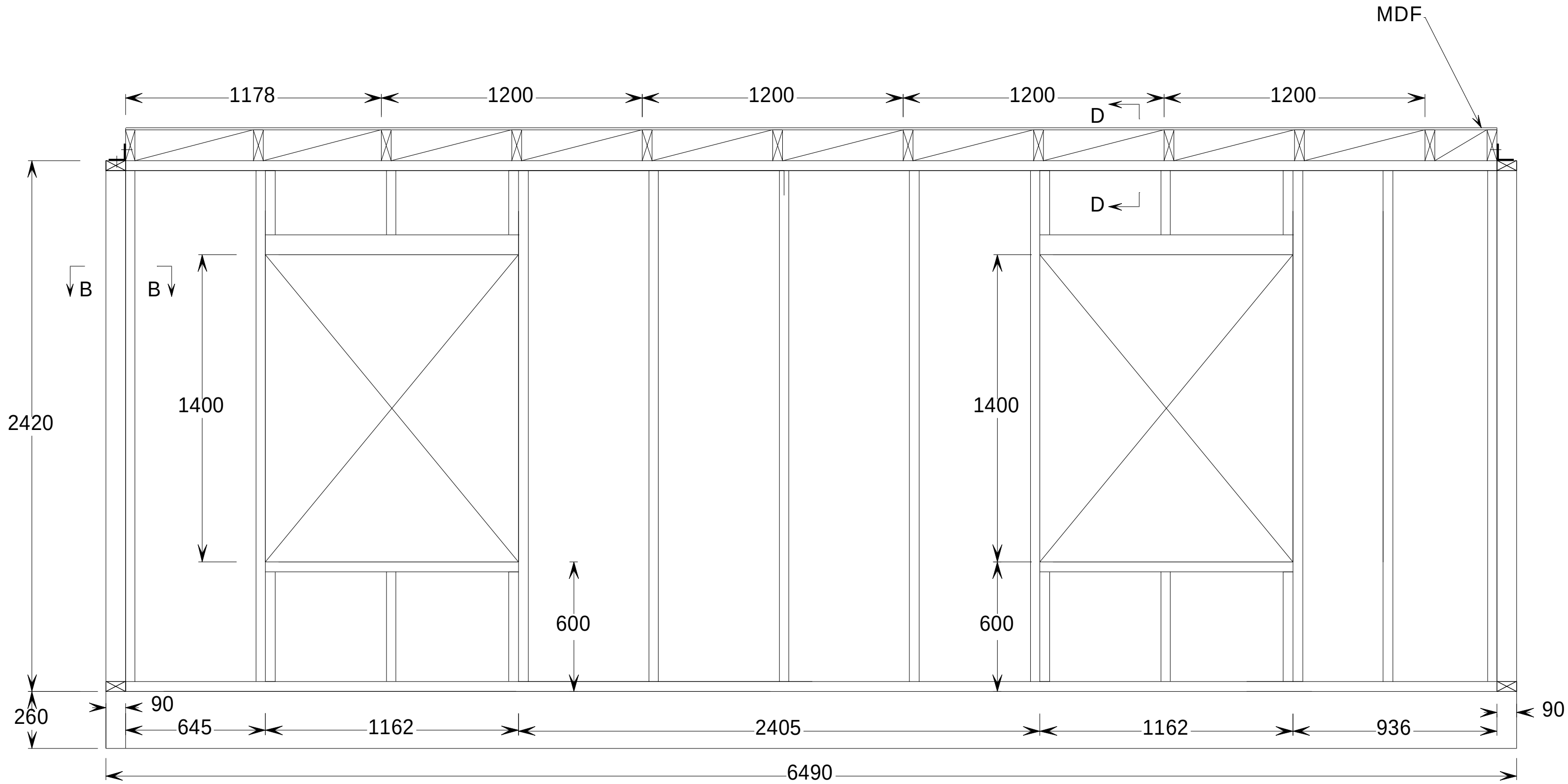


**Figure 34. Room 1 Side 1 elevation**

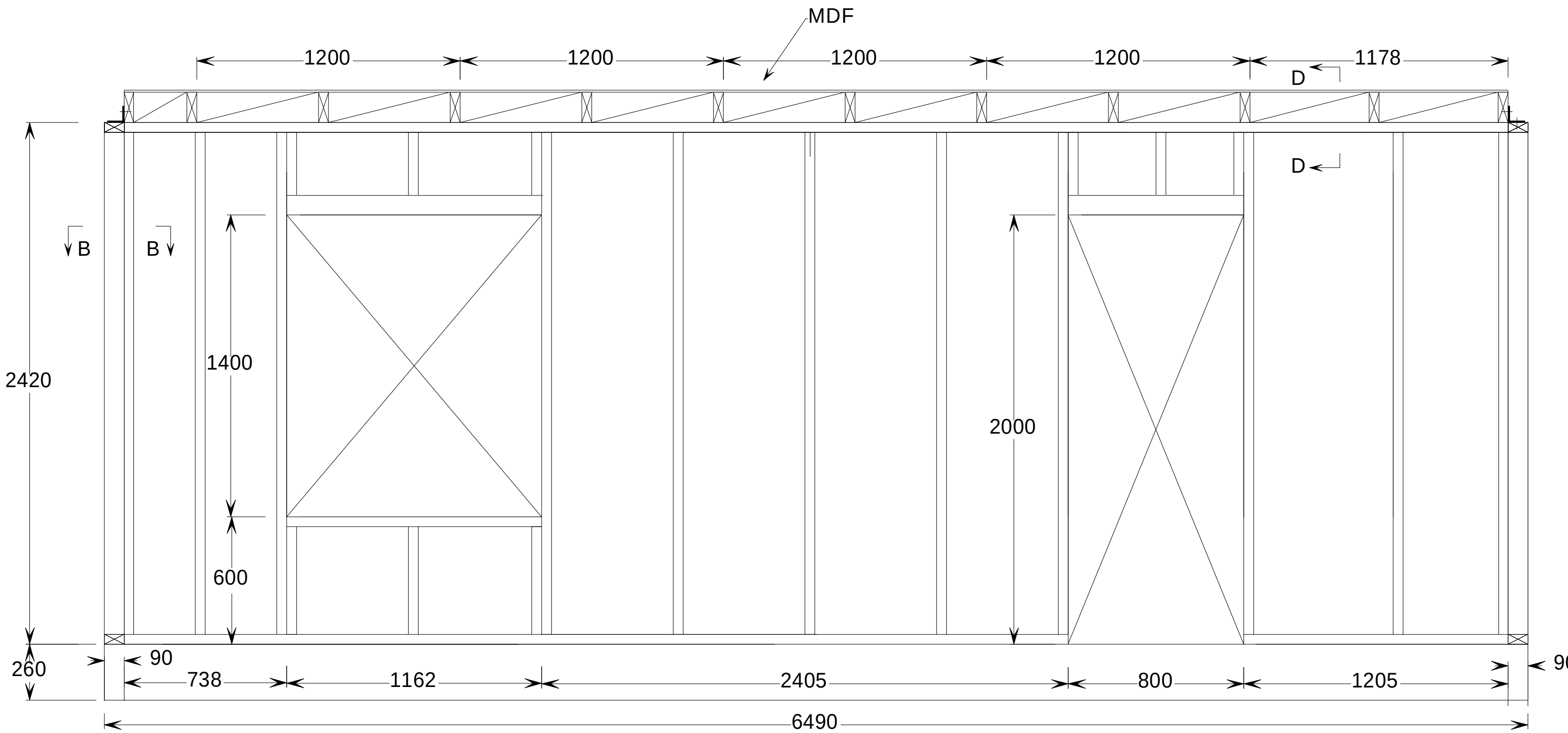


**Figure 35. Room 1 Side 2 elevation**

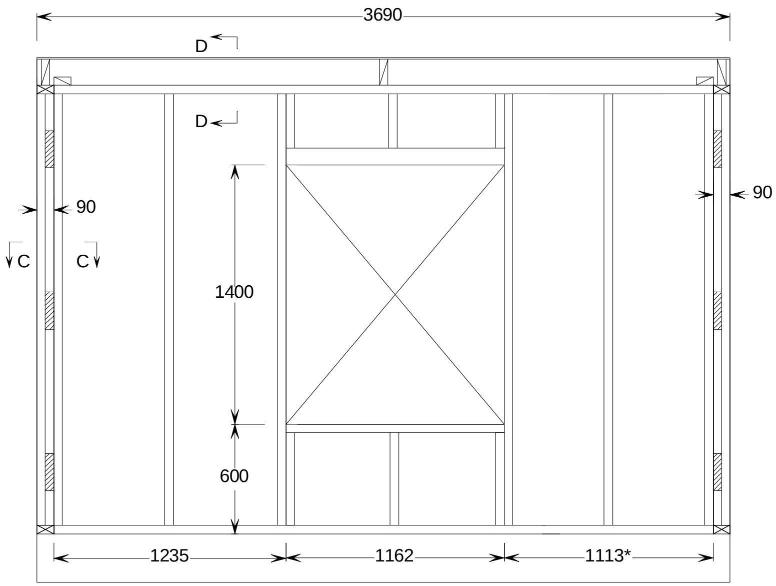


Elevation of End 2

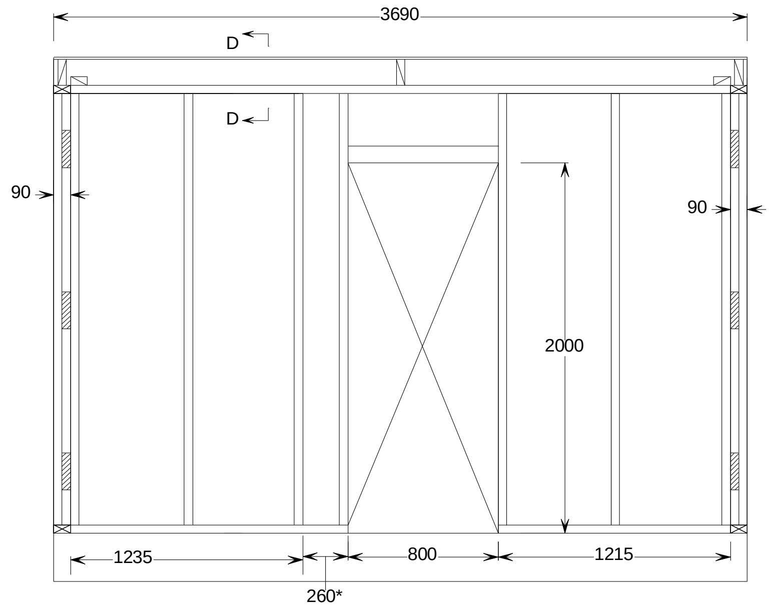


Elevation of End 1

**Figure 36. Room 1 End elevations**

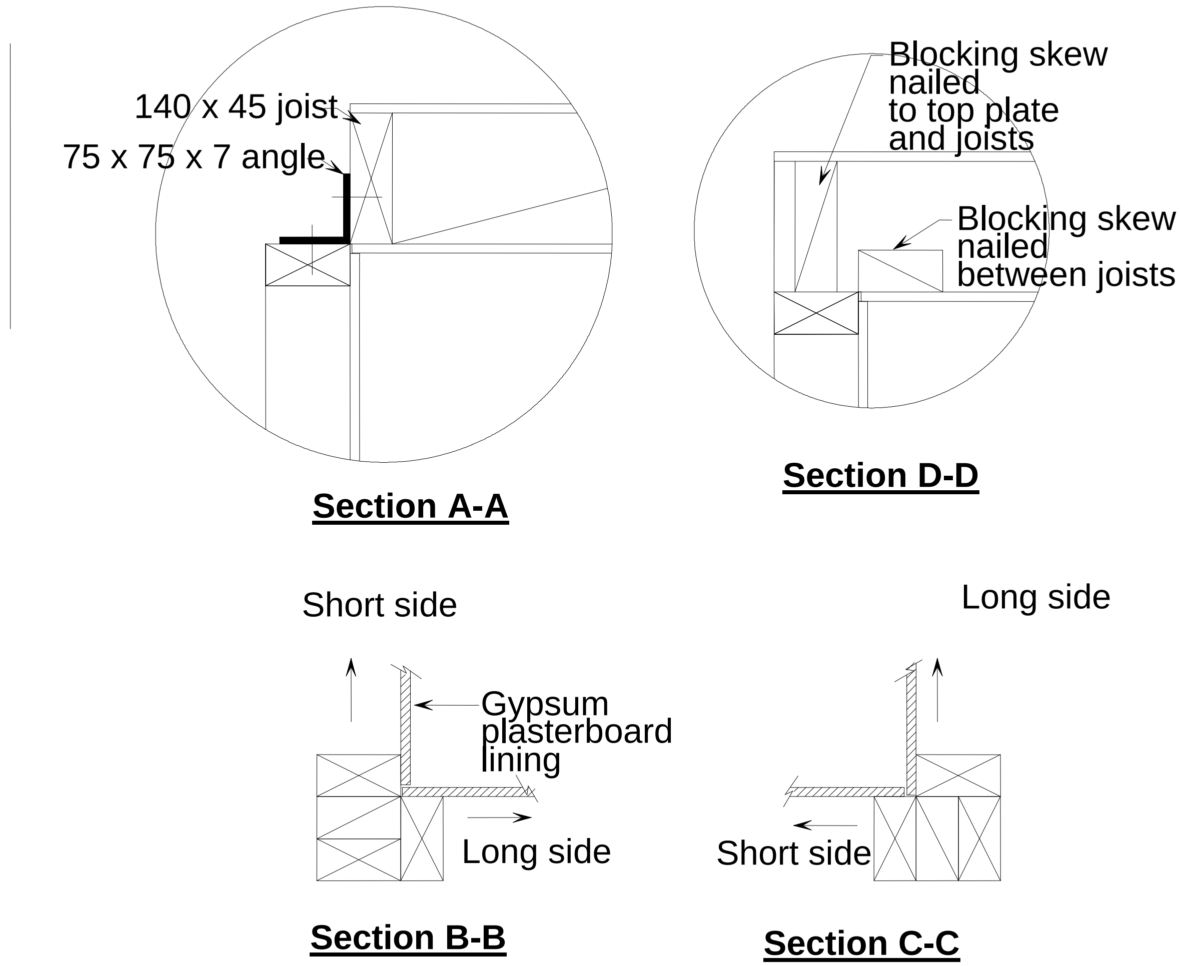


**Figure 37. Details of Room 1 LTF construction**

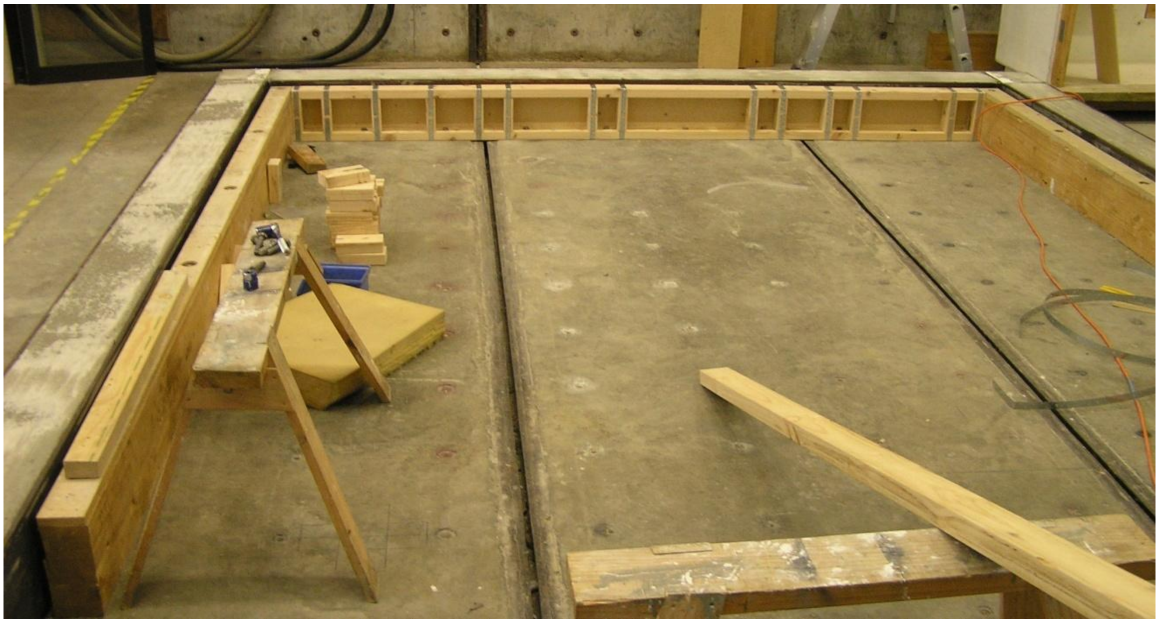

**Figure 38. Steel ring beam and timber foundation beam in place**

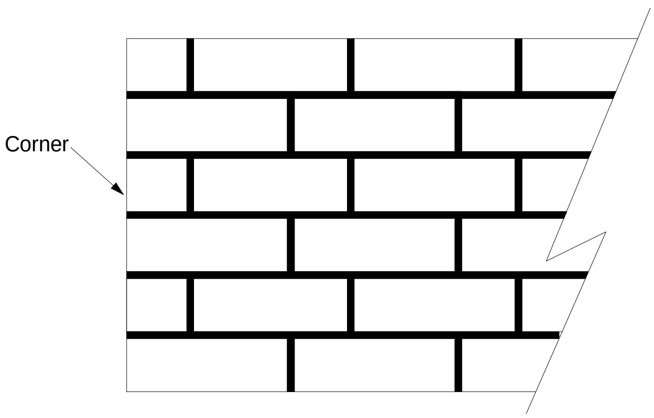


**(a) Elevation of veneer layout at a corner**

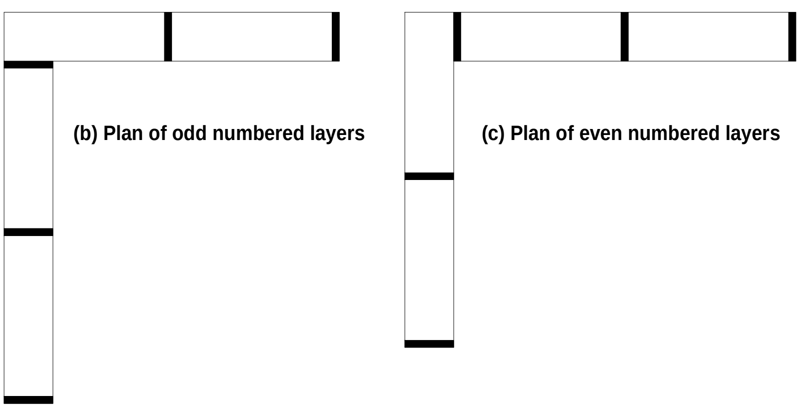


**Figure 39. Interlocking of brick veneer at corners**

**Figure 40. Gauge measuring differential horizontal displacement between LTF and brick veneer**

**Figure 41. Brick veneer tie**

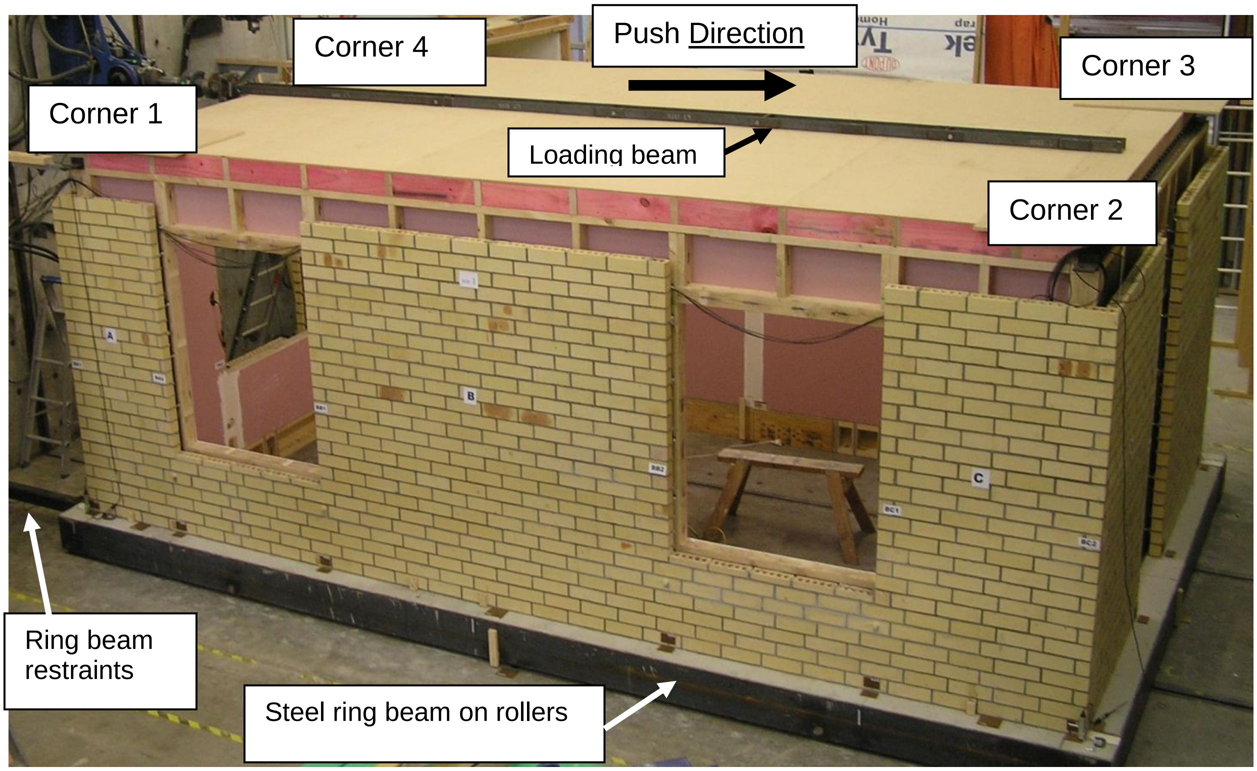


**Figure 42. Side 1 of Room 1**


**Figure 43. L-shaped veneer at Corner 1 of Room 1**


**Figure 44. Window framing used in Stage II and framing above window used in Stage III testing**


**Figure 45. Door on Side 2 and framing above door added in Stage III**

**Figure 46. Cracking on Side 2 of Room 1**

**Figure 47. Cracking on Side 1 of Room 1**

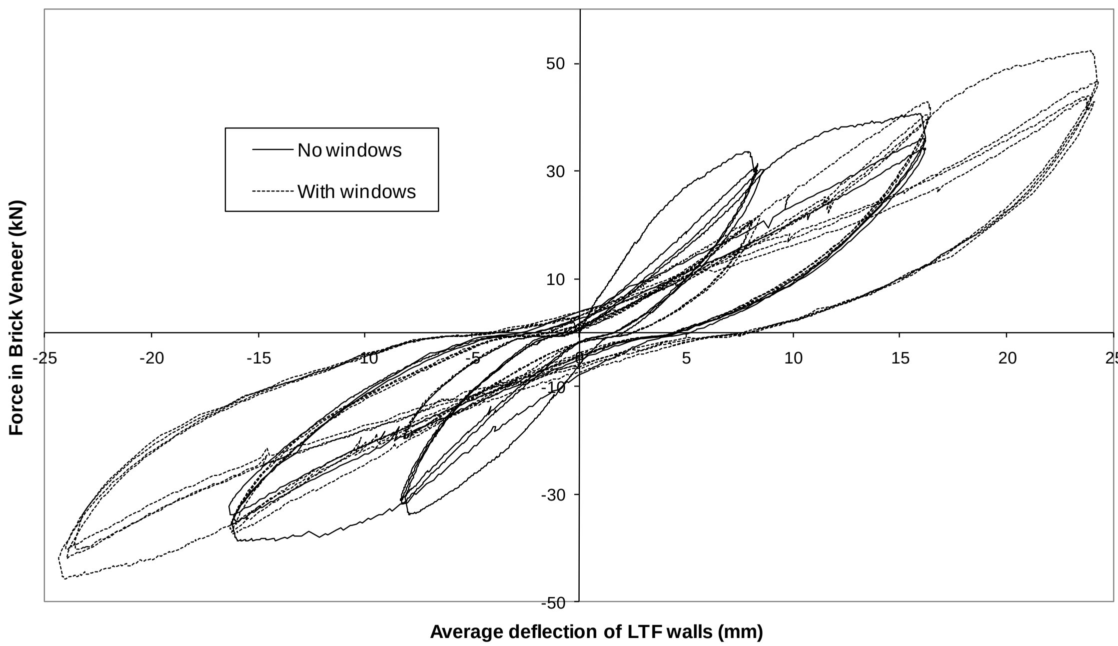


**Figure 48. Room 1 total load in brick veneer versus average deflection of side walls for Stage I and II**

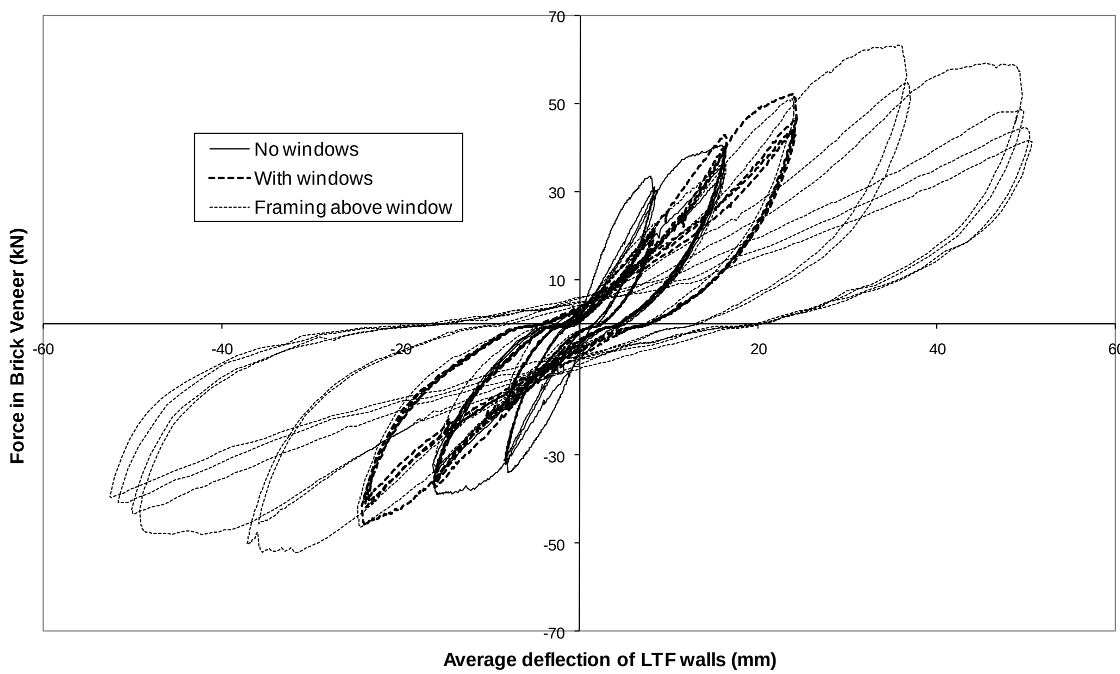


**Figure 49. Room 1 total load in brick veneer versus average deflection of side walls for the complete test series**

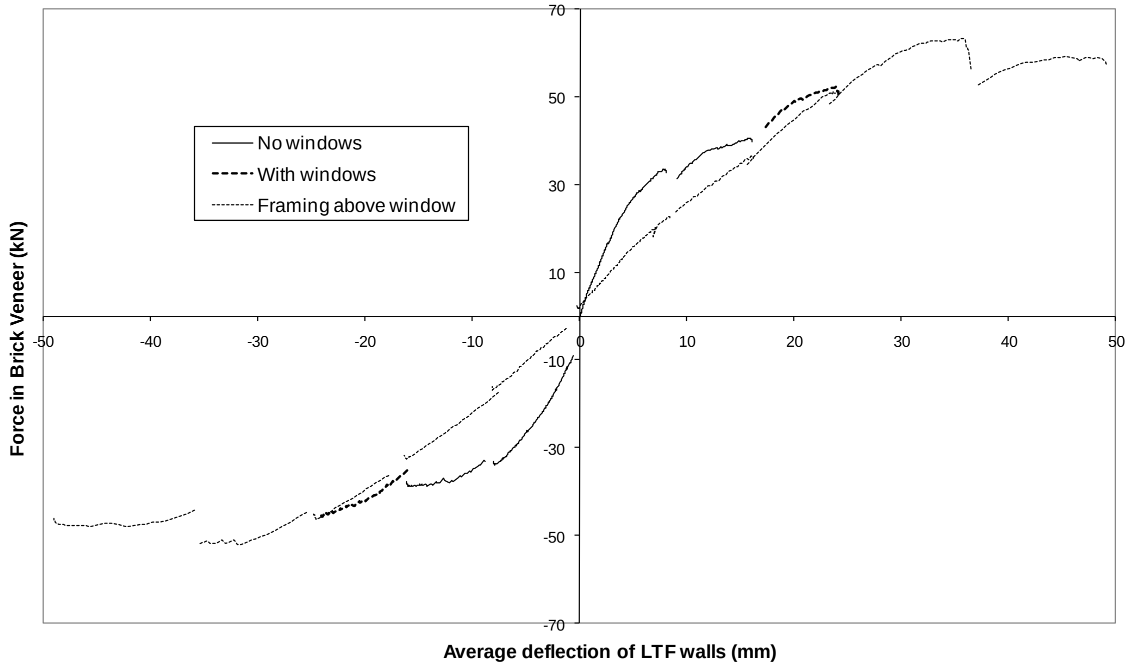


**Figure 50. Room 1 - Backbone curve of total load in brick veneer versus average deflection of side walls for the complete test series**

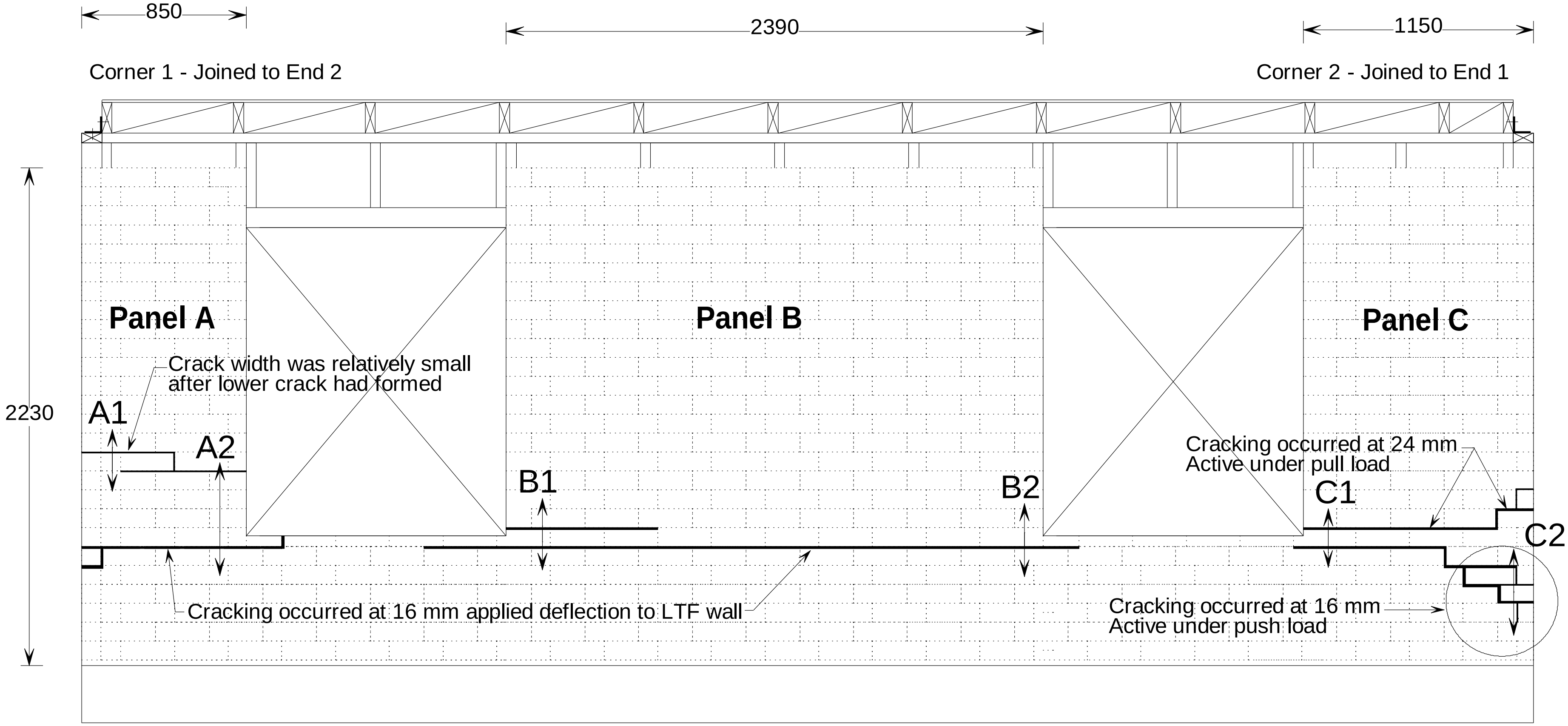


**Figure 51. Cracking observed in brickwork on Side 1 of Room 1**

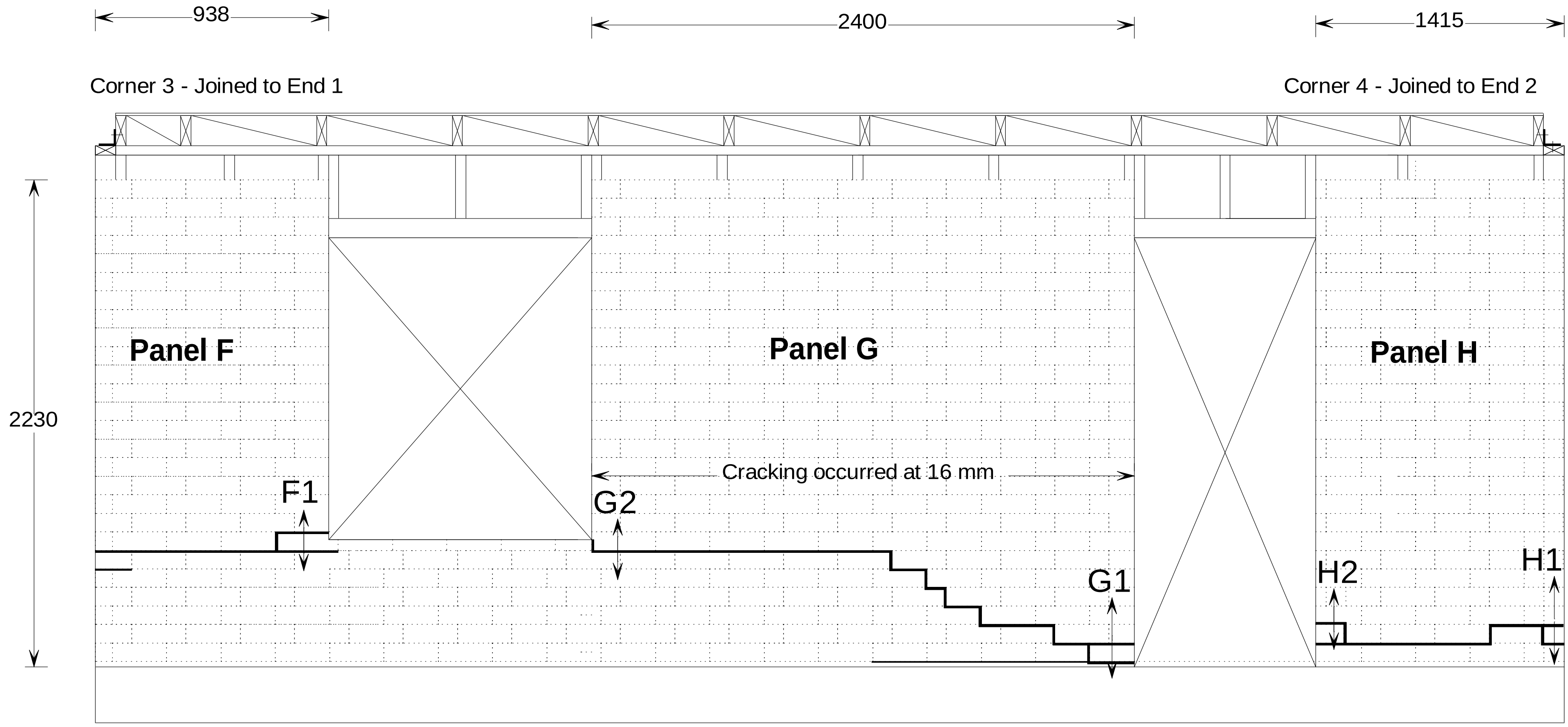


**Figure 52. Cracking observed in brickwork on Side 2 of Room 1**

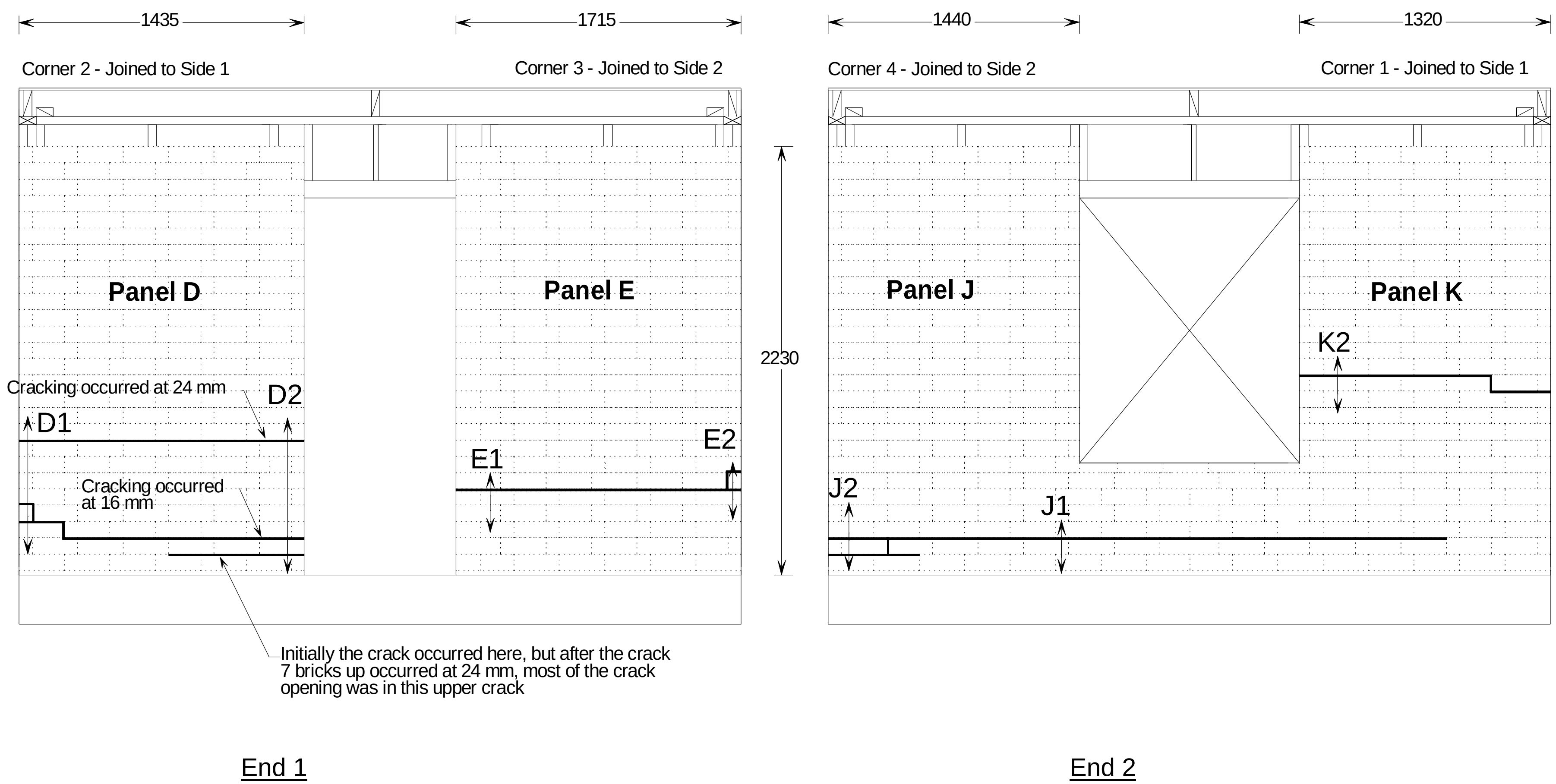


**Figure 53. Cracking observed in brickwork on End 1 and End 2 of Room 1**

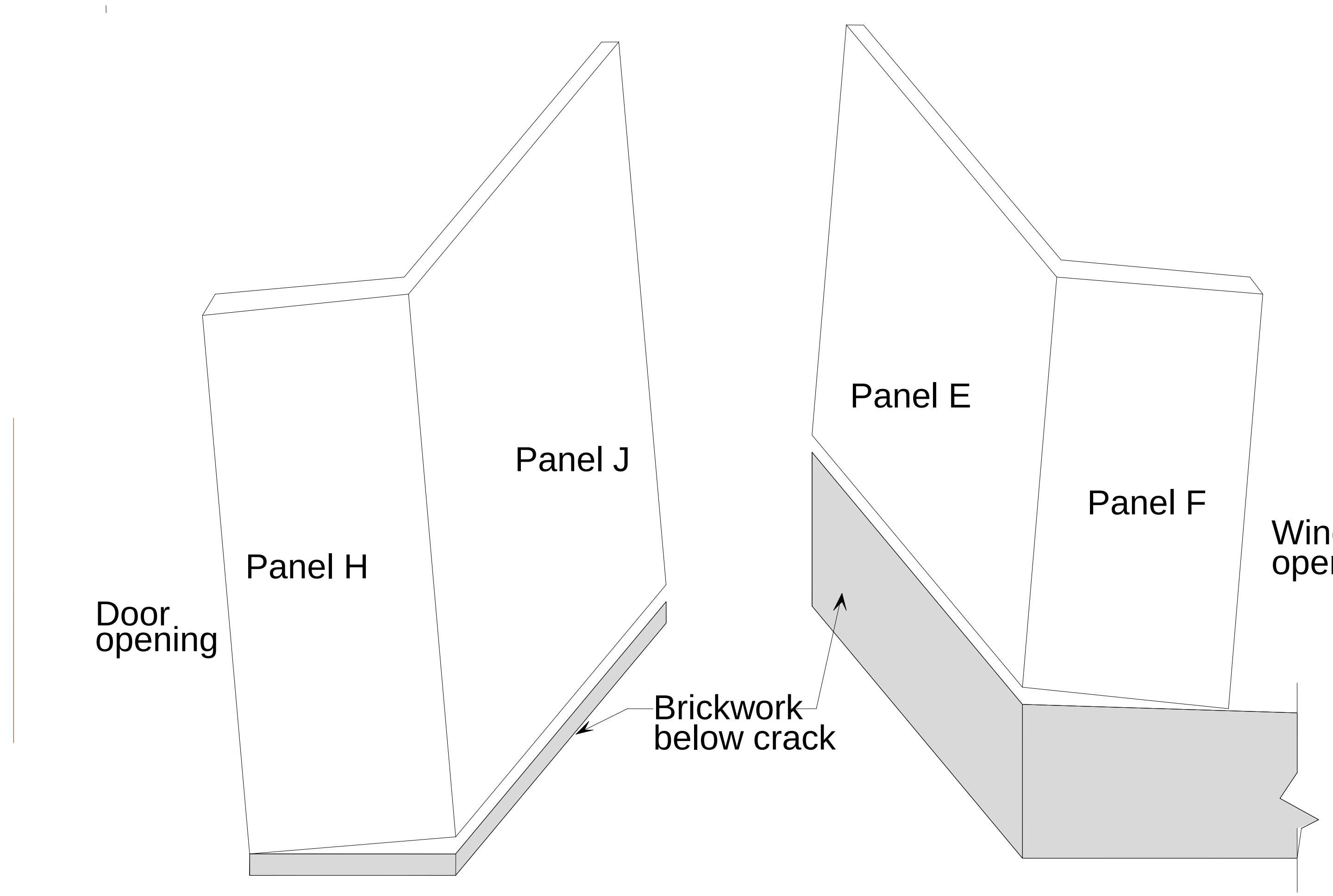


(a) L-shaped corner veneer by a side wall doorway (b) L-shaped corner veneer by a side wall window

**Figure 54. Rocking of L-shaped corner veneer elements**


**Figure 55. Brickwork cracking in Side 1 under "push" load**

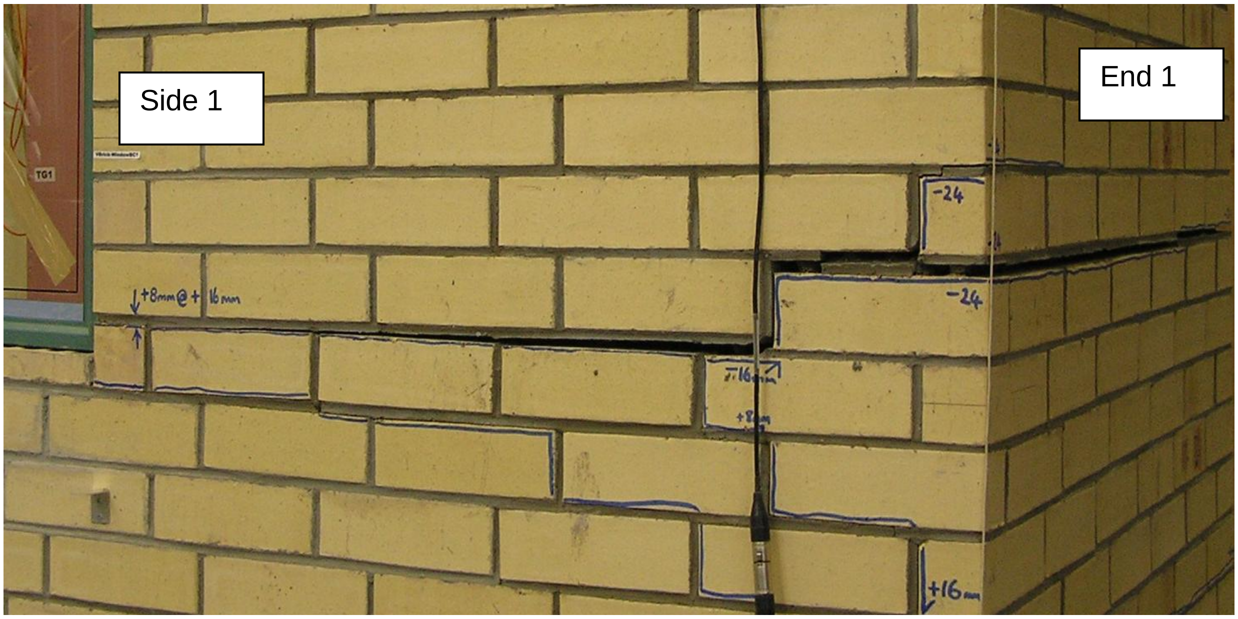


**Figure 56. Brickwork cracking at Corner 2 under “pull” load**


**Figure 57. Brickwork cracking in Panel H (Side 2) under “pull” load**


**Figure 58. Brickwork cracking in Panel G (Side 2) under "pull" load**


**Figure 59. Brickwork cracking in Panel G (Side 2) under "push" load**


**Figure 60. Brickwork crack at L-shaped veneer of Corner 3 under "pull" load**


**Figure 61. Interaction of windows and window header with brickwork on Side 1 under "pull" load**

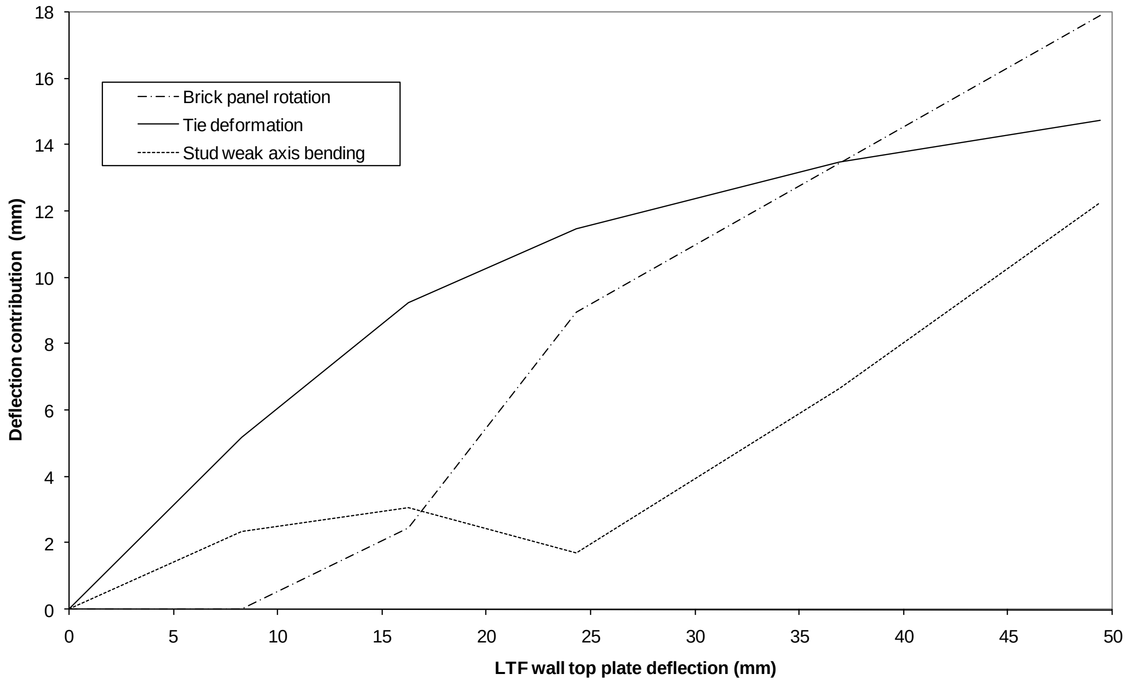


**Figure 62. Components of brickwork deflection at the top of 2.4 m long panels**

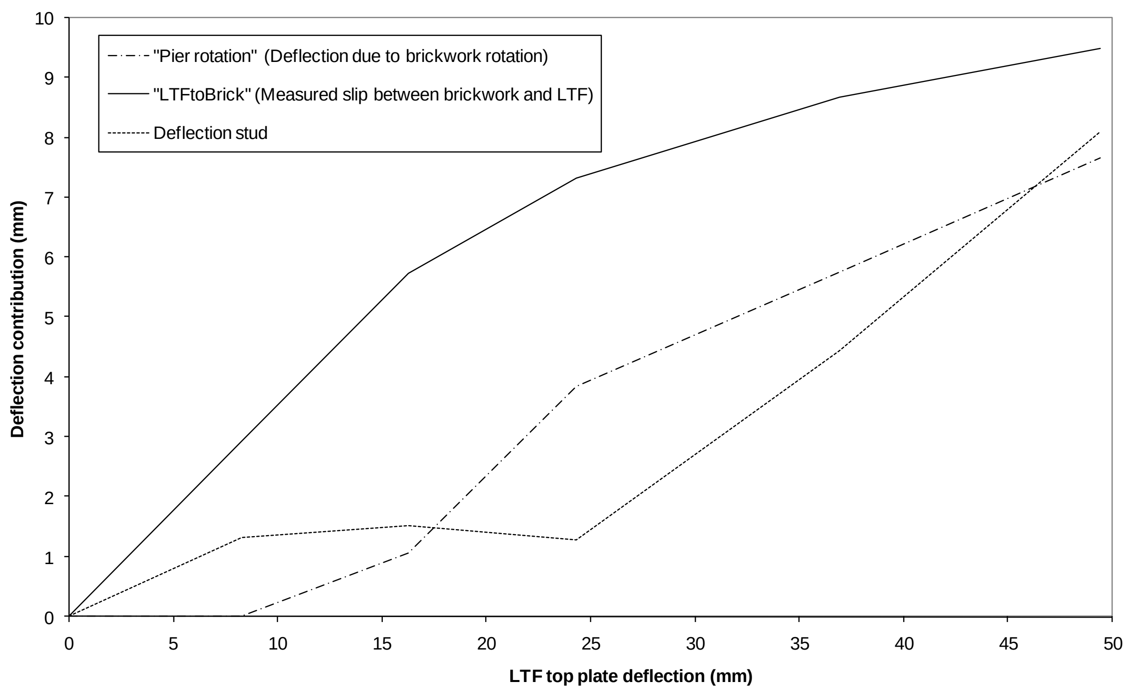


**Figure 63. Components of brickwork deflection near mid-height of 2.4 m long panels**

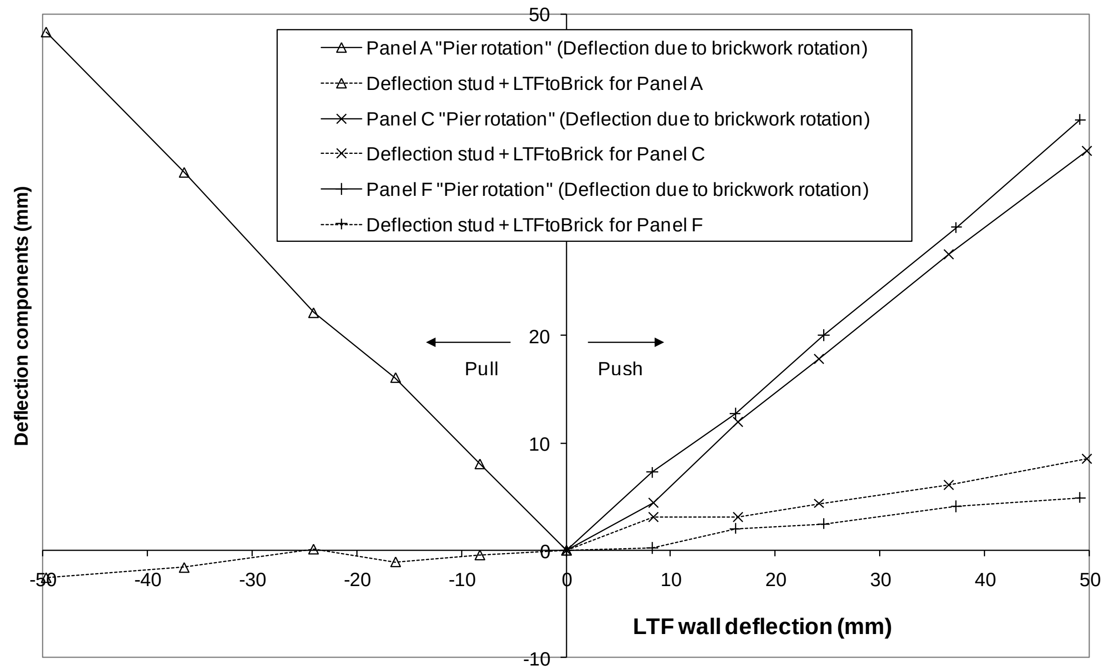


**Figure 64. Components of brickwork deflection for L-shaped veneer elements at Corners 1, 2 and 3**

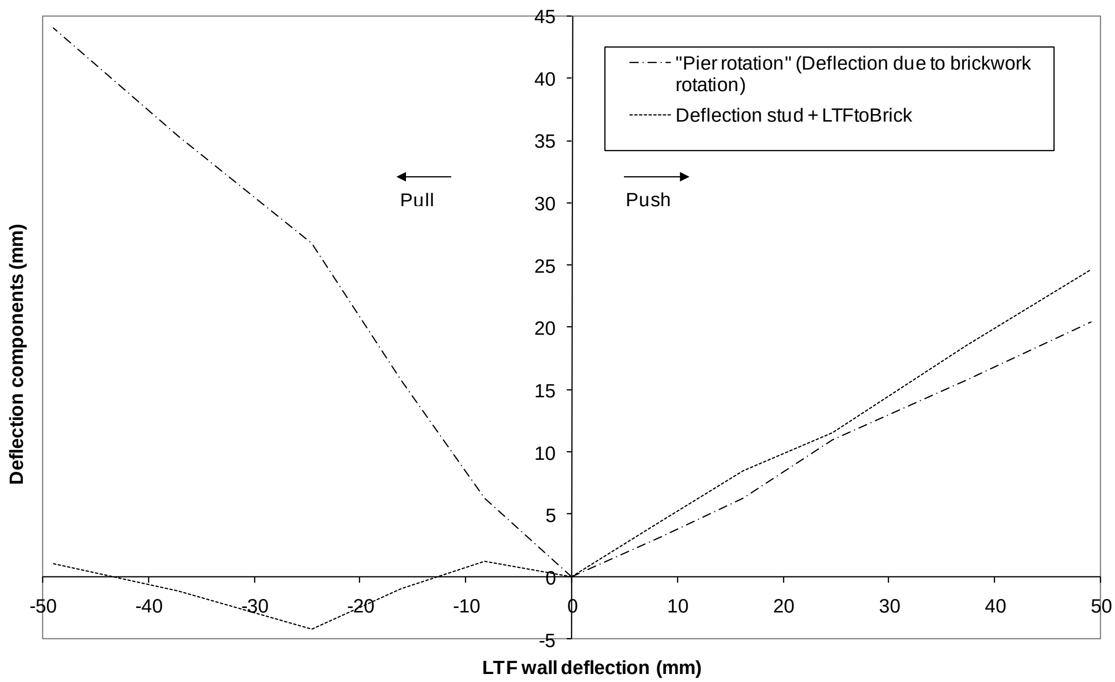


**Figure 65. Components of brickwork deflection for the L-shaped veneer element of Corner 4**

# APPENDIX B CYCLIC TESTING OF ROOM 2

## B.1 Construction

Room 2 was a single-storey nominally 2.4 m high room, as shown in Figure 66 to Figure 69. It had plasterboard-lined light timber-framed (LTF) walls and a timber-framed plasterboard-lined ceiling. There were three separate sections of brick veneer. These were an isolated 4.82 m long panel on Side 1, an isolated 3.20 m long panel on Side 2 (Figure 66 to Figure 68) and an L-shaped corner veneer element on Side 2 (Figure 69). Figure 66 defines the labelling of the corners, sides and ends. The details of the LTF, brick veneer and foundation construction are as described in Appendix A.

## B.2 Test method

The deflection regime imposed on the side LTF walls is summarised in Table 5.

## B.3 Instrumentation

Potentiometers were used to measure:

- The deflection of the brickwork relative to the timber framing at four places on the side walls for the direction parallel to the brick veneer, as shown in Figure 40.
- The uplift deflection of the brickwork relative to the timber framing at six places at wall ends.
- The in-plane horizontal deflection of the top of Side 1 and also Side 2 LTF walls relative to the ground.
- The horizontal displacement of the ceiling relative to the ground at the actuator loading point.

A steel rule was used to measure:

- Uplift and horizontal slip of the LTF walls at many places.
- Horizontal slip of the brick veneer relative to the foundation beam.
- Vertical changes in length (effectively brickwork crack widths) between lines drawn on the brickwork between which brick cracks were expected to occur or subsequently did occur at the locations A1, A2, B1, B2, C1, C2 and D1 shown in Figure 66.

The following forces were measured by load cells:

- Horizontal load in the brick veneer was measured by the load cells in the horizontal ring beam restraint elements shown in Figure 31 and Figure 33.
- The total load applied to Room 2 at the ceiling level at mid-width of the room.

## B.4 Room 2 test results

### B.4.1 Measured forces in brick veneer

A plot of Side 1 brickwork horizontal load versus adjacent LTF side wall deflection is shown in Figure 80. Once cracks had formed peak loads were approximately ±8.6 kN irrespective of the LTF wall deflection. This is consistent with the wall slipping on the concrete foundation at a constant slip coefficient.

The only brickwork on Side 1 was Panel A (see Figure 66 and Figure 67). This deformed by sliding on a crack between the brick veneer and the foundation concrete and had almost zero rotation. The weight of the panel is estimated to be 130 x 4.82 x 2.22 = 1391 kg = 13.6 kN. The slip force was estimated from Figure 80 to be approximately 8.6 kN. Thus, the effective slip coefficient of friction was 8.6/13.6 = 0.63.

A plot of Side 2 brickwork horizontal load versus adjacent LTF side wall deflection is shown in Figure 81.

The brickwork on Side 2 was Panel B and an L-shaped corner veneer element called Panel C on Side 2 and Panel D on End 2 (see Figure 66 and Figure 68). Panel B deformed by sliding on a crack between the brick veneer and the foundation concrete but also exhibited significant rotation. Based on a slip coefficient of friction of 0.63 and its self-weight of 9.05 kN the expected slip force = 5.70 kN. The theoretical performance of Panel B is plotted in Figure 81 which after a LTF deflection of 16 mm is governed by shear slip.

Panel C had negligible shear slip. This was expected as the connection between end brick veneer and LTF walls would have resisted such slip. The relationship between load in the L-shaped corner veneer element and the deflection of the adjacent LTF walls was calculated using the theory developed in Section 5.2. The total theoretical relationship (slip of Panel B + rocking of Panel C) is plotted in Figure 81. The theory gives a reasonable agreement with the measurements, particularly after Panel B had cracked at the base (i.e. after 8 mm LTF deflection). The theory was slightly conservative compared to test measurements.

**Table 5. Deflections imposed on LTF Side 1 and Side 2 walls**

| Deflections imposed (mm) | Number of cycles |
|---|---|
| ± 4 | 2 |
| ± 8 | 3 |
| ± 12 | 2 |
| ± 16 | 3 |
| ± 24 | 3 |
| ± 36 | 3 |
| ± 50 | 3 |
| ± 74 | 3 |

### B.4.2 Estimate of brickwork tension bond strength ($f_{mt}$)

It was noted that a fine crack had formed at the bottom of the 3.2 m long Panel B (Side 2 in Figure 66) after cycling to ±8 mm deflection. The corresponding loads in Side 2 brick veneer were 13.3 and -12.8 kN. If the strength of the L-shaped corner veneer element is assumed to rock at 4.37 kN, as predicted by the theory in Section 5.2, then the shear load taken by Panel B at first cracking is estimated to be (13.3+12.8)/2 – 4.37 = 8.68 kN. This can be used to provide a rough approximation of the tension bond strength of the brickwork to concrete foundation, $f_{mt}$.

Assuming the force on the brickwork is applied effectively at 2/3 of the total height, then the applied moment =

8.68 x 2/3 x 2.22 = 12.8 kNm

The resistance due to self-weight =

1.27 x 2.22 x $3.2^2$/2 = 14.4 kNm which is almost the same amount.

Hence the moment of the section at first cracking is 12.8 – 14.4 kNm (i.e. slightly negative). This implies that the resistance provided by the brickwork to mortar tension bond ($f_{mt}$) is negligible.

### B.4.3 Estimate of brickwork shear bond strength ($f_{mv}$)

It was noted that a fine crack formed at the bottom of Panel A at A1 (Side 1 in Figure 66) at 8 mm deflection and at A2 at -12 mm. The corresponding loads in Side 1 brick veneer were 13.7 and -14.6 kN. This is not expected to cause the bond between brickwork and foundation to fail due to the rocking forces alone, as shown by the following calculations:

Assuming the force on the brickwork is applied effectively at 2/3 of the total height, the overturning moment = 0.5 x (13.7 + 14.6) x 2/3 x 2.22 = 20.9 kNm.

The resisting moment due to the brickwork self-weight is given by:

= 1.27 x 2.22 x $4.82^2$/2 = 32.2 kNm,

where the veneer self-weight is 1.27 kN/$m^2$.

As the resisting self-weight moment exceeds the imposed overturning moment, Panel A is not expected to rock even when a crack has formed, as indeed was the case. The shear bond strength between the brickwork and concrete foundation, $f_{sbc'}$ is therefore taken as the failure shear less the shear friction. (Note: the average compressive stress, hence shear friction, is not affected by the overturning moment.) The shear friction is estimated in Section B.4.1 to be 0.63, thus:

0.5 x (13.7 + 14.6) = 0.63 x 1.27 x 2.22 x 4.82 + $f_{mv}$ x 4.82 x 0.07

or $f_{mv}$ = 16.6 kPa. This is very small and thus $f_{mv}$ can be assumed to be zero.

### B.4.4 Brickwork cracking

Cracks observed in the brickwork mortar were marked by felt pen at the peak loads. No cracks occurred within the bricks themselves. The cracks are sketched in Figure 88. Panels A and B simply cracked along the mortar course at the intersection of the brickwork and concrete foundation. Based on the cracking load, calculations in Sections B.4.2 and B.4.3 indicated that the tension and shear bond strengths along these joints was very low.

With the L-shaped corner veneer element, cracks occurred in the mortar course one brick above the intersection of the brickwork and concrete foundation.

Panel A brickwork movement was purely sliding along the base crack and there was no rocking. The shorter isolated Panel B exhibited both sliding along the base crack and rocking by pivoting at the crack ends. The L-shaped corner veneer element exhibited no sliding but purely rocking. It is likely that the brick-ties connecting Panel D to the adjacent LTF wall forced Panel D to deform the same amount as the LTF wall by rocking at the base, thus preventing the veneer from sliding along the base crack.

### B.4.5 Movement of brick veneer relative to LTF wall

Uplift of both the LTF wall and base beam was measured at wall opening edges and room corners and horizontal slip was measured at mid-length of wall elements. The maximum movement monitored did not exceed 1 mm.

The components of deflection are plotted below using Eqn. (11) in the same manner as for Room 1. This is reproduced below for ease of reference, although slightly reordered.

$$\Delta_{\text{Stud at gauge}} = \text{LTFdef x GaugeHeight / LTFheight} - \Delta_{\text{LTFtoBrick}} - \Delta_{R} - \Delta_{\text{shear}} \quad \dots (12)$$

Figure 83 plots $\Delta_{\text{LTFtoBrick}}$, $\Delta_R$, $\Delta_{\text{shear}}$ and $\Delta_{\text{Stud at gauge}}$ for a gauge near the top of Panel A veneer versus LTF deflection where $\Delta_{\text{Stud at gauge}}$ is calculated from Eqn. (12). The notation in the plot is as defined in Table 4. The figure averages the results from the “push” and “pull” directions.

The plot shows that the magnitude of $\Delta_{\text{Stud at gauge}}$ and brickwork rotation were low for all LTF deflections. Up to 16 mm LTF deflections, the brickwork ties accommodated most of the horizontal displacement of the ceiling. Beyond 16 mm the slip of the brickwork on the concrete foundation took up most of the additional LTF deflections.

Figure 84 was plotted for a gauge near mid-height of Panel A veneer shows that $\Delta_{\text{Stud at gauge}}$ was of similar magnitude to $\Delta_{\text{LTFtoBrick}}$ and $\Delta_{\text{shear}}$ for deflections greater than 24 mm. This corresponds to the deflection when the lining became ineffective or fell off and was unable to restrain stud bending. The magnitude of $\Delta_{\text{LTFtoBrick}}$ was similar at mid-height of the brickwork to that at the top of the brickwork.

Figure 85 and Figure 86 show similar plots, but for Panel B similar conclusions apply except that $\Delta_{\text{shear}}$ was slightly less and $\Delta_R$ greater than for Panel A.

The relative deflection between veneer and LTF wall (i.e. $\Delta_{\text{LTFtoBrick}}$) was not measured in Panel C. Thus, $\Delta_{\text{LTFtoBrick}}$ was moved to the LHS of Eqn. (12) and

Figure 87 plots $\Delta_R$, $\Delta_{shear}$ and $\Delta_{Stud\ at\ gauge}$ + $\Delta_{LTFtoBrick}$ for the top of the veneer. The figure plots the results for both the "push" and "pull" directions as a different performance is expected for both directions due to the "L" shape of the brickwork. The magnitude of ($\Delta_{Stud\ at\ gauge}$ + $\Delta_{LTFtoBrick}$) was low for all LTF deflections, indicating that most of the movement of the panels was due to rocking.

As the brickwork did not crack vertically at the corner, it is not surprising that $\Delta_{LTFtoBrick}$ was low as the ties between the end wall and LTF would have prevented this movement unless they buckled in compression or extended in tension.

The horizontal movement at the top of the brickwork relative to the ground was measured directly and gave good agreement with $\Delta_R$ + $\Delta_{shear}$ for all three panels.

### B.4.6 Summary on deflection components

As the three brick elements were effectively isolated from each other, a single crack formed at the base of the veneer and the brickwork above either slipped horizontally or rotated on these cracks.

Stud flexural deflection was not significant near the top of panels.

At mid-height of the panels stud flexural deflection was not significant for LTF deflections up to 24 mm. Subsequently, the lining became ineffective and significant stud bending deflection occurred.

Deflection taken up by pier rotation was effectively zero for the 4820 mm long Panel A. The adjacent LTF wall deflection was largely taken up by deformation of the brick-ties and slippage of the brickwork along the crack between the brickwork and the concrete foundation.

Deflection taken up by pier rotation was significant for the 3200 mm long Panel B, being greater than the base slip ($\Delta_{shear}$) for LTF wall deflections less than 22 mm. The calculated brickwork rotation-induced horizontal deflection, based on measured crack widths, was approximately 50% of the measured brickwork horizontal movement at 16 mm LTF wall deflection but this decreased to 25% at 50 mm LTF wall deflection.

In the L-shaped corner veneer element, the magnitudes of $\Delta_{Stud\ at\ gauge}$, $\Delta_{LTFtoBrick}$, and $\Delta_{shear}$ were very low for all LTF deflections showing that almost the entire movement of the panel was due to pier rocking. It was concluded that the L-shaped corner veneer element rocked with little horizontal load being transferred from LTF to brickwork via the brick-ties in the side wall Panel C (i.e. only minor tie deformations). As the brickwork did not crack vertically at the corner, it is not surprising that slip between the LTF and brickwork was low as the ties between the end wall and LTF would have prevented this movement unless they buckled or extended in tension.

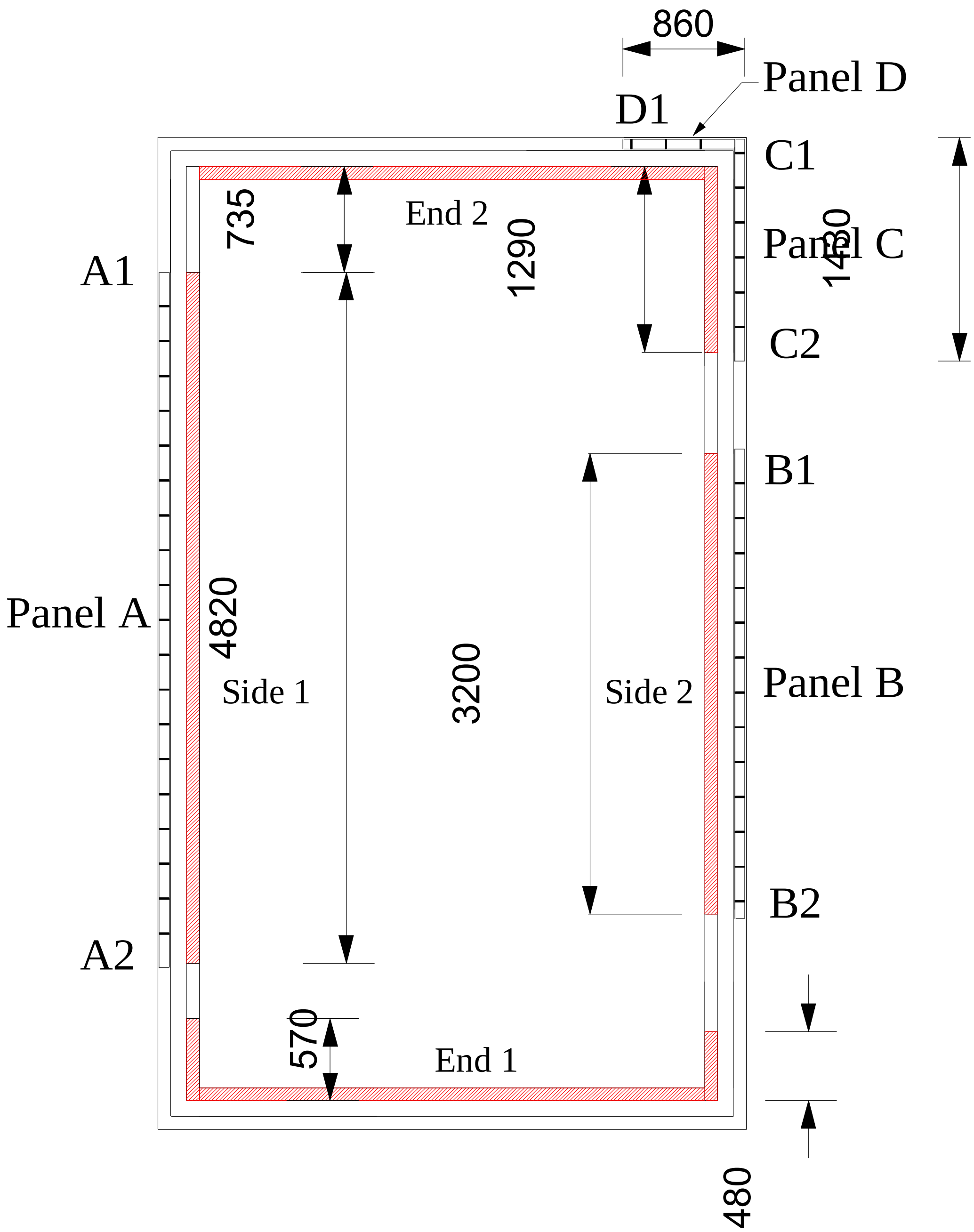


**Figure 66. Plan view of Room 2**


**Figure 67. Room 2 - Panel A on Side 1**


**Figure 68. Room 2 - Panel B and C on Side 2**

**Figure 69. Room 2 - End 1 - no brick veneer.**


**Figure 70. Room 2 - Panel C on End 2**

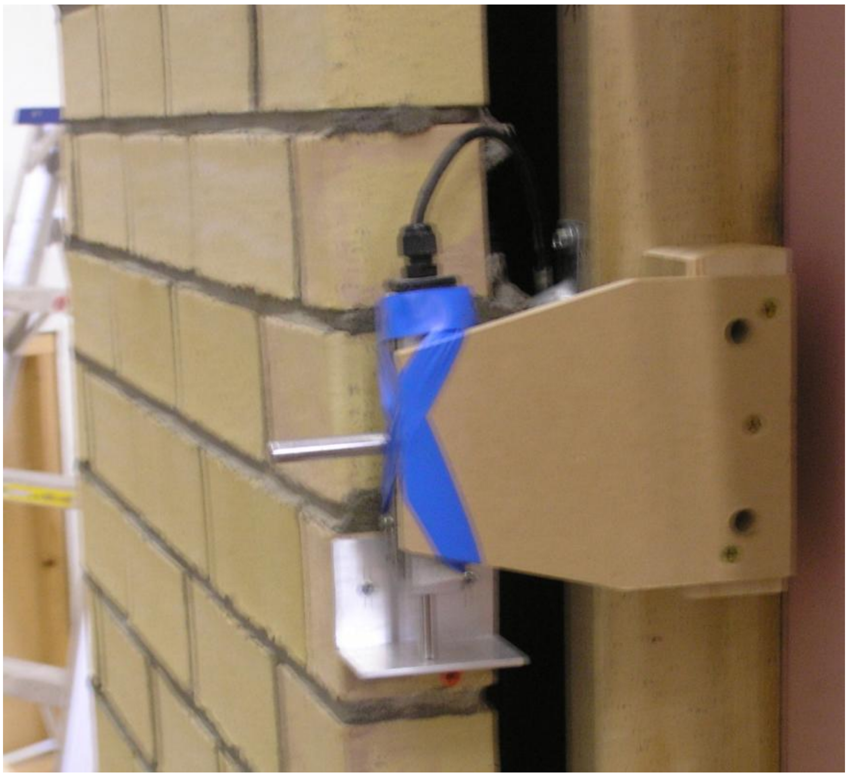

**Figure 71. Vertical deflection gauge**

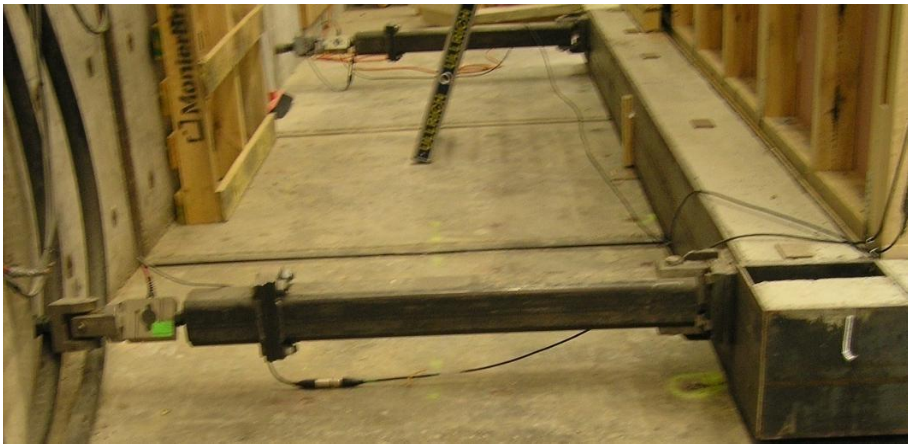

**Figure 72. Ring beam end restraints**

**Figure 73. Crack in Panel C**

**Figure 74. Cracking of the L-shaped corner veneer element under push load**

**Figure 75. Panel sliding and crack opening on Panel B**


**Figure 76. Tie distortion due to pier uplift**

**Figure 77. Stud curvature and brick pier sliding**


**Figure 78. Stud curvature**

**Figure 79. Stud curvature and pier sliding**

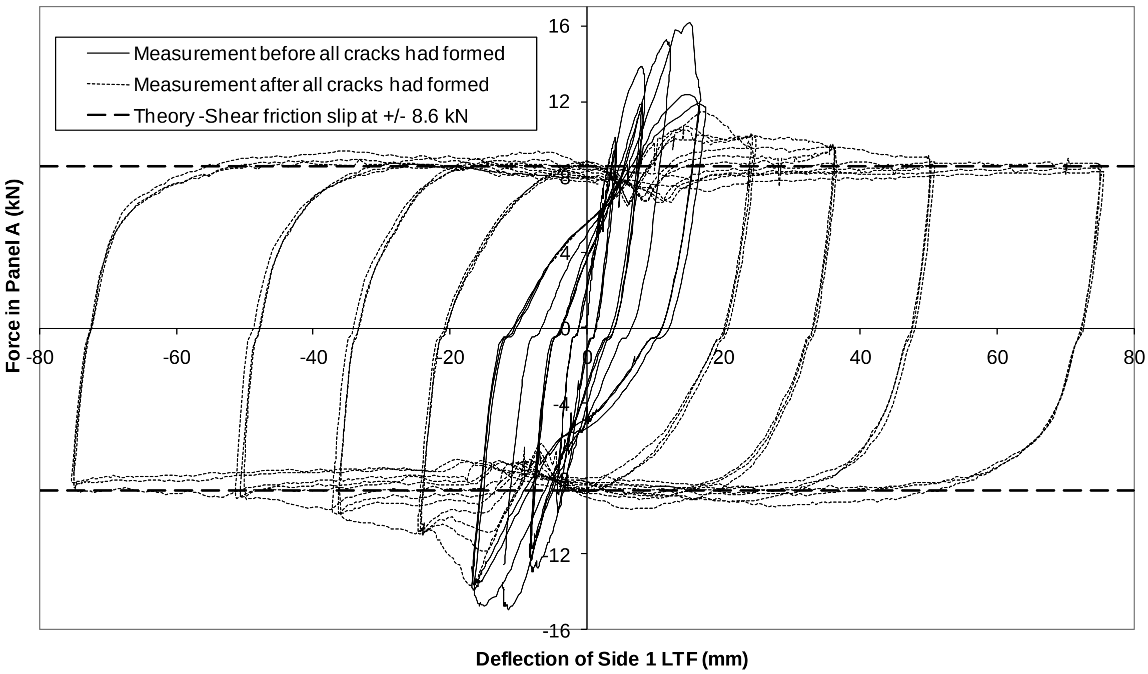


**Figure 80. Room 2 - load in Side 1 brick veneer versus deflection of adjacent LTF - comparison of theory and experiment**

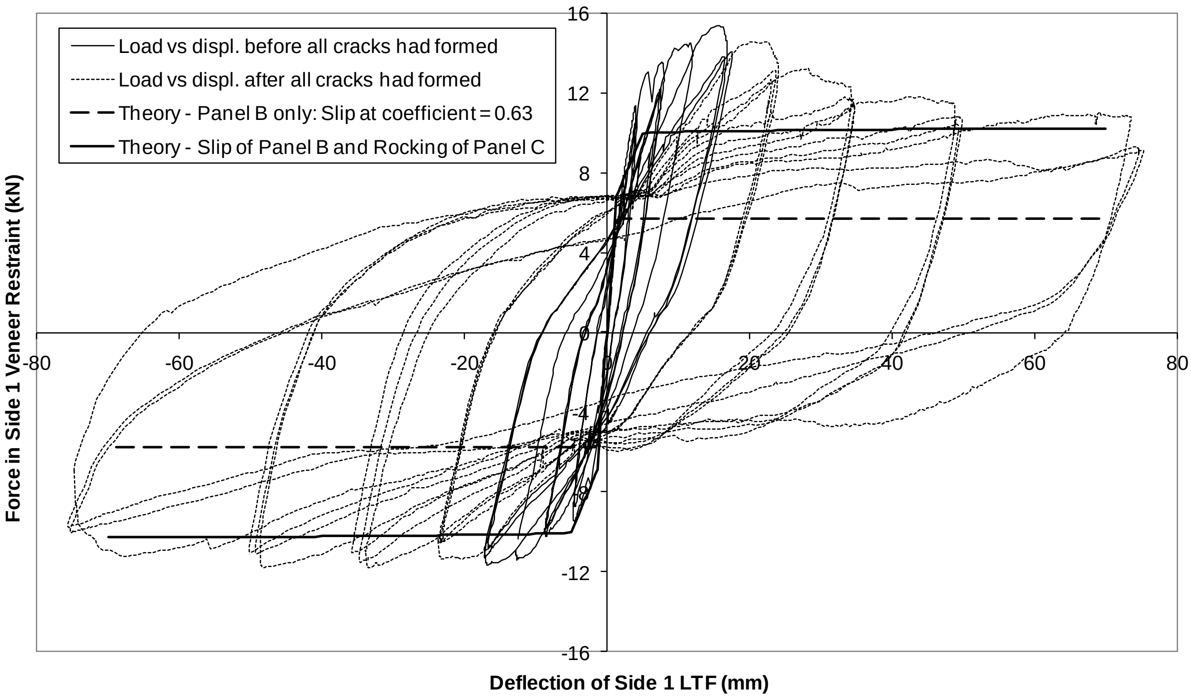


**Figure 81. Room 2 - load in Side 2 brick veneer versus deflection of adjacent LTF wall - comparison of theory and experiment**

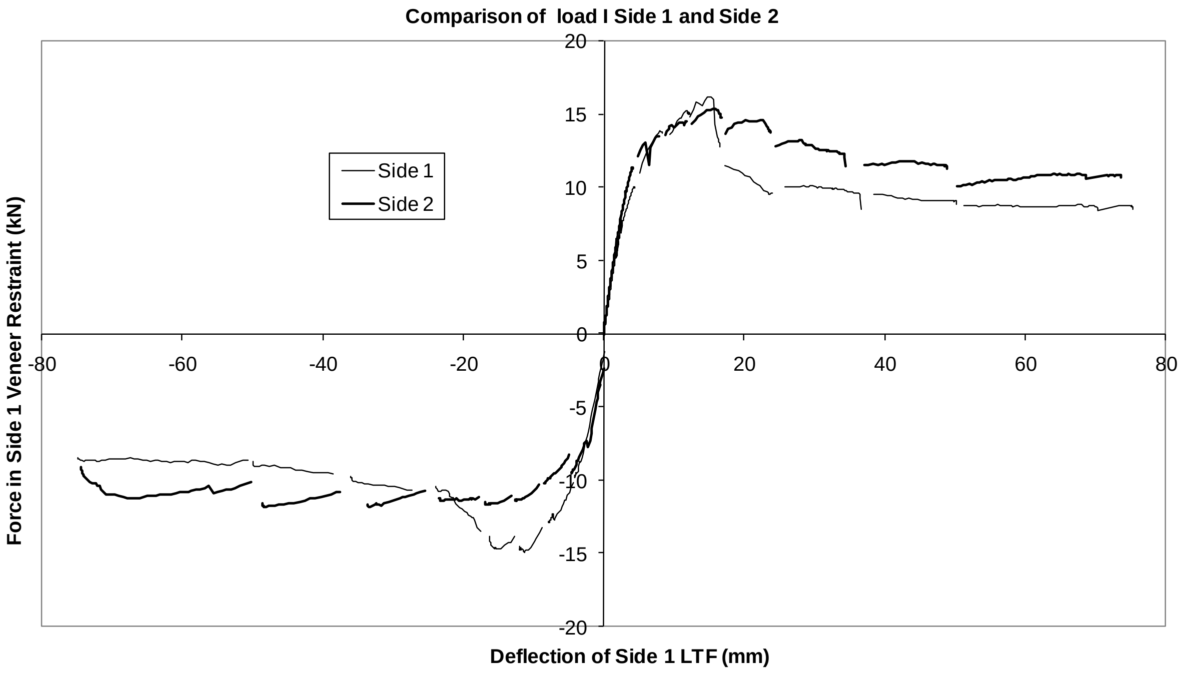


**Figure 82. Room 2 - backbone curve of load in Side 1 and Side 2 brick veneer versus deflection of the adjacent LTF walls**

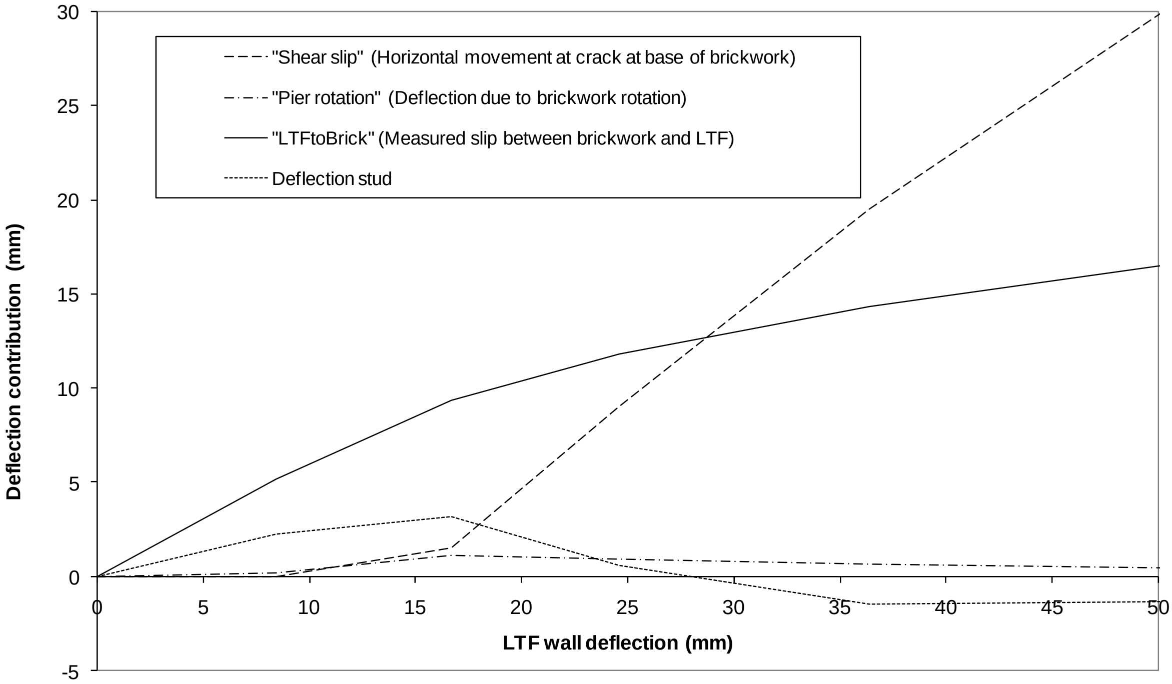


**Figure 83. Room 2 - components of brickwork deflection at the top of Panel A**

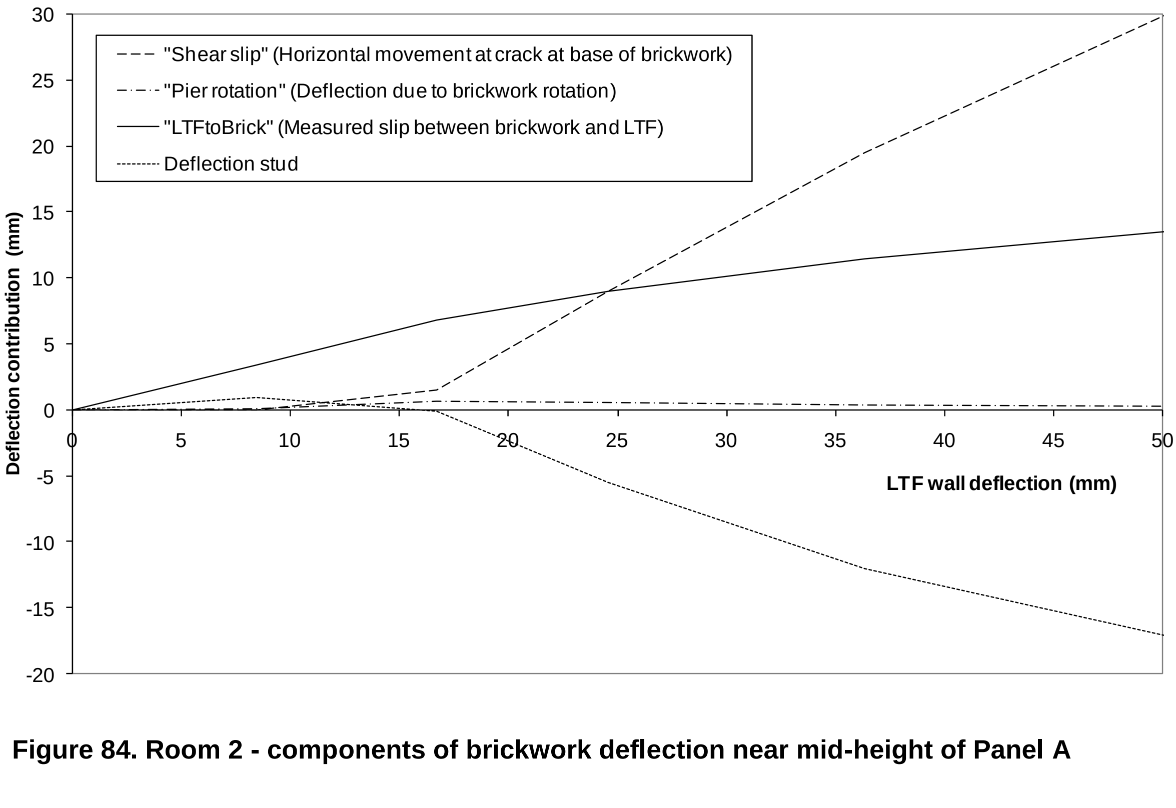


**Figure 84. Room 2 - components of brickwork deflection near mid-height of Panel A**

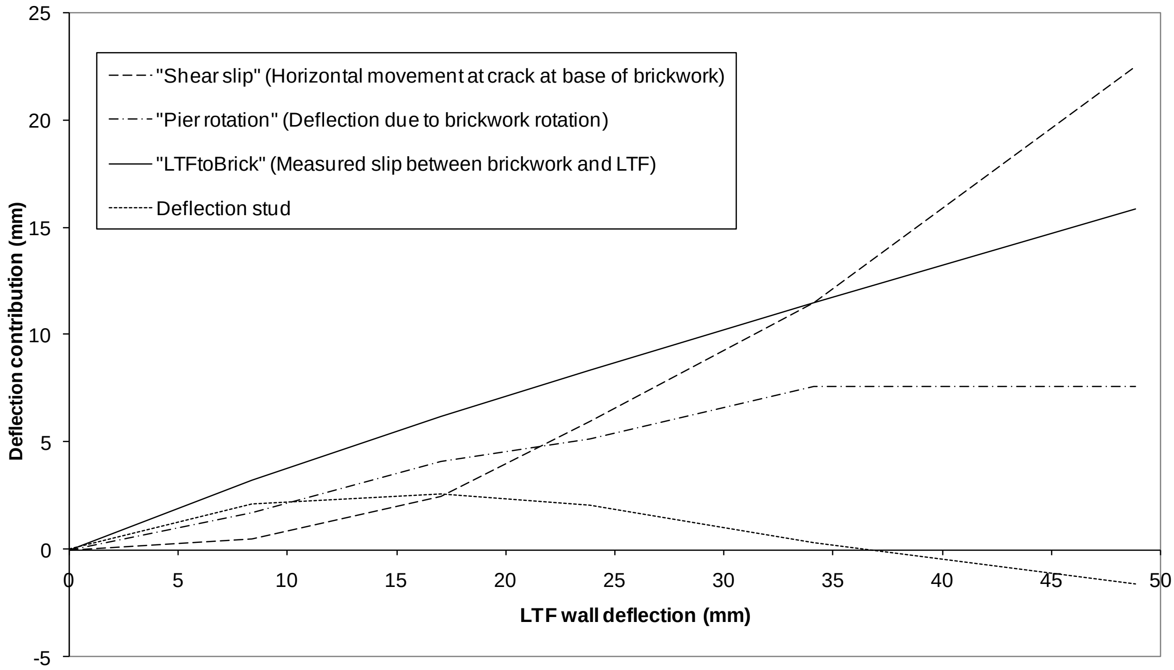


**Figure 85. Room 2 - components of brickwork deflection near the top of Panel B**

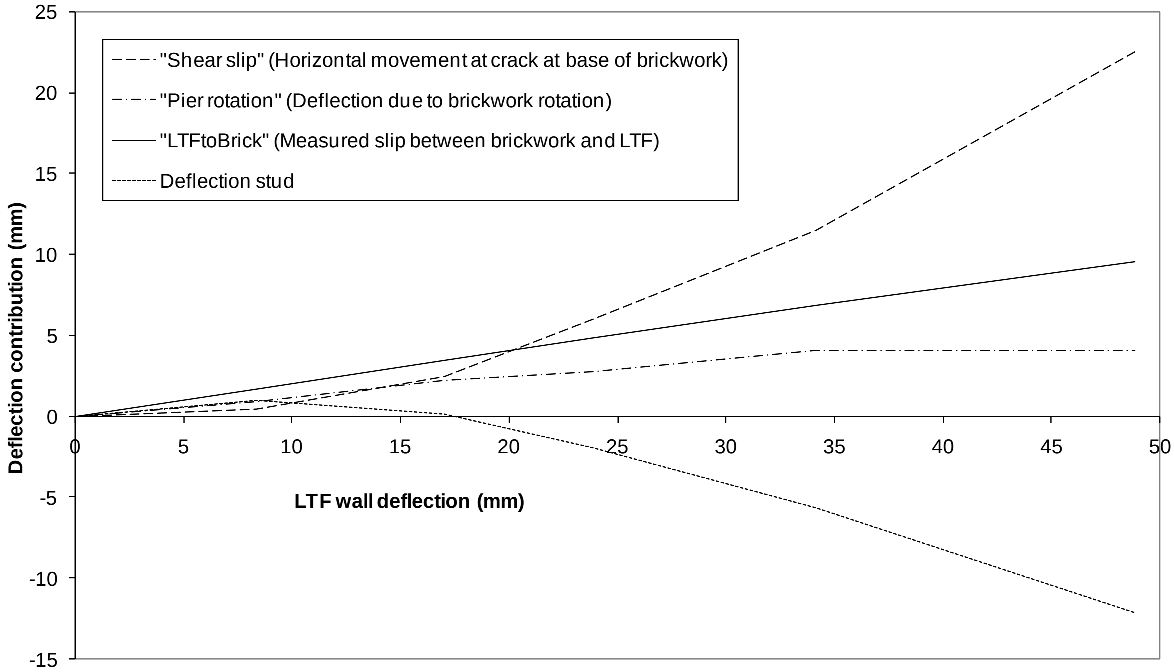


**Figure 86. Room 2 - components of brickwork deflection near mid-height of Panel B**

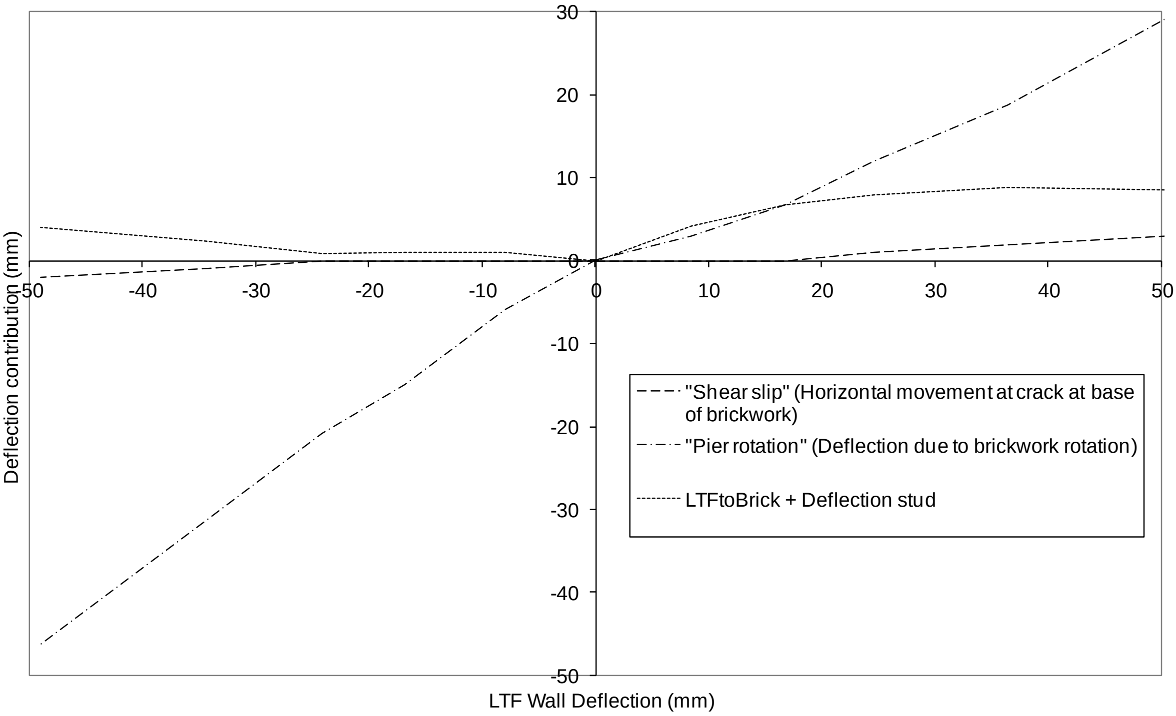


**Figure 87. Components of brickwork deflection for the L-shaped corner veneer element**

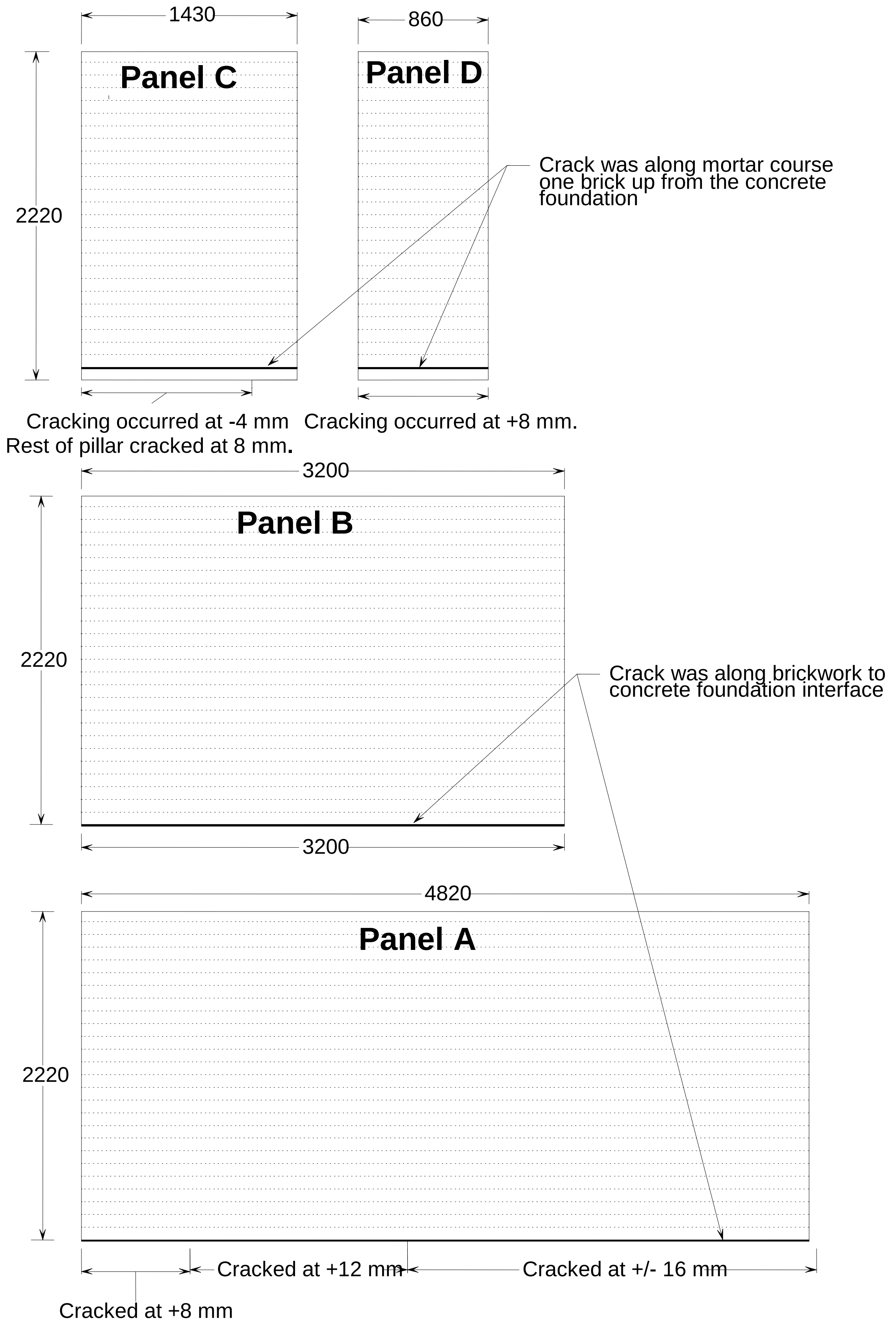


**Figure 88. Room 2 brickwork cracking**

# APPENDIX C SMALL SPECIMEN TESTING

## C.1 Introduction

Three foundations were made from concrete as shown in Figure 89. The top surface of one of these was painted with two coats of Mulseal™ (a bitumen impregnated liquid which dried to give a surface texture and appearance much like tar). As is normal practice on building sites, the long top edges of the foundation were rebated 45 mm deep by 90 mm wide using lengths of timber. When the concrete flows under this formwork, air bubbles are trapped on the top surface of the fresh concrete, creating pockets in the concrete surface.


**Figure 89. Concrete beam used as a foundation to fix bricks**

## C.2 Specimen construction

A tradesman laid the bricks shown in Figure 89. The bricks shown up-ended on the top surface have already been “plucked” off, as described in Section C.4, and the photograph shows the mortar residue left on the bricks and concrete. Horizontal shear tests were performed on the brick wall elements laid along the foundation edges shown in Figure 89, as described in Section C.3.

Separate bond wrenching tests were performed, as described in Section C.5.

The concrete bases were approximately two weeks old and the Mulseal™ three days old at the time the bricks were mortared into position. All brick veneer specimens were left outside to weather for approximately eight months before testing.

## C.3 Shear tests on brick wall elements

Each foundation shown in Figure 89 had two brick wall elements, each being only two bricks high. Two shear tests were performed on each element, as shown in Figure 90. An axial load applied to the element helped resist overturning and provided shear friction resistance representative of veneer above the joint.

In the first test a horizontal load was applied to the bottom layer of bricks and a reaction applied at the bottom of the foundation beam, thus measuring the brick-to-foundation shear strength. Results are summarised in Table 6 for brick mortared to a bare concrete foundation and Table 7 for brick mortared to a Mulseal™ coated concrete foundation. In all cases failure was between the mortar and concrete foundation or mortar and Mulseal™ rather than along the mortar-to-brick interface.

In the second test a horizontal load was applied to the top layer of bricks and a reaction applied at the bottom layer, thus measuring the brick-to-brick shear strength. Test results are summarised in Table 8. An example is given below to explain how the values were obtained.

An example plot of measurements for the first test is shown in Figure 92. An axial load of 3.95 kN was initially applied to the brick element. In this test the wall was 968 mm long whereas in all the others it was 1200 mm long. The 70 mm wide bricks protruded 10 mm over the edge of the foundation, thus only 60 mm were supported on the concrete. Hence, the axial stress due to the applied load was 3.95/0.060/0.968 = 68 kPa. The axial load due to two layers of brick (3.4 kPa) needed to be added to this giving a total of 71 kPa. (To relate this to typical axial pressures for brick veneer in actual construction, note that a 2.2 m high brick veneer of the construction tested has a self-weight axial load of approximately 47 kPa.)

As can be seen in Figure 92, at a peak shear load of 17.4 kN (i.e. 17.4/0.060/0.968 = 299 kPa shear stress) the brick-to-concrete foundation joint cracked between the mortar and concrete and the resisted load fell quickly and began to flatten out. At 28 mm actuator deflection the shear load had reduced to 4.08 kN (i.e. 4.08/0.060/0.968 = 70 kPa residual shear stress) which indicates an effective shear friction, μ, of 68/70 = 0.97. (This is shown in Table 6 as 0.98 as calculated by the spreadsheet without rounding.)

At this stage the axial load was increased to 7.25 kN (128 kPa) and the load to continue shearing the interface was 7.15 kN. The axial load was then reduced to 3.95 kN again and subsequently the shear load continued to decrease with greater applied deflection at this load.

The shear friction values given in the tables are at the maximum applied deflection. Clearly the shear friction is a function of slip deflection and the reduction may have been due to “lubrication” provided by the crushed mortar at the interface. Values given are significantly greater than the shear friction values of 0.63 measured for Room 2. Several causes of this incompatibility are possible:

- The brick ties may have been applying a net uplift force on the veneer panels in the room tests.
- The concrete surface in Room 2 was trowelled smoother than used for the small sample tests.
- The measurement of shear force in the veneer may have been underestimated due to friction in the support beam rollers.

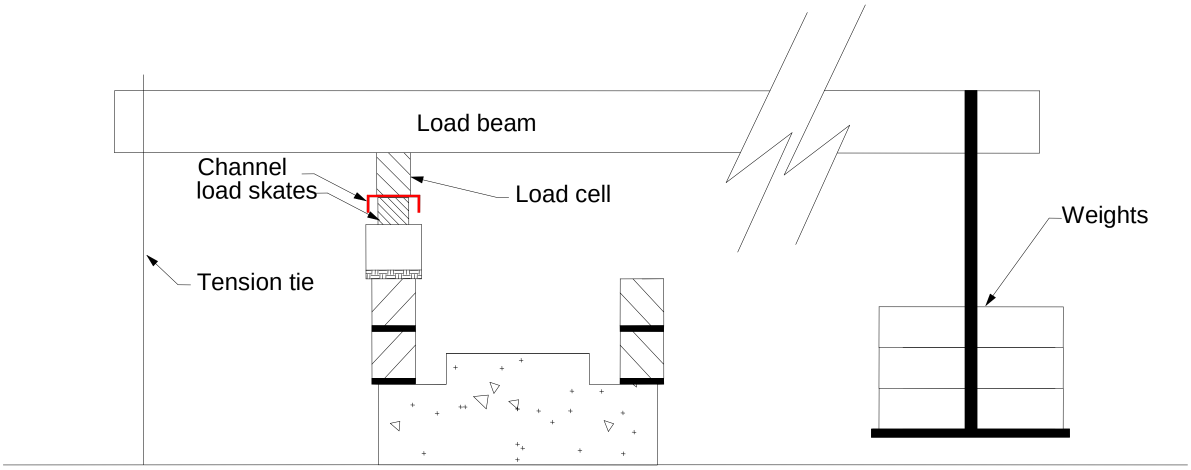


Cross Section

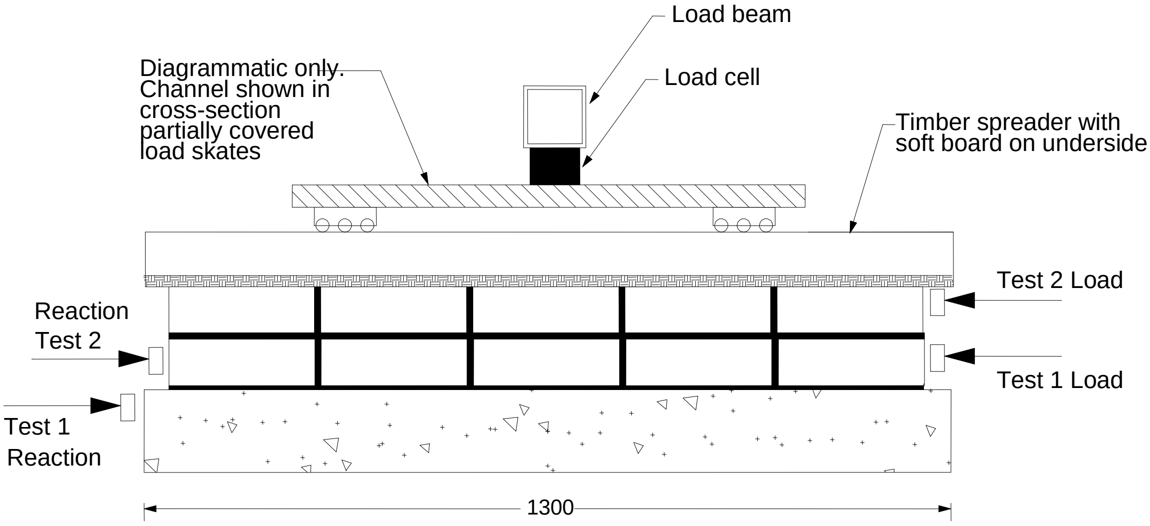


Elevation

**Figure 90. Shear test setup**

The peak shear strength of the brick-to-brick interface (Table 8) averaged 516 kPa across the test elements, which is 26% more than the corresponding value for the brick-to-concrete foundation interface (Table 6, 409 kPa). This may be partially due to the weaker bond of the mortar cast against bare concrete which may have “sucked” moisture from the mortar or otherwise from the mechanical action of the brick mortar dowels between the brick courses shown in Figure 10.

No cracks occurred at the base of the Room 1 veneer except for a small length of Panel G (Figure 51 to Figure 53). As the total length of brickwork (including the end walls) was 13.5 m, the predicted total bond strength between brickwork and concrete foundation = 13.5 x 0.07 x 409 = 387 kN which is far greater than the applied loads shown in Figure 27. So it is not surprising that no brick veneer base slip was observed in Room 1. The slip observed in Panels A and B of Room 2 is expected to be because the bond was ruptured by rocking before slip occurred. No brick-to-brick slip occurred along crack lines in either room. It is expected that once the bond had been ruptured by rocking the mechanical action of the dowels resisted any slip.

The peak shear strength of the brick-to-coated concrete foundation averaged 619 kPa, which is 51% more than that for the brick-to-uncoated concrete foundation. The failure was at the mortar-to-Mulseal™ interface rather than the brick-to-mortar interface. Post-cracking, the shear friction coefficient was only half that measured for joints with no coating. Thus, if a coated joint at the bottom of a panel is pre-cracked by rocking, it will slip at a lower shear load than a corresponding panel on an uncoated concrete foundation. However, based on the test results, from a structural perspective Mulseal™ is still considered to be a suitable damp-proof course.

## C.4 Plucking tests

Plucking tests were performed as shown in Figure 93 with the results summarised in Table 9. Steel plates sandwiched the bricks, thus allowing them to be pulled from the foundations. These were lifted off and the peak load was measured using a load cell.

The results initially reported in this section brick-to-concrete specimens are considered to be suspect as they were so low. It is likely that they were damaged and then autogenously healed. The tests were repeated and tested at age 6 months and the results replaced those initially in the table.

The mean of the brick-to-concrete specimens was 254 kPa. The four test specimens with bricks bonded to Mulseal™ coated concrete had an average strength of 175 kPa.

In all cases the failure of the brick-to-concrete specimens occurred at the interface of the mortar and concrete whereas in the Mulsealed concrete specimens the failure was between the mortar and brick.

Although an effort was made to make the loading concentric, accidental eccentricities are likely to have influenced results.

**Figure 91. Coated foundation test specimen showing end condition after brick plucking tests**

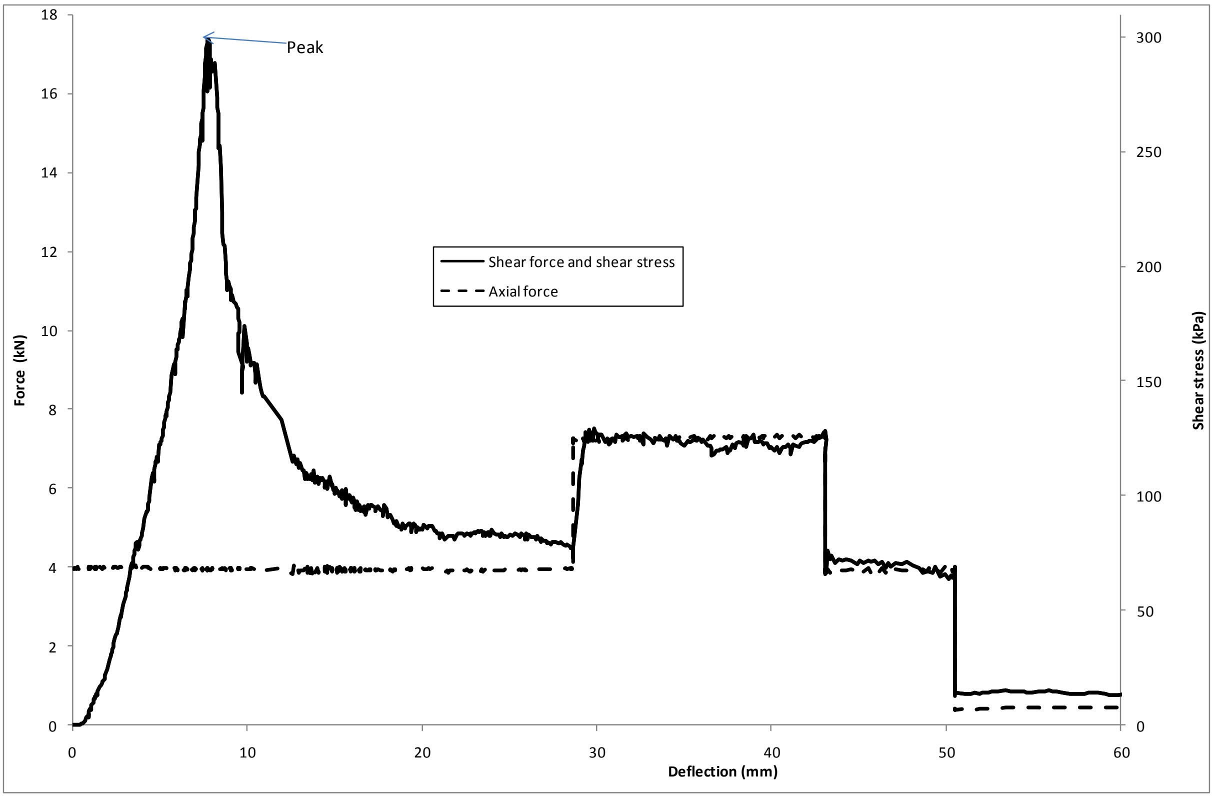


**Figure 92. Plot of shear force and axial load versus actuator movement in brick-to-foundation shear test on Specimen 1**

**Table 6. Strength of brick-to-concrete foundation bond strength**

| Specimen Number | Axial stress (kPa) | Peak shear stress (kPa) | Residual shear stress (kPa) | Shear Friction μ |
|---|---|---|---|---|
| **1** | 71 | 299 | 70 | 0.98 |
| | 128 | | 123 | 0.96 |
| **2** | 60 | 468 | 56 | 0.94 |
| | 106 | | 88 | 0.83 |
| **3** | 59 | 454 | 46 | 0.77 |
| | 108 | | 81 | 0.75 |
| **4** | 60 | 417 | 64 | 1.07 |
| | 107 | | 94 | 0.88 |
| **Mean** | | **409** | | **0.90** |
| **COV** | | **0.19** | | **0.12** |

**Table 7. Bond strength of brick-to-coated concrete foundation**

| Specimen Number | Axial stress (kPa) | Peak shear stress (kPa) | Residual shear stress (kPa) | Shear Friction μ |
|---|---|---|---|---|
| **5** | 109 | 666 | 59 | 0.54 |
| **6** | 108 | 571 | 39 | 0.36 |
| **Mean** | | **619** | | **0.45** |

**Table 8. Strength of brick-to-brick bond strength**

| Specimen Number | Axial stress (kPa) | Peak shear stress (kPa) | Residual shear stress (kPa) | Shear Friction μ |
|---|---|---|---|---|
| **1** | 71 | 461 | 66 | 0.92 |
| **2** | 58 | 434 | 46 | 0.78 |
| **3** | 105 | | 85 | 0.80 |
| **4** | 104 | 517 | 88 | 0.85 |
| **5** | 107 | 575 | 92 | 0.86 |
| **6** | 105 | 590 | 89 | 0.85 |
| **Mean** | | **516** | | **0.84** |
| **COV** | | **0.13** | | **0.06** |

Figure 93. Plucking test setup

Table 9. Plucking tests results

| Sample | Brick/concrete | | Brick/Mulseal | |
|---|---|---|---|---|
| 1 | 3.475 | kN | 4.962 | kN |
| 2 | 4.025 | kN | 3.149 | kN |
| 3 | 6.51 | kN | 2.241 | kN |
| 4 | 2.535 | kN | 1.423 | kN |
| 5 | 4.785 | kN | | |
| 6 | 3.975 | kN | | |
| 7 | 4.270 | kN | | |
| 8 | 4.565 | kN | | |
| **Mean** | 4.268 | kN | 2.944 | kN |
| **SDEv** | 1.144 | kN | 1.519 | kN |
| **Cov** | 0.268 | | 0.516 | |
| **Mean** | 254 | kPa | 175 | kPa |

## C.5 Brick bond wrench tests

Tests were performed in accordance with NZS 4210 (SNZ 2001). This specifies a code compliance value of 200 kPa for the average mortar flexural tension results. A view of the test setup is shown in Figure 94. Results are given in Table 11.

There is a large scatter of results, but the mean value of 1334 kPa is far higher than that obtained from the plucking tests (254 kPa). This theoretical load is compared with Room 1 test measurements in Table 10. This shows that a tension bond strength of

1334 kPa grossly overestimates the horizontal force to induce pier rocking and 254 kPa is also too great. The last column of Table 10 gives the bond strength required to get a match with test measurements. These calculations show that cracking of piers occurs far earlier than simple strength calculations based on elemental test results predict.

**Table 10. Brick bond wrench tests results**

| | Failure stress (kPa) |
|---|---|
| 1 | 333 |
| 2 | 718 |
| 3 | 2210 |
| 4 | 2313 |
| 5 | 1120 |
| 6 | 889 |
| 7 | 1757 |
| **Mean** | 1334 |
| **Standard Dev.** | 767 |
| **Cov** | 0.58 |

## C.5 Possible issue with brick bond test procedure

The discrepancy is possibly due to the mortar dowels in the bricks wedging in the bricks and therefore resisting the moment applied to the bond wrench test specimens. It is therefore concluded that the plucking test may give more reliable tension bond strengths.

## C.6 Mortar crushing strength

The measured crushing strength of test cylinders, made from the mortar taken from the tradesman's barrow, is summarised in Table 12. The tests were done to NZS 3112: Part 2 (SNZ 1986). The average strength of the standard cured 28 day mortar was 20.2 MPa which is 62% more than the 12.5 MPa minimum strength specified by NZS 4210 (SNZ 2001).

**Table 11. Force to rock Panels B and G of Room 1**

| Panel | Length (m) | LTF deflection at cracking (mm) | Estimated cracking force (kN) | Prediction assuming $f_t$ = 1334 kPa kN | Prediction assuming $f_t$ = 254 kPa kN | Bond stress to match cracking load (kPa) |
|---|---|---|---|---|---|---|
| B | 2.4 | 16 | 8.1 | 101.6 | 18.1 | 36.2 |
| G | 2.4 | 16 | 6.8 | 101.6 | 18.1 | 17.9 |

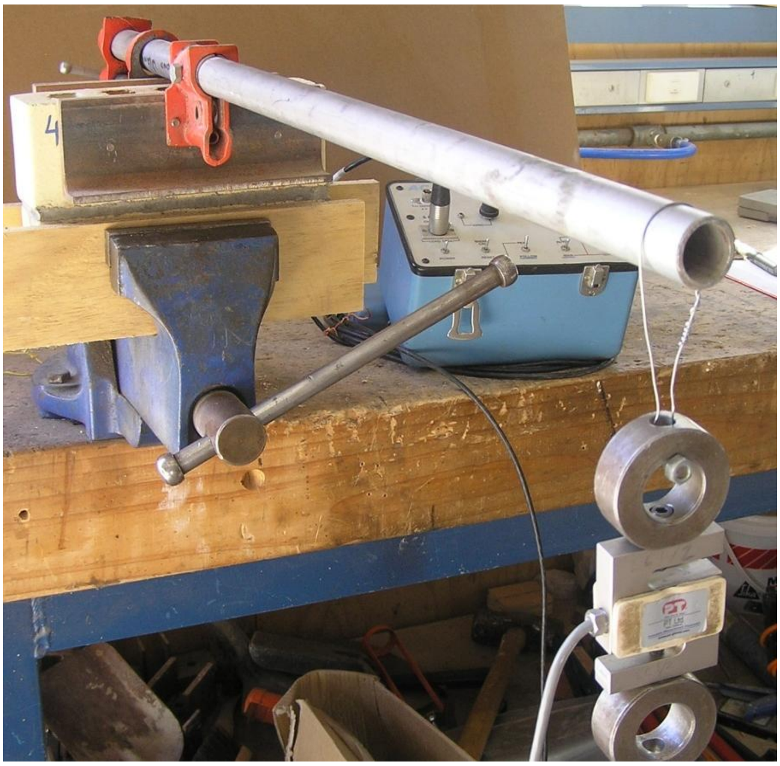

Figure 94.  Bond wrench test

Figure 95.  Plot of horizontal load required to rock brick panels for various tension bond strengths

### Table 12. Measured mortar crushing strength

| Cylinder number | Age (days) | Density kg/m$^3$ | Strength (MPa) | Group average (MPa) | Curing |
|---|---|---|---|---|---|
| 1 | 15 | 1890 | 17.5 | 17.3 | Standard curing |
| 2 | | 1900 | 17.5 | | |
| 3 | | 1890 | 17.0 | | |
| 4 | 15 | 1870 | 15.0 | 16.2 | Double bagged sealed and stored by test room |
| 5 | | 1870 | 16.5 | | |
| 6 | | 1880 | 17.0 | | |
| 7 | 15 | 1760 | 12.5 | 12.8 | Stored in air by test room |
| 8 | | 1750 | 12.5 | | |
| 9 | | 1750 | 13.5 | | |
| 10 | 28 | 1920 | 20.5 | 20.2 | Standard curing |
| 11 | | 1900 | 20.0 | | |
| 12 | | 1900 | 20.0 | | |

# APPENDIX D STRENGTH AND STIFFNESS OF BRICK TIES

## D.1 Shear load-deflection behaviour of brick veneer ties

When a veneer panel rocks, the tie displaces in both a horizontal and vertical direction relative to the LTF. When it does not rock and either remains stationary or slips along a base-course, then the tie displaces in only a horizontal direction relative to the LTF. The relationship between tie horizontal deflection and horizontal load per tie was measured as described below. The set-up ensured the timber framing remained parallel to the plane of the veneer but did not provide restraint against the timber framing moving closer to the veneer, as this was considered to best simulate the constraints that occur in real construction (Figure 96).

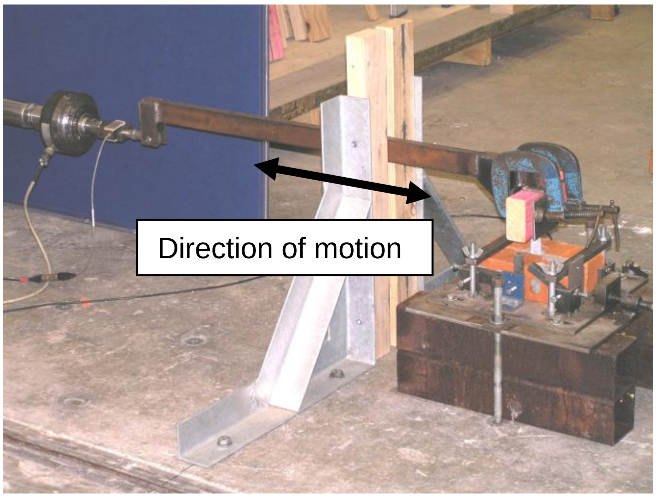


**Figure 96. Test set-up for in-plane shear testing of the veneer ties**

Specimens were constructed using a commonly available stiff brick veneer tie. A couplet of bricks and a section of studs were connected with the ties in much the same fashion as the specimens required to undertake testing to AS/NZS 2699.1.

A selection of the ties were subjected to specified cyclic displacements and several were subjected to increasing cyclic displacements. The plot below provides a backbone curve of the average first cycle load peaks from the tests.

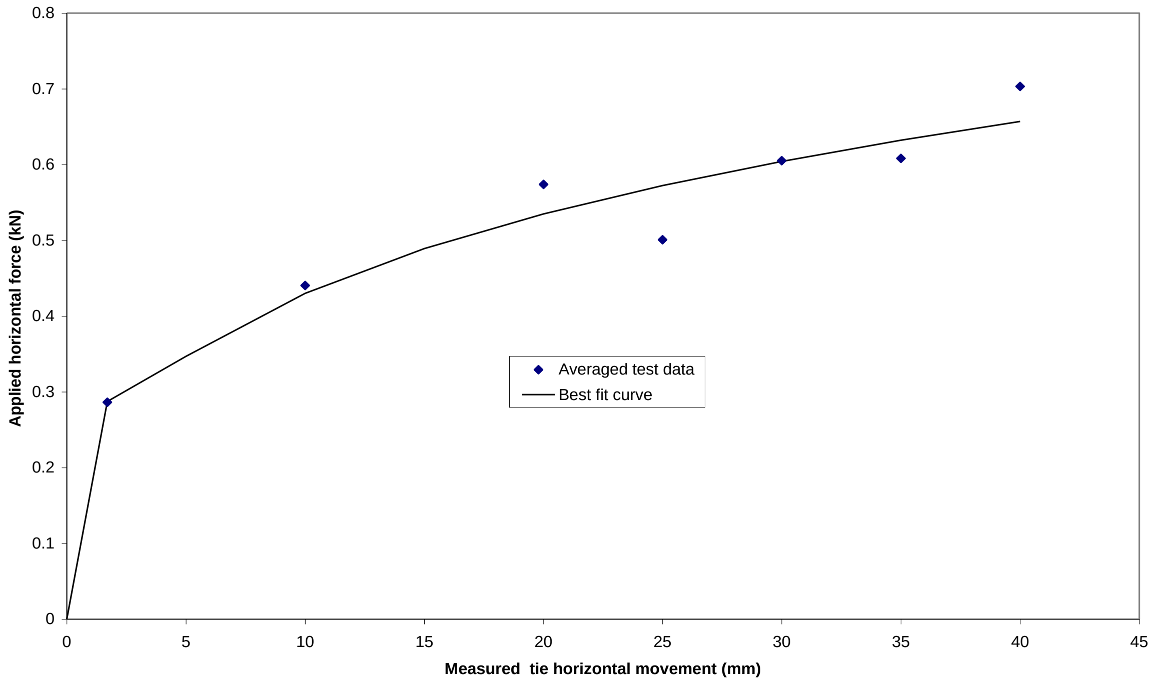


**Figure 97. Measured tie horizontal load versus slip characteristics**

## D.2 Vertical load in brick tie versus vertical tie deflection

The relationship between tie vertical deflection and vertical load was measured as illustrated in Figure 98 for three specimens for the case where the veneer was restrained from moving closer to the LTF and in Figure 99 for three specimens for the case where the veneer was not restrained from moving closer to the LTF. The brick veneer was simulated by a timber stud and the tie to brick veneer mortar bond was simulated by the tie being glued into a slot cut into this stud.

The set-ups ensured the timber stud remained parallel to the plane of the veneer as it was moved in the direction parallel to its long axis. Near veneer corners and the bottom of the veneer there is expected to be close to full restraint against this movement in real construction but near the top of the veneer, well away from corners, the restraint is likely to be small.

It is noted that a tie force versus displacement relationship at an angle (say 45˚) to the timber stud is unlikely to be the simple vector addition of the vertical and horizontal relationships due to twisting of the tie.

As a veneer panel can only move in the upward direction as it rocks (i.e. not in the downward direction), the test regime simulated this as follows. The timber stud simulating the brick veneer was displaced for two cycles between each of the displacement limits of 0 to 10 mm, 0 to 20 mm, 0 to 30 mm, 0 to 40 mm and 0 to 40 mm. Typical hysteresis loops for the two cases are given in Figure 100 and Figure 101. Note, these are given as load per test specimen – ie per two ties. The backbone curves were extracted from the load-displacement loops and peak points are summarised in Table 13 as load per single tie. This table also includes the average load resisted from the three specimens at each displacement. Table 1(b) also includes the mean loads from the two tables (i.e., Table 1(a) + Table 1(b))/2 and the ratio of corresponding loads from Table 1(b)/Table 1(a). The mean loads are adopted in this report as the best estimate of the relationship in real buildings.

**Figure 98. Measured tie vertical load versus horizontal displacement relationship for the case of stud stays the same distance from veneer**

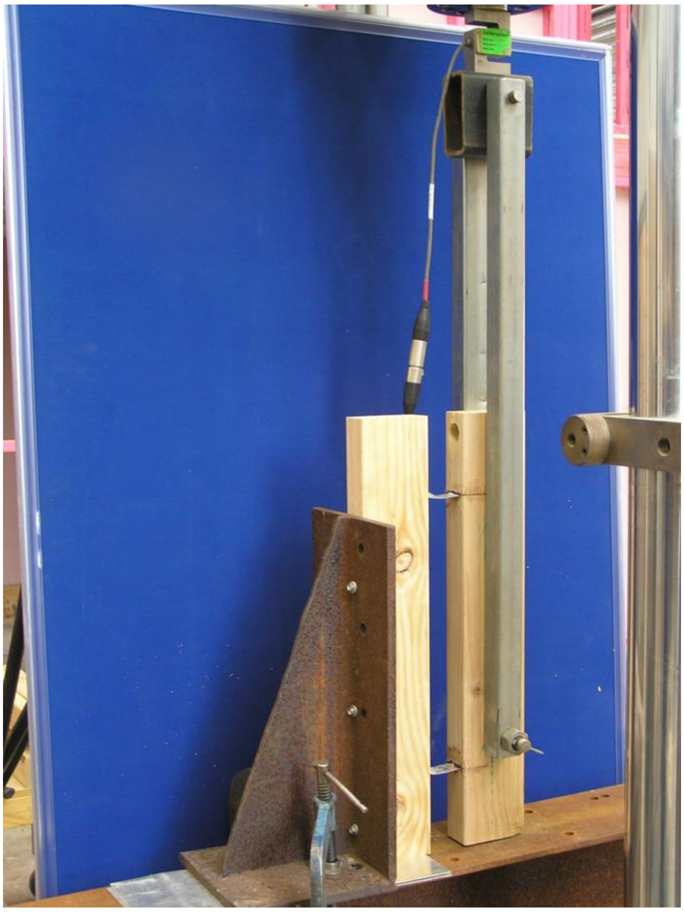

**Figure 99. Measured tie vertical load versus horizontal displacement relationship for the case of stud can move freely closer or further away from veneer**

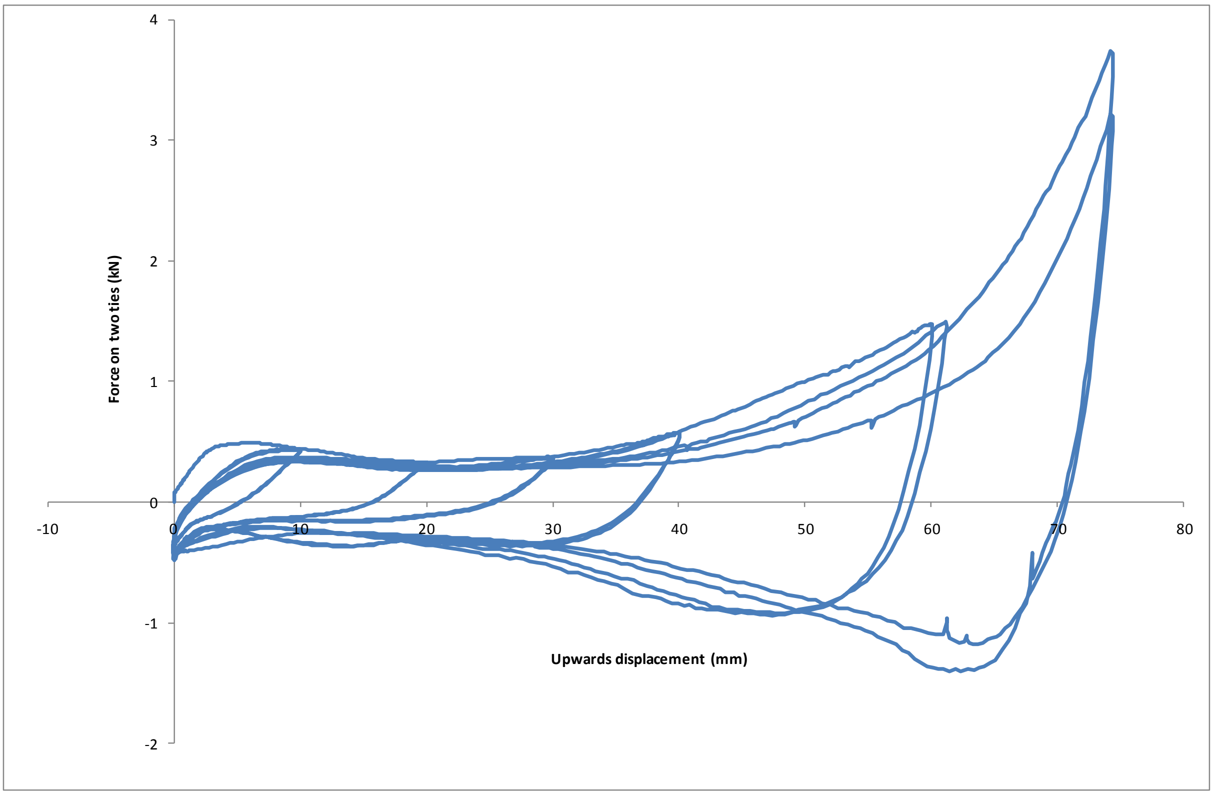


**Figure 100. Measured tie vertical load versus horizontal displacement relationship for the two cases where there was some tie slip in the mortar**

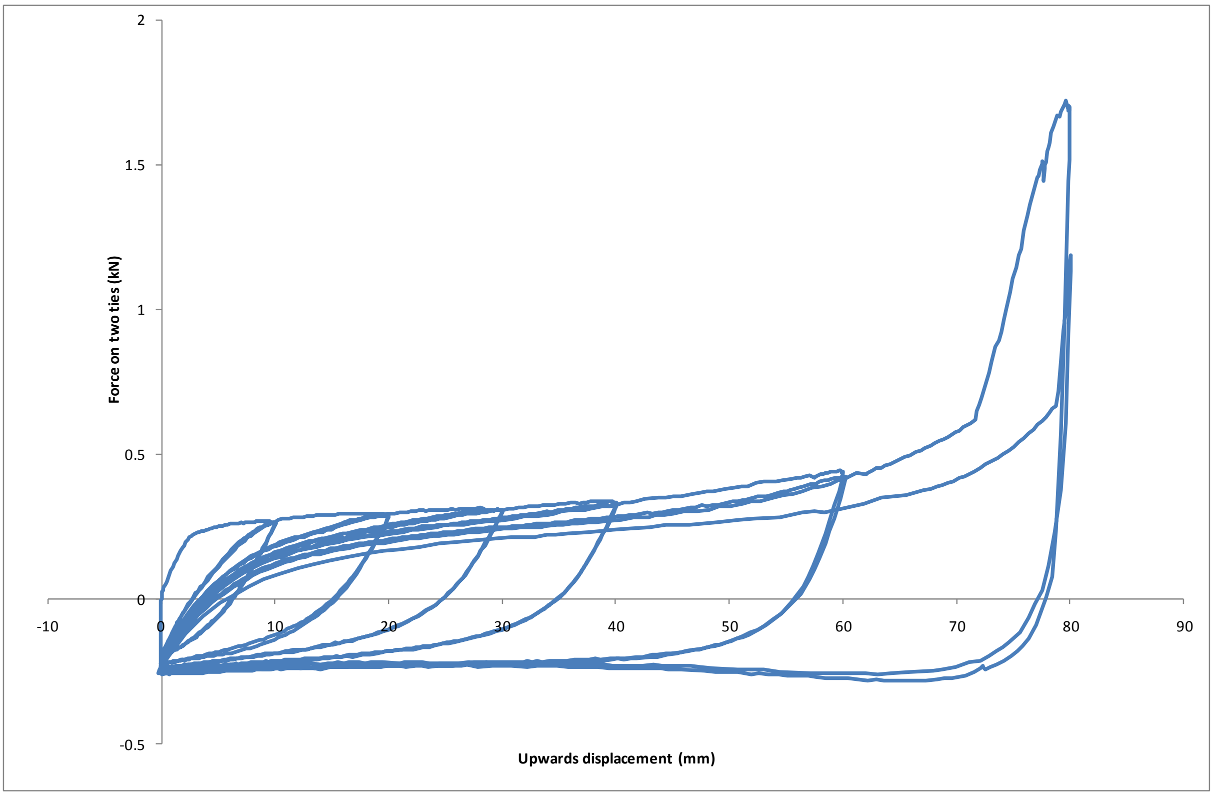


**Figure 101. Measured tie vertical load versus horizontal displacement relationship for the two cases where there was some tie slip in the mortar**

**Table 13. Tie vertical displacement (mm) versus vertical load (kN/tie) from test backbone curves**

**(a) Out-of-plane movement between veneer and LTF fully restrained**

| Specimen No. | 1 | 2 | 3 | |
|---|---|---|---|---|
| Vertical Displacement | | | | Average |
| 3 mm | 0.213 | 0.220 | 0.199 | 0.210 |
| 10 mm | 0.247 | 0.246 | 0.217 | 0.237 |
| 20 mm | 0.230 | 0.217 | 0.182 | 0.209 |
| 30 mm | 0.196 | 0.187 | 0.154 | 0.179 |
| 40 mm | 0.254 | 0.290 | 0.335 | 0.293 |
| 60 mm | 0.669 | 0.749 | 0.796 | 0.738 |

**(b) Out-of-plane movement between veneer and LTF not restrained**

| Specimen No. | 1 | 2 | 3 | | | |
|---|---|---|---|---|---|---|
| Vertical Displacement | | | | Average | Mean | Ratio |
| 3 mm | 0.112 | 0.132 | 0.085 | 0.110 | 0.160 | 0.521 |
| 10 mm | 0.134 | 0.155 | 0.105 | 0.131 | 0.184 | 0.554 |
| 20 mm | 0.147 | 0.156 | 0.111 | 0.138 | 0.174 | 0.658 |
| 30 mm | 0.155 | 0.147 | 0.113 | 0.138 | 0.158 | 0.772 |
| 40 mm | 0.169 | 0.157 | 0.124 | 0.150 | 0.221 | 0.512 |
| 60 mm | 0.221 | 0.201 | 0.165 | 0.196 | 0.467 | 0.265 |